

Louisiana State University

LSU Scholarly Repository

LSU Historical Dissertations and Theses

Graduate School

1995

Polynuclear Aromatic Hydrocarbons With Curved Surfaces: Models and Precursors for Fullerenes.

Atteye Houssein Abdourazak

Louisiana State University and Agricultural & Mechanical College

Follow this and additional works at: https://repository.lsu.edu/gradschool_disstheses

Recommended Citation

Abdourazak, Atteye Houssein, "Polynuclear Aromatic Hydrocarbons With Curved Surfaces: Models and Precursors for Fullerenes." (1995). *LSU Historical Dissertations and Theses*. 6081.

https://repository.lsu.edu/gradschool_disstheses/6081

This Dissertation is brought to you for free and open access by the Graduate School at LSU Scholarly Repository. It has been accepted for inclusion in LSU Historical Dissertations and Theses by an authorized administrator of LSU Scholarly Repository. For more information, please contact gradetd@lsu.edu.

INFORMATION TO USERS

This manuscript has been reproduced from the microfilm master. UMI films the text directly from the original or copy submitted. Thus, some thesis and dissertation copies are in typewriter face, while others may be from any type of computer printer.

The quality of this reproduction is dependent upon the quality of the copy submitted. Broken or indistinct print, colored or poor quality illustrations and photographs, print bleedthrough, substandard margins, and improper alignment can adversely affect reproduction.

In the unlikely event that the author did not send UMI a complete manuscript and there are missing pages, these will be noted. Also, if unauthorized copyright material had to be removed, a note will indicate the deletion.

Oversize materials (e.g., maps, drawings, charts) are reproduced by sectioning the original, beginning at the upper left-hand corner and continuing from left to right in equal sections with small overlaps. Each original is also photographed in one exposure and is included in reduced form at the back of the book.

Photographs included in the original manuscript have been reproduced xerographically in this copy. Higher quality 6" x 9" black and white photographic prints are available for any photographs or illustrations appearing in this copy for an additional charge. Contact UMI directly to order.

UMI

**A Bell & Howell Information Company
300 North Zeeb Road, Ann Arbor MI 48106-1346 USA
313/761-4700 800/521-0600**

**POLYNUCLEAR AROMATIC HYDROCARBONS WITH CURVED
SURFACES: MODELS AND PRECURSORS FOR FULLERENES**

A Dissertation

**Submitted to the Graduate Faculty of the
Louisiana State University and
Agricultural and Mechanical College
in partial fulfillment of the
requirements for the degree of
Doctor of Philosophy**

in

The Department of Chemistry

by

Atteye H. Abdourazak

B.S., Université de Reims Champagne-Ardenne, 1986

M.S., Université de Reims Champagne-Ardenne, 1987

December 1995

UMI Number: 9618271

UMI Microform 9618271
Copyright 1996, by UMI Company. All rights reserved.

**This microform edition is protected against unauthorized
copying under Title 17, United States Code.**

UMI
300 North Zeeb Road
Ann Arbor, MI 48103

SI TU PEUX

Si tu peux voir détruit l'ouvrage de ta vie
Et sans dire un seul mot te mettre à rebâtir,
Ou perdre en un seul coup le gain de cent parties
Sans un geste et sans un soupir,

Si tu peux être amant sans être fou d'amour,
Si tu peux être fort sans cesser d'être tendre,
Et, te sentant haï, sans haïr à ton tour,
Pouvant lutter et te défendre,

Si tu peux supporter d'entendre tes paroles
Travesties par des gueux pour exciter les sots,
Et d'entendre mentir sur toi leurs bouches folles
Sans mentir toi-même d'un mot,

Si tu peux rester digne en étant populaire,
Si tu peux rester peuple en conseillant les rois,
Et si tu peux aimer tous tes amis, en frères,
Sans qu'aucun d'eux soit tout pour toi,

Si tu sais méditer, observer et connaître,
Sans jamais devenir sceptique ou destructeur,
Rêver, mais sans laisser ton rêve être ton maître,
Penser sans n'être qu'un penseur,

Si tu peux être dur sans jamais être en rage,
Si tu peux être brave et jamais imprudent,
Si tu sais être bon, si tu sais être sage,
Sans être moral ni pédant,

Si tu peux rencontrer Triomphe après Défaite,
Et recevoir ces deux menteurs d'un même front,
Si tu peux conserver ton courage et ta tête,
Quand tous les autres la perdront,

Alors les Rois, les Dieux, la Chance et la Victoire
Seront à tout jamais tes esclaves soumis,
Et, ce qui vaut mieux que les Rois et la Gloire,
Tu seras un homme, mon fils.

RUDYARD KIPLING (traduit par Andre Maurois)

IF -----

If you can keep your head when all about you
Are losing theirs and blaming it on you,
If you can trust yourself when all men doubt you,
But make allowance for their doubting too;
If you can wait and not be tired by waiting,
Or being lied about, don't deal in lies,
Or being hated, don't give way to hating,
And yet don't look too good, nor talk too wise;

If you can dream- and not make dreams your master;
If you can think- and not make thoughts your aim;
If you can meet with Triumph and Disaster
And treat those two imposters just the same;
If you can bear to hear the truth you've spoken
Twisted by knaves to make a trap for fools,
Or watch the things you gave your life to, broken,
And stoop and build'em with worn-out tools;

If you can make one heap of all your winnings
And risk it on one turn of pitch-and-toss,
And lose, and start again at your beginnings
And never breathe a word about your loss;
If you can force your heart and nerve and sinew
To serve your turn long after they are gone,
And so hold on when there is nothing in you
Except the Will which says to them: " Hold on!"

If you can talk with crowds and keep your virtue,
Or walk with Kings-nor lose the common touch,
If neither foes nor loving friends can hurt you,
If all men count with you, but none too much;
If you can fill the unforgiving minute
With sixty seconds'worth of distance run,
Yours is the Earth and everything that' in it,
And-which is more-you'll be a Man, my son!

RUDYARD KIPLING

" Brother Square-Toes" - Rewards and Fairies.

*A mes pères: Houssein Hirab Dembil
 Mahmoud Hirab Dembil
 Houssein Atteye Guirreh*

*A mes mères: Saada Cheik Hersi
 Daahabo waddad
 Aicha Meraneh*

A tous mes nombreux oncles, frères, soeurs, cousins , cousines.

*A ma femme: Fathia Djama Yassin et à ma famille "adoptive": la famille
Djama Yassin.*

A tous mes amis.

Je vous dédie cette dissertation.

ACKNOWLEDGMENTS

I could not have reached this goal without the support and help of a lot of people, and especially that of Dean Peter W. Rabideau and his research group. I would like to take a moment to thank them, and let them know how much I really appreciate them.

I would like to thank Dean Peter W. Rabideau for being more than just an advisor; for giving me the independence, encouragments, ideas and enthusiasm for succeeding in my goals. I would like to extend my warm thanks to his family: his wife Jennifer and his children, Leah and Mark. I will always cherish the memories of Christmas and Thanksgiving dinners in the warmth of their home.

My deep gratitudes go to Dr. Andrzej Sygula, his wife and the Lady of the group; Renata Sygula, and their son Peter. Thanks for being there for me all the times, the good and the bad, for giving me all the encouragments and advises both in my academic and personal life. Thank you for your friendships, support and resourcefulness. I could never thank you enough just for being the very good friends that you are.

I would like to thank Dr. Zbigniew Marcinow and his family; his wife Barbara and their two daughters; Anna and Justina. My labmate for all these years, you worked on these projects as much as I did and your help has been very valuable for me in attaining this goal, and I wanted to thank you sincerely.

I would like to remember Haskell E. Folsom "the old texan", a very good friend and his familly: his wife Anna, his daughter Christina and

the soon to be born baby. Good Luck to you on the road that you have chosen.

And finally from the Rabideau's group, a very fine young man from the "Blue Grass State", Mark Clayton and his wife Kendra, thank you for being the very good friends that you are.

I would also like to say welcome to the new member of this group, Dr. Charles Liu.

The Rabideau's group would like to thank Professor Larry Scott for helpful discussions and for sharing his most recent procedures for the preparation of corannulene.

I wish to express my gratitudes to the faculty, staff and graduate students of the chemistry department of Louisiana State University. In particular: Dr. Mark L. McLaughlin and his graduate student Alfonso Davila for their valuable assistance in the hydrogenation experiments; Dr. George G. Stanley and his graduate student Barry Misquitta for kindly providing us the homogeneous catalyst; Dr. Nikolaus H. Fischer, Dr. Frank K. Cartledge and Dr. Dana Browne for all their help and fruitful discussions. Dr. James G. Traynham for his help and advises regarding organic nomenclature.

I would also like to extend my deepest appreciation to Dr. Frank R. Fronczek for the determination of the X-ray crystal structures; Dr. David Vargas and Mr. Marcus Nauman for taking their time to teach me the use of the NMR instrumentation; Dr. Tracy McCarley, Mr. Rolly Singh and Mr. Jeff Corkern for all their help in the mass spectrometry resolutions; the Master scientific glassblower, Mr. Christian Bousset and his assistant Vincent Guerrini; my friends Youssouf Farah Ahmed,

Mohamed Guedi Qayad, Dadi Mohamed Atman his wife Christine and their son Killian, Hassan Omar Mahadallah, Charo Benites, Laurie Brown, Jean-Noël Lemercier, Hong Fan, Kipronoh Rugutt, Alicia James, Maria Fernandez, Javier Macossay, Guillermo Morales.

TABLE OF CONTENTS

DEDICATION	ii
ACKNOWLEDGMENTS	v
LIST OF TABLES	xi
LIST OF FIGURES	xiii
LIST OF SCHEMES	xiv
LIST OF ABBREVIATIONS	xv
ABSTRACT	xvii
 CHAPTER ONE. CYCLOPENTACORANNULENE: THE FIRST CONFORMATIONALLY "LOCKED", FULLERENE-RELATED, BOWL-SHAPED MOLECULE	
1.1 Introduction	1
1.1.1 Literature review	1
1.1.1.1 Synthesis of corannulene	1
1.1.1.2 Dynamic of the corannulene system	6
1.2 Results and Discussion	9
1.2.1 Synthesis of cyclopentacorannulene	9
1.2.2 Dynamic ¹H NMR of cyclopentacorannulene	14
1.2.3 Crystal structure of cyclopentenocorannulene	22
1.3 Conclusions	24
1.4 Experimental	25
1.4.1 Materials and Methods	25
1.4.2 Synthesis of 5,6-dihydrocyclopent[<i>f, g</i>]acenaphthylene-1,2-dione, (11)	26
1.4.3 Synthesis of 5,7-diacetyl-1,2-dihydro-6H-dicyclopent[<i>a, fg</i>]acenaphthylen-6-one, (12)	28
1.4.4 Synthesis of 1,1'-(1,2-dihydrocyclopent[<i>cd</i>]fluoranthene-5,8-diyl)bis-ethanone, (14)	29
1.4.5 Synthesis of 5,8-bis(1-chloroethenyl)-1,2-dihydrocyclopenta[<i>cd</i>]fluoranthene, (15)	30
1.4.6 Flash vacuum pyrolysis of 5,8-bis(1-chloroethenyl)-1,2-dihydrocyclopent[<i>cd</i>]fluoranthene, (15)	31
1.4.7 Selective hydrogenation of dibenzo[<i>ghi, mno</i>]cyclopenta[<i>cd</i>]fluoranthene, (16)	32
1.4.8 Synthesis of 7,10-diacetyl-3,4-(1,2-dibromoethano)-fluoranthene, (18)	33
1.4.9 Synthesis of 7,10-diacetyl-3,4-ethenofluoranthene, (19)	33

1.4.10 Attempted synthesis of 7,10-di(1-chloroethenyl)-3,4-ethenofluoranthene (22) from 7,10-diacetyl-3,4-ethenofluoranthene, (19)	34
1.4.11 Synthesis of 7,10-(1-chloroethenyl)-3,4-(dibromoethano)-fluoranthene, (21)	35
1.4.12 Synthesis 7,10-di(1-chloroethenyl)-3,4-ethenofluoranthene, (22)	36
1.4.13 Flash vacuum pyrolysis of 7,10-di(1-chloroethenyl)-3,4-etheno-fluoranthene, (22)	37
1.4.14 Heterogeneous selective deuteration of dibenzo[ghi, -mno]cyclopenta[cd]fluoranthene, (16)	37
1.4.15 Homogeneous selective deutrogenation of dibenzo[ghi, -mno]cyclopenta[cd]fluoranthene, (16)	39
1.4.16 Kinetic study of the equilibration of the stereoisomers of 23	39

CHAPTER TWO. BUCKYBOWLS! SYNTHESIS AND CHARACTERIZATION OF SEMIBUCKMINSTERFULLERENES (C₃₀H₁₂)

2.1 Introduction	47
2.2 Results and Discussion	49
2.2.1 Synthesis and characterization of diacenaphtho[3,2,1,8-cdefg: 3',2',1',8'-lmnop]chrysene, (24)	49
2.2.1.1 Attempted synthesis of 24 from bis(4H-cyclopenta[def]phenanthren-4-ylidene), (30)	49
2.2.1.2 Synthesis of cyclopent[fg]acenaphthylene-1,2,5,6-tetrone, (31)	50
2.2.1.3 Synthesis of diacenaphtho[3,2,1,8-cdefg: 3',2',1',8'-lmnop]chrysene, (24)	51
2.2.2 Synthesis of benz[5,6]-as-indaceno[3,2,1,8,7-mnopqr]indeno[4,3,2,1-cdef]chrysene, (25)	54
2.3 Conclusions	58
2.4 Experimental	59
2.4.1 Synthesis of diacenaphtho[3,2,1,8-cdefg: 3',2',1',8'-lmnop]-chrysene, (24)	59
2.4.1.1 Synthesis of 5,6-dibromo-5,6-dihydrocyclopent[fg]-acenaphthylene-1,2-dione, (33)	59
2.4.1.2 Synthesis of 5,6-dihydro-5,6-bis(nitrooxy)-cyclopent[fg]acenaphthylene-1,2-dione, (34)	60
2.4.1.3 Synthesis of cyclopent[fg]acenaphthylene-1,2,5,6-tetrone, (31)	61
2.4.1.4 Synthesis of 1,4,7,10-tetraethanone-indeno[1,2,3-cd]-fluoranthene, (35)	62
2.4.1.5 Synthesis of 1,4,7,10-tetrakis(1-chloroethenyl)-indeno[1,2,3-cd]fluoranthene, (36)	63
2.4.1.6 Flash vacuum pyrolysis of 1,4,7,10-tetrakis(1-chloroethenyl)-indeno[1,2,3-cd]fluoranthene, (36).	64

2.4.2 Synthesis of benz[5,6]-as-indaceno[3,2,1,8,7- <i>mnopqr</i>]indeno- [4,3,2,1- <i>cdef</i>]chrysene, (25)	65
2.4.2.1 Synthesis of 5H-diindeno[1, 2- <i>a</i> : 1', 2'- <i>c</i>]fluorene- 5,10, 15-trione, (27)	65
2.4.2.2 Synthesis of 5,10,15-tris(dichloromethyl)-5,10,15- trihydroxy-5H-diindeno[1, 2- <i>a</i> ; 1', 2'- <i>c</i>]fluorene, (40)	66
2.4.2.3 Synthesis of 5,10,15-tris(dichloromethylene)-5H- diindeno[1, 2- <i>a</i> : 1', 2'- <i>c</i>]fluorene, (41)	67
2.4.2.4 Flash vacuum pyrolysis of 5,10,15-tridichloro- methylene)-5H-diindeno[1, 2- <i>a</i> : 1', 2'- <i>c</i>]fluorene, (41)	68
2.4.2.5 Synthesis of 5,10-bis(chloromethylene)-15- dichloromethylene-5H-diindeno[1, 2- <i>a</i> : 1', 2'- <i>c</i>]- fluorenes, (42)	69
2.4.2.6 Flash vacuum pyrolysis of 5,10-bis(chloromethylene)- 15-dichloromethylene-5H-diindeno[1, 2- <i>a</i> : 1', 2'- <i>c</i>]- fluorenes, (42)	70
BIBLIOGRAPHY	96
APPENDIXES	100
VITA	144

LIST OF TABLES

Table 1.1	Barriers for the ring inversion of corannulene derivatives	8
Table 1.2	Rates constants, half-life times and free energy activation of the stereoisomers of 23 by ¹H NMR experiment	22
Table 1.3	Crystal data and collection parameters for 16	40
Table 1.4	Coordinates and equivalent isotropic thermal parameters for 16	42
Table 1.5	Bond distances in angstroms for 16	42
Table 1.6	Coordiantes assigned to hydrogen atoms for 16	43
Table 1.7	Bond angles in degrees for 16	43
Table 1.8	Torsion angles in degrees for 16	44
Table 2.1	Crystal data and collection parameters for 31	72
Table 2.2	Bond distances in angstroms for 31	74
Table 2.3	Coordinates and equivalent isotropic thermal parameters for 31	74
Table 2.4	Coordiantes assigned to hydrogen atoms for 31	75
Table 2.5	Bond angles in degrees for 31	75
Table 2.6	Crystal data and collection parameters for syn-40	76
Table 2.7	Bond angles in degrees for syn-40	79
Table 2.8	Bond distances in angstroms for syn-40	80
Table 2.9	Coordinates and equivalent isotropic thermal parameters for syn-40	81
Table 2.10	Coordiantes assigned to hydrogen atoms for syn-40	82
Table 2.11	Torsion angles in degrees for syn-40	83
Table 2.12	Crystal data and collection parameters for 41	87
Table 2.13	Bond angles in degrees for 41	90
Table 2.14	Bond distances in angstroms for 41	91

Table 2.15	Coordiantes assigned to hydrogen atoms for 41	91
Table 2.16	Coordinates and equivalent isotropic thermal parameters for 41	92
Table 2.17	Torsion angles in degrees for 41	93

LIST OF FIGURES

Figure 1.1	Buckminsterfullerene	2
Figure 1.2	400 MHz ^1H NMR spectrum of the aliphatic region of 17	15
Figure 1.3	Stacked plots showing the equilibration of the stereoisomers of 23 at 85.1 °C with time (minutes).....	20
Figure 1.4	Plot of $\log(a/a-2x)$ vs. time	21
Figure 1.5	Stacked bowls of cyclopentacorannulene 16	23
Figure 1.6	Bowl depth from x-ray diffraction as measured from the rim aromatic carbons to the best plane containing the central five-membered ring	24
Figure 1.7	Flash vacuum pyrolysis apparatus	26
Figure 1.8	ORTEP drawing of cyclopentacorannulene (16)	41
Figure 2.1	ORTEP drawing of cyclopent[<i>g</i>]acenaphthylene-1,2,5,6-tetrone, (31)	73
Figure 2.2	ORTEP side view of 5,10,15-tris(dichloromethyl)-5,10,15-trihydroxy-5H-diindeno[1, 2-<i>a</i>, 1', 2'-<i>c</i>]fluorene, (40)	77
Figure 2.3	ORTEP top view of 5,10,15-tris(dichloromethyl)-5,10,15-trihydroxy-5H-diindeno[1, 2-<i>a</i>, 1', 2'-<i>c</i>]fluorene, (40)	78
Figure 2.4	ORTEP side view of 5,10,15-tris(dichloromethylene)-5H-diindeno[1, 2-<i>a</i>: 1', 2'-<i>c</i>]fluorene, (41)	88
Figure 2.5	ORTEP top view of 5,10,15-tris(dichloromethylene)-5H-diindeno[1, 2-<i>a</i>: 1', 2'-<i>c</i>]fluorene, (41)	89

LIST OF SCHEMES

Scheme 1.1	The first synthesis of corannulene	3
Scheme 1.2	Craig and Robin's approach to corannulene	3
Scheme 1.3	Scott's route to corannulene	4
Scheme 1.4	Siegel's route to corannulene	5
Scheme 1.5	Zimmerman and Nuechter's route to corannulene	5
Scheme 1.6	Scott's improved version of corannulene synthesis	6
Scheme 2.1	Chapman et al. attempts to 25	48
Scheme 2.2	Retrosynthetic routes proposed for 24	49
Scheme 2.3	Synthesis of 1,2,3,4-tetraketopyracene (31)	51
Scheme 2.4	Synthesis of 24	52
Scheme 2.5	Previous attempts to 25 by our group	55

LIST OF ABBREVIATIONS

AcOH	Acetic acid
anh.	anhydrous
bs	broad singlet (in NMR spectra)
CDCl ₃	deuterated chloroform
d	doublet (in NMR spectra)
dd	doublet of doublet (in NMR spectra)
DCM	Dichloromethane
DEPT	Distortionless Enhancement by Polarization Transfer (in NMR spectra)
DMSO	Dimethylsulfoxide
DMSO-d ₆	deuterated dimethylsulfoxide
FAB	Fast Atom Bombardment
FVP	Flash Vacuum Pyrolysis
GC/MS	Gas Chromatography/Mass Spectrometry
Hz	Hertz
HRMS	High Resolution Mass Spectrometry
J	coupling constant
LC/MS	Liquid Chromatography/Mass Spectrometry
m	multiplet (in NMR spectra)
MgSO ₄	Magnesium sulfate
mp	melting point
PD/MS	Plasma Desorption/Mass Spectrometry
¹ H NMR	Proton Nuclear Magnetic Resonance
¹³ C NMR	Carbon Nuclear Magnetic Resonance
NBD	Norbornadiene

s	singlet (in NMR spectra)
t	triplet (in NMR spectra)
THF	Tetrahydrofuran
n-BuLi	n-butyllithium
PPh₃	Triphenylphosphine
BF₄	Boron tetrafluoride
NOE	Nuclear Overhauser Effect

ABSTRACT

This dissertation deals with the synthesis and characterization of polynuclear aromatic hydrocarbons with curved surfaces whose carbon frameworks may be identified on the C_{60} surface. C_{60} , known as buckminsterfullerene, is the most important member of the fullerene family, the recently discovered new form of elemental carbon.

Chapter one presents the synthesis and the dynamic 1H NMR behavior of cyclopentacorannulene (CPC), the first conformationally "locked", fullerene-related, bowl-shaped aromatic hydrocarbon. The determined barrier for the ring inversion of CPC is more than twice as large as that of corannulene. In contrast to the crystal structure of corannulene, the crystal structure of the unsaturated cyclopenteno-corannulene shows remarkable long range bowl stacking in a concave-convex orientation.

Chapter two presents the synthesis and characterization of the first two known semibuckminsterfullerenes ($C_{30}H_{12}$). These polynuclear aromatic hydrocarbons represent one half of C_{60} .

CHAPTER ONE. CYCLOPENTACORANNULENE: THE FIRST CONFORMATIONALLY "LOCKED", FULLERENE-RELATED, BOWL-SHAPED MOLECULE

1.1 INTRODUCTION.

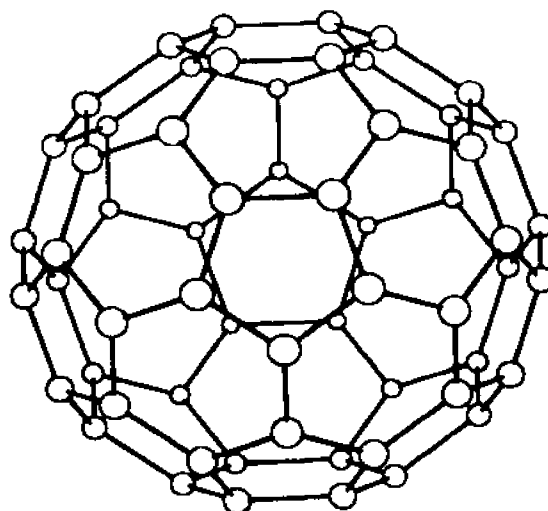
1.1.1 Literature review.

1.1.1.1 Synthesis of corannulene

One of the most exciting developments in organic chemistry has been the discovery of a third allotropic form of carbon, besides graphite and diamond, called carbon cages or fullerenes.¹ The most important member of the fullerene family is the icosahedral C_{60} , known as buckminsterfullerene (1) (Figure 1.1), named after the American engineer, architect and designer R. Buckminster Fuller (1895-1983) who invented stable, geodesic domes formed of hexagons and pentagons. In a process first reported in 1985,^{1b} C_{60} and higher fullerenes were produced by vaporization of graphite by laser irradiation.

While graphite and diamond exist as an infinite arrangement of carbon atoms with dangling bonds at the external carbon atoms saturated with other atoms, buckminsterfullerene or "buckyball" and the fullerenes in general are the purest and the only form of carbon that is a molecule since there are no dangling bonds (closed cage structure).

Publications on fullerene chemistry became very abundant in the last decade. This is especially true for buckminsterfullerene which, among other transformations, has been doped with alkali-metals, inflated to large sizes, oxidized, reduced, used as a sponge for free radicals, changed from isolator to conductor to superconductor, married to diamond on films, and so on.²⁻¹⁰ Buckminsterfullerene won the title "Molecule of the year" in the Dec. 20, 1991, issue of Science.

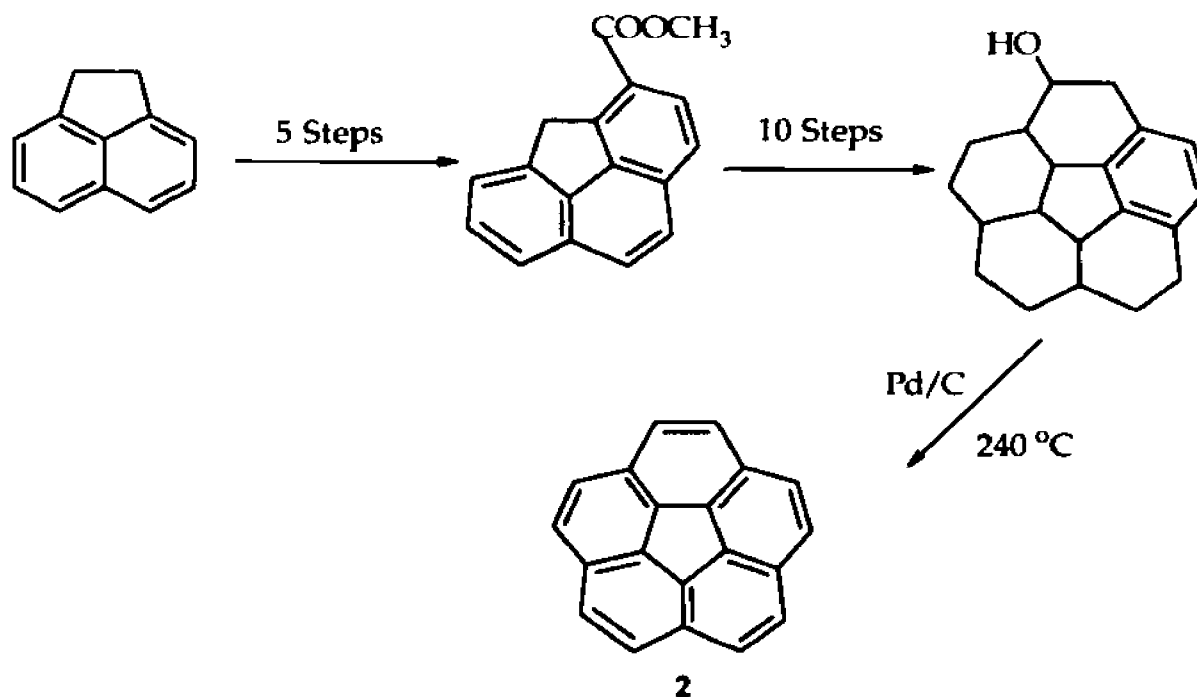


1

Figure 1.1 Buckminsterfullerene

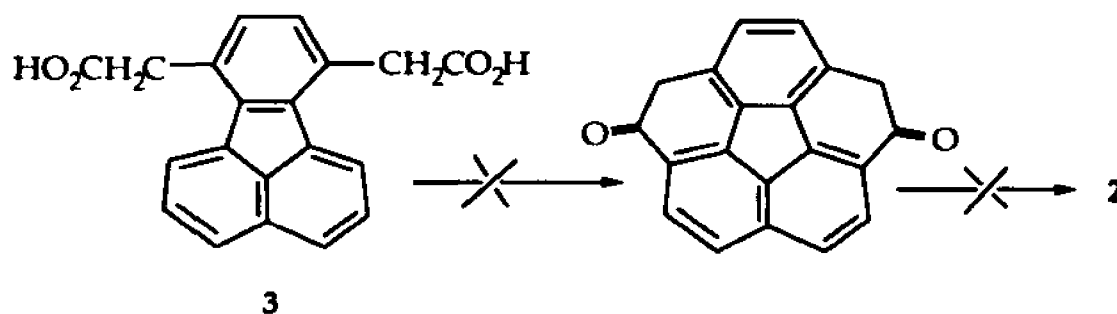
The discovery of fullerenes has also generated a renewed interest in polynuclear aromatic hydrocarbons with curved surfaces whose carbon networks are represented on fullerene surfaces. These hydrocarbons may serve as models for understanding the chemical behavior of fullerene, and also as potential precursors for the chemical synthesis of fullerenes.

Corannulene (**2**), the smallest buckminsterfullerene subunit with a curved surface, was first synthesized in 1966 by Barth and Lawton in sixteen steps (Scheme 1.1) starting with acenaphthene.¹¹ A recent comment in Chemical and Engineering News, March 1991, stated: "it (the synthesis) was so torturous that no one other than Barth and Lawton ever repeated it."¹²



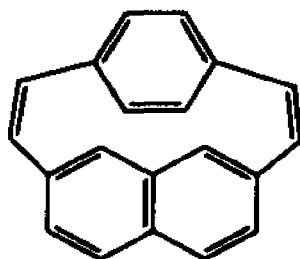
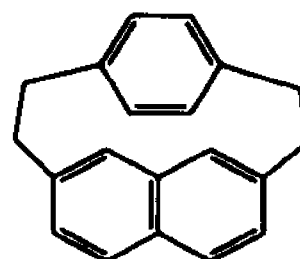
Scheme 1.1 The first synthesis of corannulene.

Two years later, Craig and Robins reported a new synthetic approach to corannulene using fluoranthene derivatives having substituents in the 7- and 10-positions,¹³ but failed at the final step of cyclization of the diacetic acid (**3**) under Friedel-Crafts conditions with strong acids (**Scheme 1.2**).

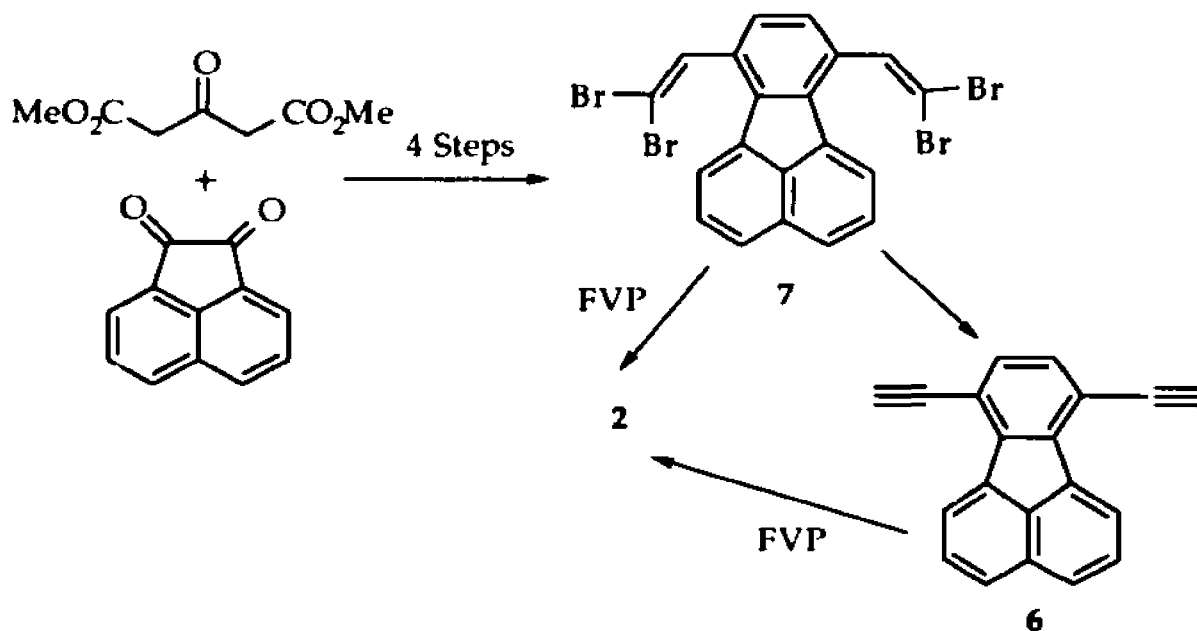


Scheme 1.2 Craig and Robins's approach to corannulene.

Attempts by Davy, Iskander and Reiss to photochemically or chemically form the central five-membered ring in [2,2](2,7)-naphthalenocyclophanediene (**4**) and [2,2](2,7)-naphthalenocyclophane (**5**) failed also.¹⁴

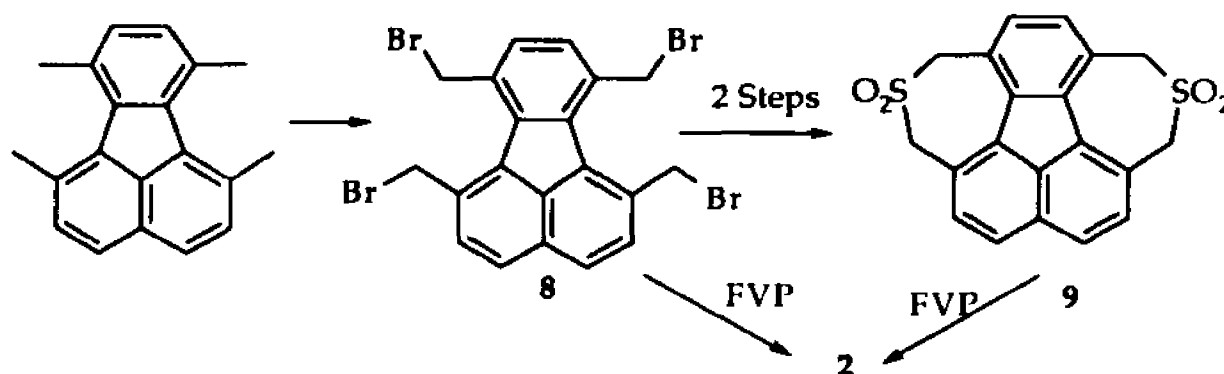
**4****5**

In 1991, Scott and coworkers made the breakthrough to a short and convenient synthesis of corannulene in six steps (Scheme 1.3) by Flash Vacuum Pyrolysis (FVP) of 7,10-diethynylfluoranthene (**6**) or 7,10-bis(2,2-dibromovinyl)fluoranthene (**7**) in the crucial ring closure step.¹⁵



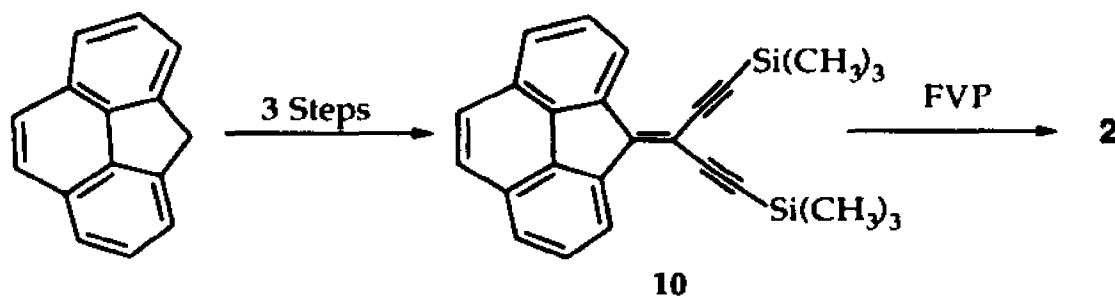
Scheme 1.3 Scott's route to corannulene.

A year later, Siegel et al., using a different pathway, also succeeded in synthesizing corannulene from 1,6,7,10-tetra-(bromomethyl)-fluoranthene (**8**) and the sulfone **9** (Scheme 1.4).¹⁶



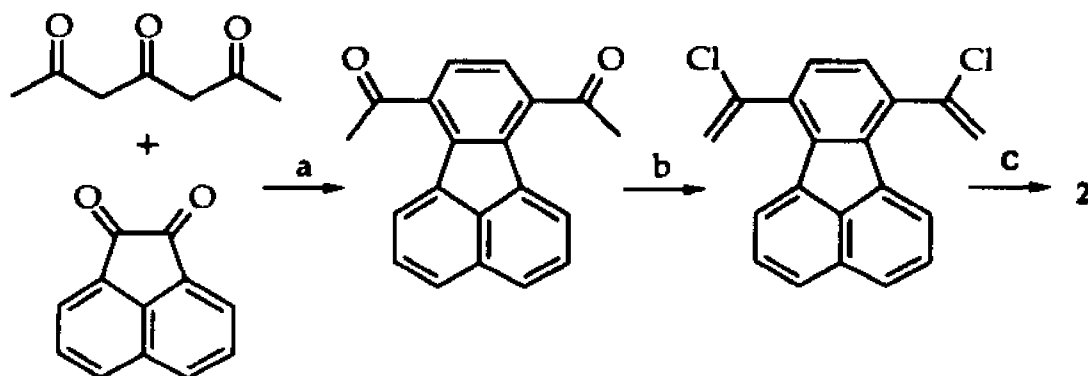
Scheme 1.4 Siegel's route to corannulene.

More recently, Zimmermann and Nuechter also used high temperature pyrolysis to obtain corannulene from 3-(4H-cyclopenta [*def*]phenanthrylidene)-1,5-bis(trimethylsilyl)-1,4-pentadiyne (**10**) (Scheme 1.5).¹⁷ Although their yield was comparable to those reported by Scott and Siegel, this route also gave smaller polynuclear aromatic hydrocarbons during the pyrolysis.



Scheme 1.5 Zimmermann and Nuechter's route to corannulene.

Currently the best method for the synthesis of corannulene is an improved version of the Scott method, a relatively simple three steps synthesis (**Scheme 1.6**) starting with acenaphthaquinone.¹⁸



a) glycine, norbornadiene/toluene, 110 °C, 3 days, 70%. b) PCl_5 , benzene, reflux, 3 hrs, 60%. c) FVP, 1100 °C, ca. 30%

Scheme 1.6 Scott's improved version of corannulene synthesis.

1.1.1.2 Dynamic of the corannulene system.

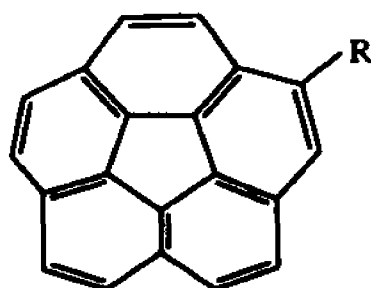
Corannulene consists of five six-membered rings which are joined along their edges forming a five-membered ring in the center. This five-membered ring introduces the curvature, giving the molecule its bowl shape. Coronene with a central six-membered ring,¹⁹ and [7] circulene with a central seven-membered ring - corannulene's analogues - have planar and saddle-shape geometries, respectively.

Corannulene is a very flexible bowl inverting itself more than 200,000 times/s in solution at room temperature²⁰ as determined by the dynamic ^1H NMR of corannulene derivatives. Since corannulene has all

equivalent protons, a suitable probe is necessary to measure the barrier for the ring inversion. Some of the probes, shown in **Table 1.1**, are dimethyl carbinol, isopropyl and benzyl groups which bear a prochiral center that make the methyl groups (in dimethyl carbinol and isopropyl) or the hydrogens (in benzyl) diastereotopic. When the bowl-to-bowl inversion is fast on the NMR time scale, the two methyl groups (or the two benzylic hydrogens) become equivalent and give a singlet for dimethyl carbinol and benzyl, or a doublet for isopropyl. When the interconversion between the conformations is slowed at lower temperatures, the methyl groups (or the benzylic hydrogens) become observable separately and ^1H NMR shows a doublet (dimethyl carbinol) or two doublets (isopropyl or benzyl). By determining the coalescence temperature (T_c), one is able to calculate the barrier for inversion (ΔG^\ddagger) using a combination of Gutowsky and Holm, and Eyring equations:

$$\Delta G^\ddagger = 4.57 T_c (9.97 + \log_{10} (T_c / \Delta\nu))$$

Despite the significant curvature of corannulene, the barrier of its bowl-to-bowl inversion is surprisingly low, being close in energy to that for the inversion of cyclohexane from one chair conformation to another ($\Delta G^\ddagger = 10.3$ kcal/mol at -67°C),²¹ and lower than that of cyclooctatetraene from one tub conformation to another ($\Delta G^\ddagger = 14.7$ kcal/mol at -2°C).²² The focus of this chapter is to answer the question of how many additional fused rings on the corannulene structure are needed to prevent the bowl-to-bowl inversion process.

Table 1.1 Barriers for the ring inversion of corannulene derivatives.

R	T _c (°C)	ΔG [#] (Kcal/mol)
$\begin{array}{c} \text{CH}_3 \\ \\ -\text{C}-\text{OH} \\ \\ \text{CH}_3 \end{array}$	- 64	10.2 ²⁰
$\begin{array}{c} \text{CH}_3 \\ \\ -\text{C}-\text{H} \\ \\ \text{CH}_3 \end{array}$	- 31	11.3 ²³
$\begin{array}{c} \text{H} \\ \\ -\text{C}-\text{C}_6\text{H}_5 \\ \\ \text{H} \end{array}$	- 39	11.2 ²³

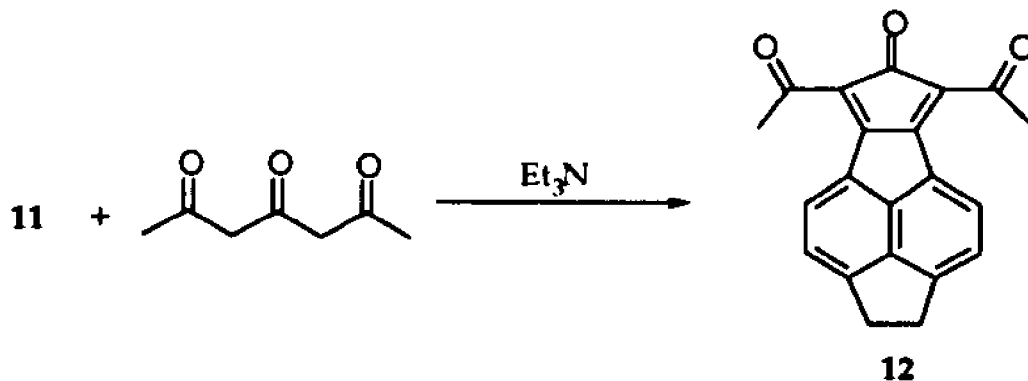
1.2 RESULTS AND DISCUSSION.

1.2.1 Synthesis of cyclopentacorannulene.

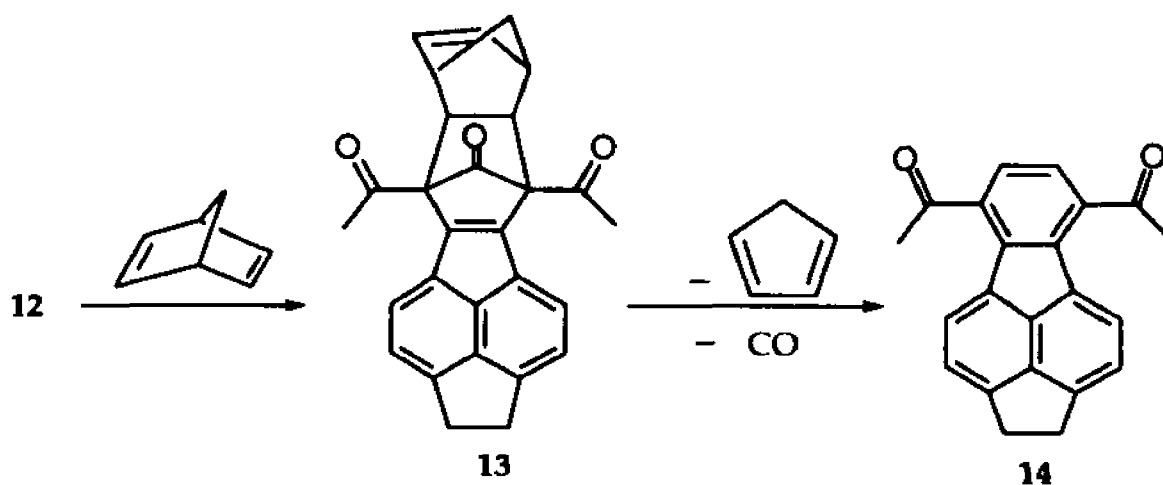
The strategy of adding a new fused ring to the corannulene structure consisted of incorporating it at the beginning of the synthetic route using the latest version of the corannulene synthesis by Scott et al. (Scheme 1.6). Consequently, 1,2-diketopyracene (**11**) seemed the best starting material for incorporating a five membered-ring. 1,2-Diketopyracene was prepared by Friedel-Crafts acylation of acenaphthene with oxalyl chloride (or oxalyl bromide) and aluminum bromide as a catalyst.²⁴



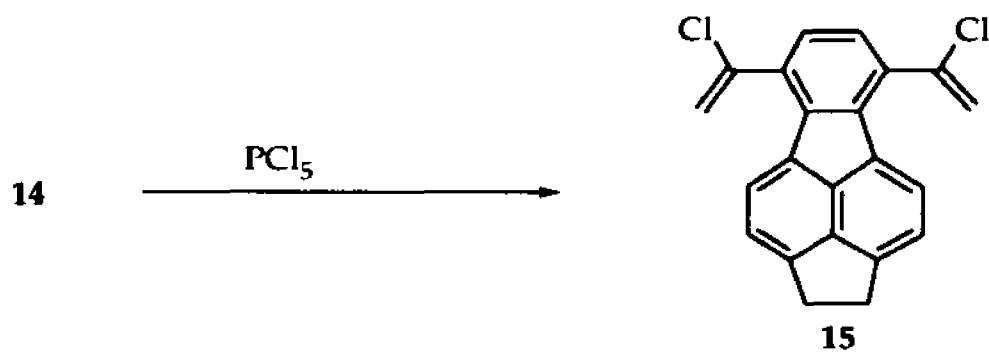
Double Knoevenagel condensation of **11** with 2,4,6-heptanetrione in methanol with triethylamine as a base afforded the cyclopentadienone **12** in 40% yield.



The crude material was subjected, without further purification, to an inverse electron demand Diels-Alder cycloaddition with norbornadiene in refluxing n-butanol. Chelotropic extrusion of carbon monoxide and expulsion of cyclopentadiene from the heptacyclic intermediate (**13**) gave the diacetyl **14** in 64% yield.

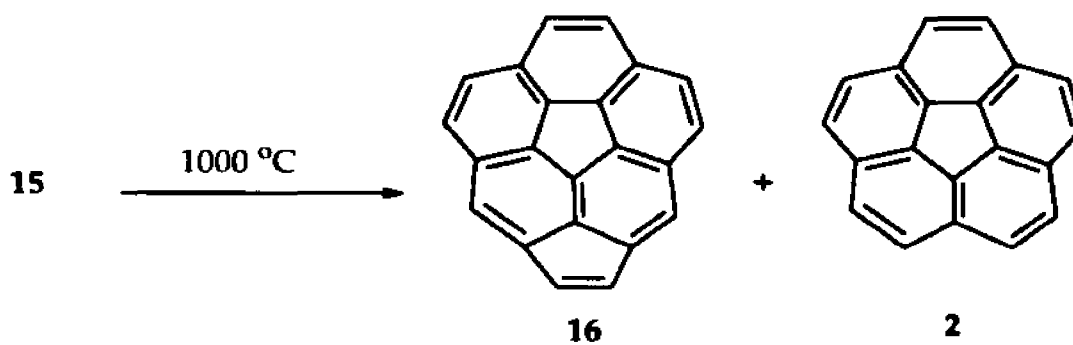


Conversion to the divinyllic dichloride **15** was achieved by treatment of **14** with three equivalents of phosphorus pentachloride in boiling benzene in 50% yield.

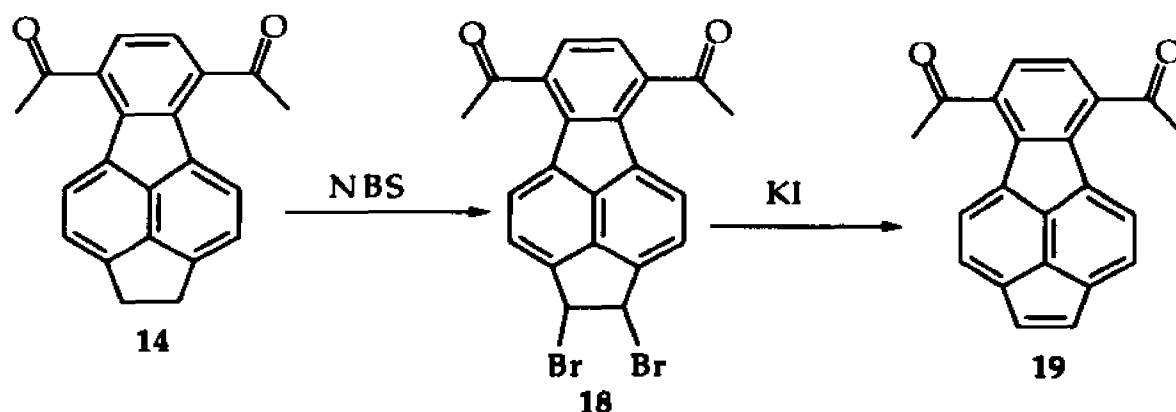


Flash pyrolysis of **15** at 1000 °C under a pressure of 1.5 mm Hg and a small flow of nitrogen not only closed the rings on both sides (in a 1,5-

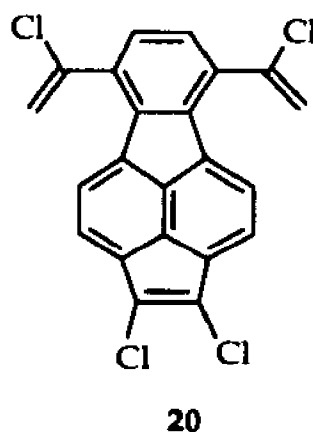
sigmatropic hydrogen shift after loss of two molecules of hydrogen chloride), but also dehydrogenated the ethano fragment and partially detached the ethane bridge producing a mixture of **16** and **2** (ca. 7:3; 10-15% yields after chromatography). A complete separation of the mixture by column chromatography was not successful, but successive recrystallizations from ethanol allowed enrichment of the mixture in **16** up to 98% (by GC).



In an effort to improve the yield of the pyrolysis, and avoid the contamination by **2**, we decided to incorporate the double bond before the pyrolytic step, expecting that detachment of the ethene bridge would not take place. Bromination of **14** at the benzylic positions by treatment with N-bromosuccinimide in benzene gave several products including the dibromo derivative **18** as the major product. Debromination of **18** utilizing powdered potassium iodide in refluxing acetone proceeded in 77% yield.



Conversion of **19** to the divinyl dichloride with phosphorus pentachloride in refluxing benzene yielded a mixture of polychlorinated with **20** as the major product instead of the desired product (**22**).

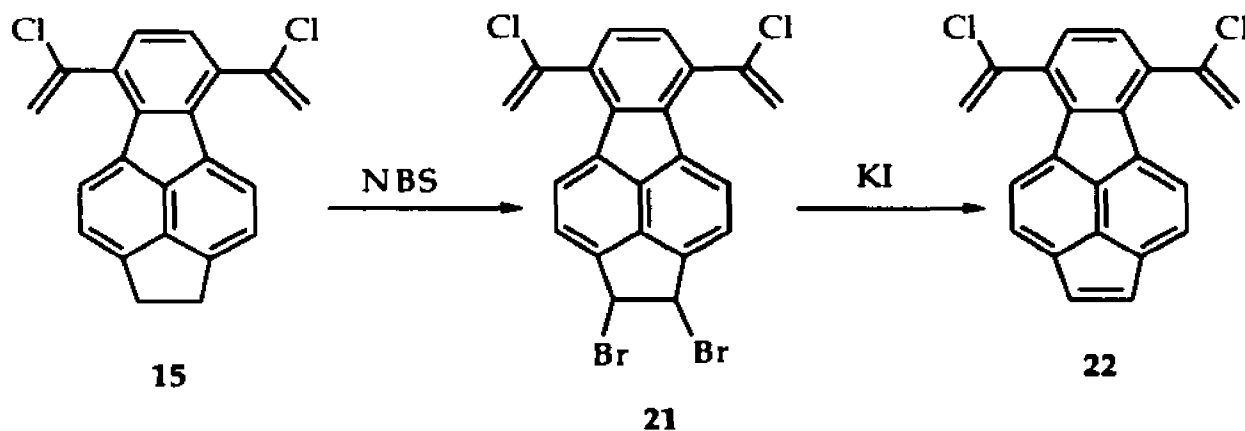


Thus the double bond is reactive towards phosphorus pentachloride, which can undergo both an auto-ionization equilibrium (1) and a dissociation equilibrium (2).²⁵ Chlorination of the alkene bridge is presumably caused by a double sequence of chlorine addition followed by hydrogen chloride elimination.



Adding a large excess of phosphorus trichloride to displace the equilibrium (2) to the left (to decrease the concentration of chlorine in solution) in order to prevent chlorination of the double bond did not improve the results.

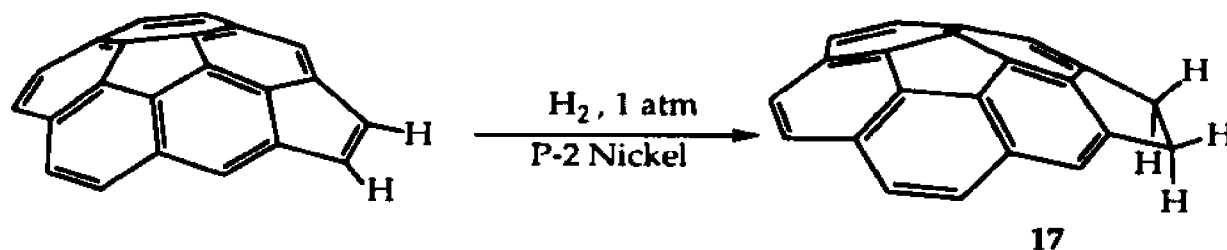
The problem was overcome by executing the above sequence of reactions (bromination and debromination) with compound **15** to finally obtain the desired precursor for pyrolysis (**22**) with the incorporated double bond.



Unfortunately, pyrolysis of **22** under the conditions used previously for **15** gave a mixture of products including **2**, **16** and unclosed materials by GC/MS. Also unlike **15**, **22** tended to polymerize before reaching the hot zone of the oven since at the end of the pyrolysis there was a significant amount of tarry products left in the boat. Therefore

improvement of the pyrolytic step was not successful, and compound **15** remains as the best precursor for the synthesis of **16**.

Heterogeneous catalytic hydrogenation of **16** with ethanolic nickel acetate treated with sodium borohydride (P-2 Nickel)²⁶ selectively reduced the etheno bridge affording **17** quantitatively.



1.2.2 Dynamic ¹H NMR of cyclopentacorannulene

Because of its symmetry, cyclopentenocorannulene (**16**), like corannulene, is not suitable for a dynamic process study by NMR. This is not the case for cyclopentacorannulene (**17**) which has non-equivalent benzylic protons due to the curvature of the molecule (endo protons; protons towards the concave side: exo protons; protons towards the convex side). At room temperature, the 400 MHz ¹H NMR spectrum (DMSO-d₆) of **17** shows two sets of aliphatic hydrogens, centered at 2.98 and 3.75 ppm (Figure 1.2), characteristic for an AA'BB' system. The non-equivalence of the endo and the exo protons proves that the bowl-to-bowl inversion is slow on the NMR time scale.

This is in contrast to the behavior of monosubstituted corannulenes which show differentiation of the diastereotopic protons

only at low temperatures (Table 1.1). By variable-temperature ^1H NMR, 17 shows no signal coalescence up to 135 $^{\circ}\text{C}$, the upper temperature limit of the instrument. At this temperature the lower limit for the barrier to ring inversion of 17 may be estimated at 18.8 Kcal/mol.

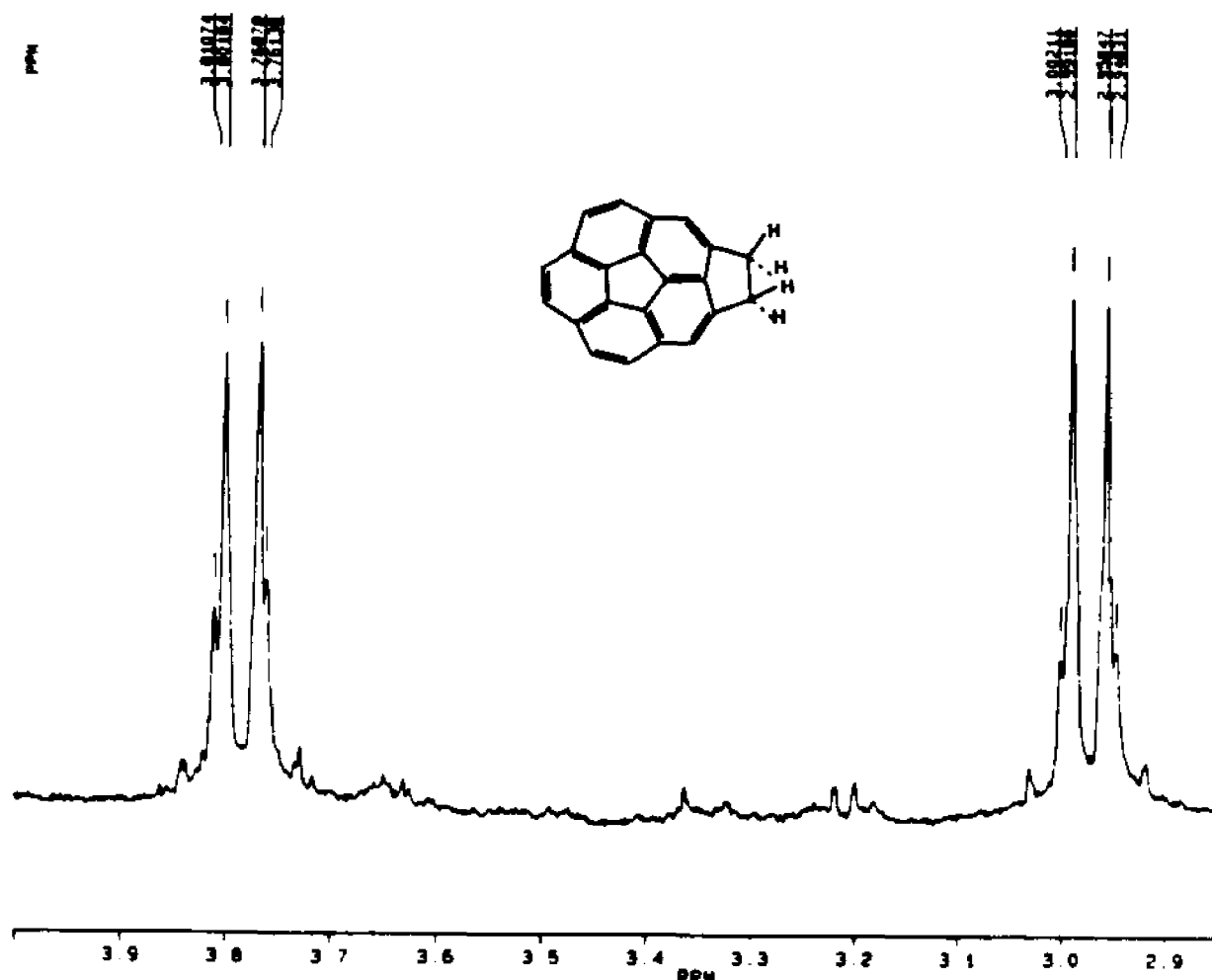
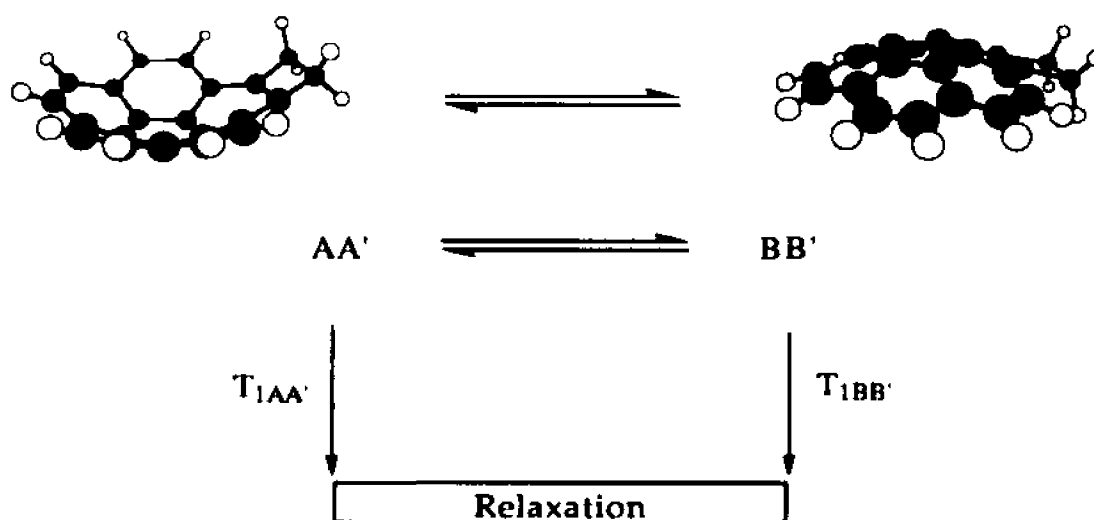


Figure 1.2 400 MHz ^1H NMR spectrum of the aliphatic region of 17.

The dynamic behavior of 17 was also studied with the spin polarization transfer method²⁷ at 127 $^{\circ}\text{C}$. This method consists of applying a selective 180° pulse to one of the doublets, in order to reverse

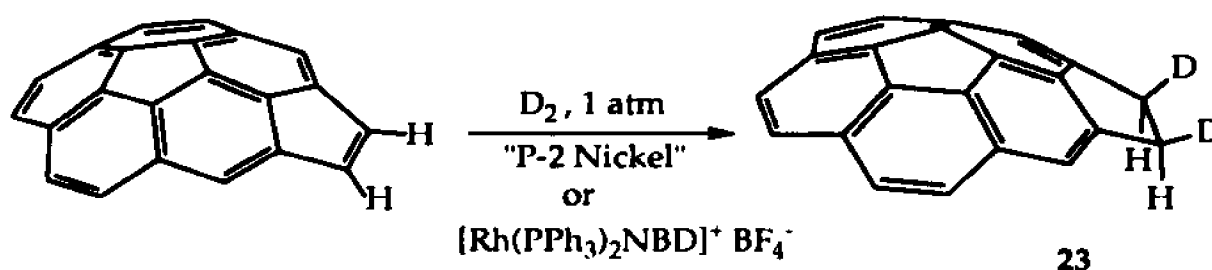
its polarization, followed by a nonselective 90° pulse after increasingly longer delay times (from $1\mu\text{s}$ to 15.0 s). A delay domain between 0.0 and 8.0 s was used. At longer delay times other time-dependent processes interfere with the measurement. The two processes considered in this method are the exchange interconverting the endo and the exo protons (the bowl-to-bowl inversion), and the relaxation time (T_1) of these protons.



When the rate of inversion is very slow (or if there is no inversion), after certain time corresponding to the relaxation time T_1 the negative signal becomes positive again without any change in the other part of the spectrum (Inversion-Recovery Technique for measuring T_1). If the rate of inversion is comparable to the relaxation process, then there should be a change in the other part of the spectrum (decrease in the intensity of the peaks) since the endo protons become exo and vice-versa. We observed very little spin polarization transfer in 17, even at 127°C ,

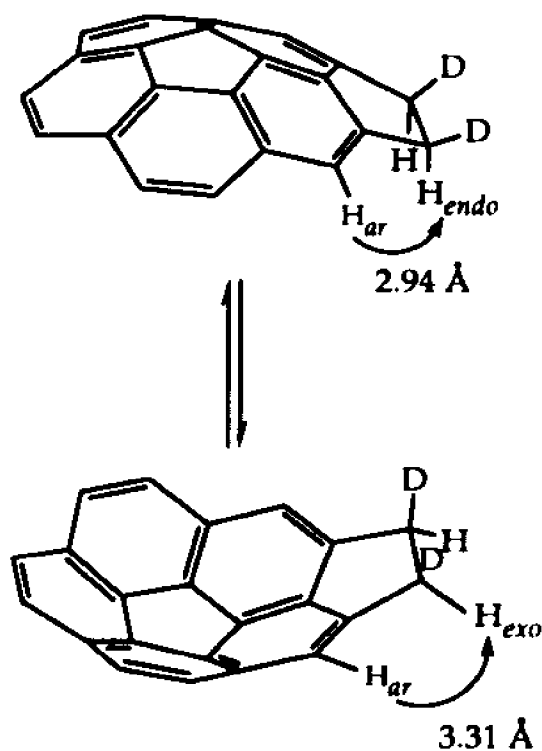
and this allowed an estimation of the lower barrier for ring inversion at 26 Kcal/mol.

The variable-temperature ^1H NMR and the spin polarization transfer methods suggest that the rate of bowl-to-bowl inversion is slower than that of the relaxation time of the benzylic protons. Therefore these methods could not be used for the determination of the barrier in CPC. Thus, an option was the synthesis of an optically active derivative, followed by separation of the enantiomers and measurement of the decay of the optical activity with time and temperature. However, due to the relatively small amount of material available, we preferred a method that could be done more easily on a milligram scale. Hence we decided to deuterogenate **16** in hope of obtaining one stereoisomer with the deuterium only on one side. We could then determine the bowl-to bowl inversion as a measure of the rate of equilibration between the two stereoisomers.



Deuterogenation of **16** was accomplished by the method used in the heterogeneous catalysis hydrogenation of **16** (section 1.2.1), replacing

hydrogen gas with deuterium gas and sodium borohydride with sodium borodeuteride. Only one stereoisomer of the dideuterated product (**23**) was detected by ^1H NMR which showed a singlet at 2.95 ppm (in CDCl_3). The sample left at room temperature for four days showed no signs of change, but when heated at $150\text{ }^\circ\text{C}$ for ten minutes, the ^1H NMR showed two singlets of equal intensities at 2.94 and 3.71 ppm (in $\text{DMSO}-d_6$). This suggested that equilibration between the two stereoisomers was established by ring inversion.



The deuterogenation reaction is π -facial stereoselective. The upfield chemical shift of the benzylic protons (due to the anisotropy of the aromatic rings) suggested that cis-deuterogenation is stereoselectively occurring on the convex side of the bowl because of the curvature of the molecule. This was confirmed by an NOE experiment conducted on the

equilibrated mixture of the exo and endo dideutero isomers (**Appendix 25**). Irradiation of the aromatic hydrogen proximal to the benzylic hydrogens (H_{ar} 7.34 ppm) enhanced the signal at 2.94 ppm twice as much as the signal at 3.75 ppm. As calculated at the HF/3-21G level of theory, the H_{ar} - H_{endo} distance is 2.92 Å, as compared to 3.31 Å for H_{ar} - H_{exo} . The convex stereoselective deuterogenation was also preferred in a homogeneous catalysis with the Wilkinson's related catalyst, $[Rh(NBD)(PPh_3)_2]^+BF_4^-$.

The rates of equilibration between the two stereoisomers of **23** at temperatures ranging from 52 to 99 °C were studied by 1H NMR by measuring the intensity of the respective peaks. An illustration is given in **Figure 1.3** with a temperature of 85.1 °C and times varying from 0 to 240 minutes.

The kinetic expression for this reversible system is given by:²⁸

$$\frac{dx}{dt} = k(a - x) - kx = k(a - 2x)$$

a = initial concentration of the given stereoisomer

x = the amount changed into the other stereoisomer after time t

k = rate constant (since the two rate constants are equal)

The integrated form of this equation is:

$$k = \frac{2.3}{2t} \log \frac{a}{a - 2x}$$

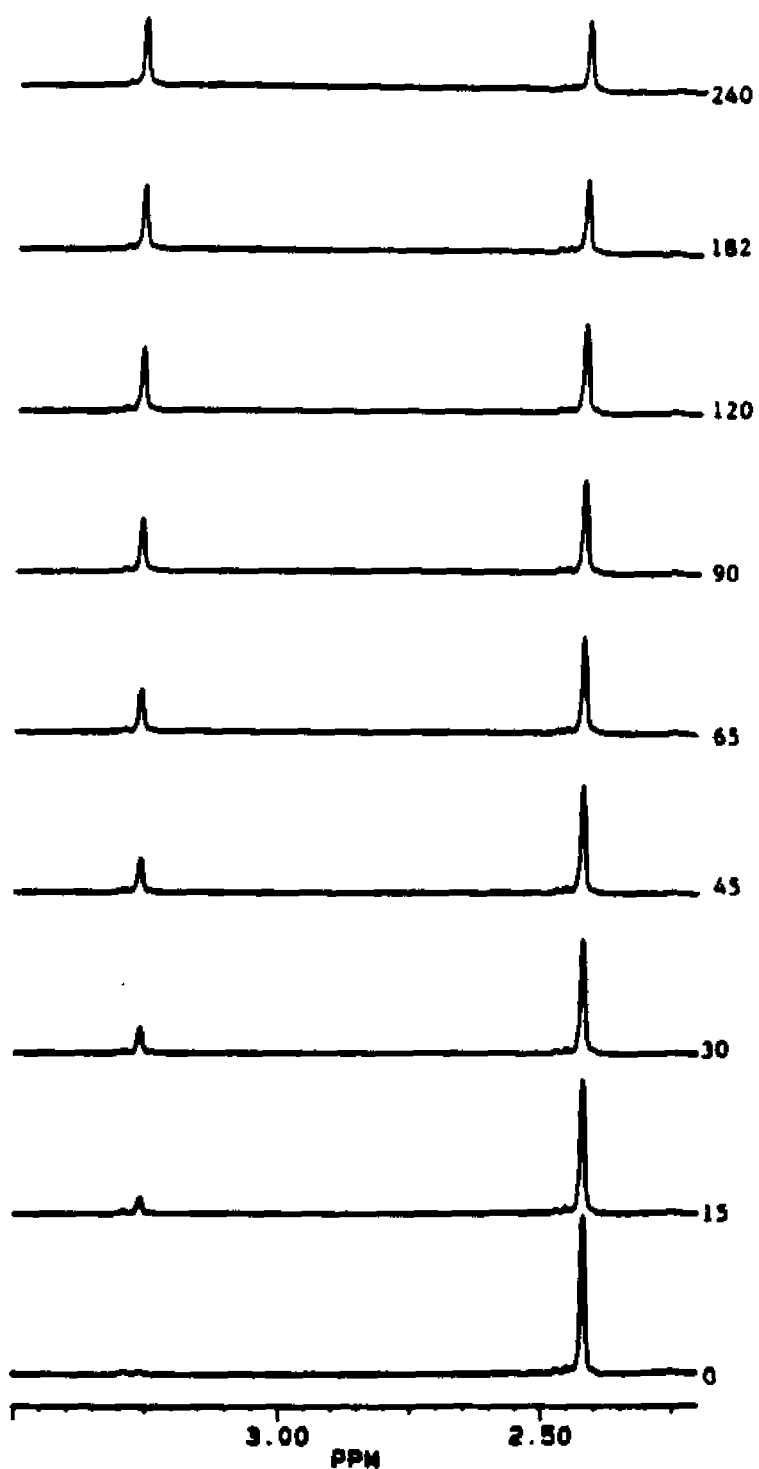


Figure 1.3 Stacked plots showing the equilibration of the stereoisomers of 23 at 85.1°C with time (minutes).

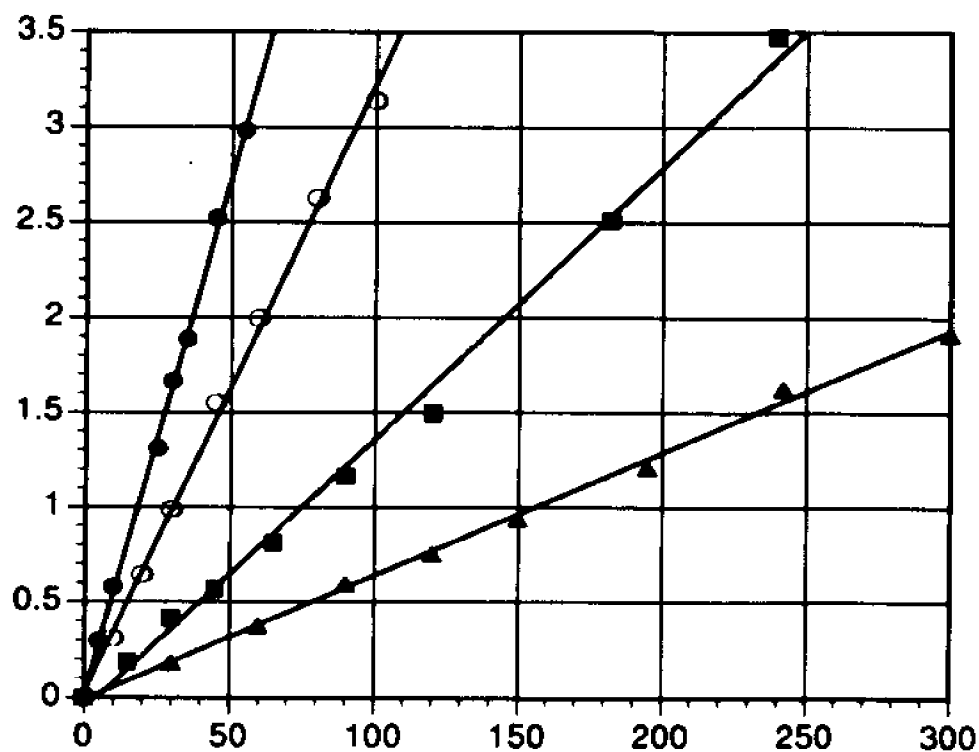


Figure 1.4 Plot of $\log(a/a-2x)$ vs. time (min)

The rate constants for different temperatures are obtained by plotting $\log(a/a-2x)$ vs. time (min) (Figure 1.4). The Free energy of activation (barrier for the ring inversion) is obtained from the Eyring equation:²⁹

$$k = K \frac{k_B T}{h} \exp(-\Delta G^\ddagger / RT)$$

k = rate constant

K = transmission coefficient (usually taken as unity)

k_B = Boltzmann constant = $3.29986 \cdot 10^{-24}$ cal k^{-1}

h = Planck's constant = $1.58369 \cdot 10^{-34}$ cal s

R = Universal gas constant = 1.98719 cal mol k^{-1}

The results are summarized in Table 1.2.

Table 1.2 Rates constants, half-life times and free energy of activation of the stereoisomers of **23** by ^1H NMR experiment.

$T(^{\circ}\text{C})$	$k_T(\text{s}^{-1})$	$t^{1/2}(\text{s})$	$\Delta G^{\#}(\text{kcal/mol})$
99.3	4.53×10^{-4}	770	27.67
94.0	2.67×10^{-4}	1283	27.65
85.1	1.19×10^{-4}	2888	27.59
78.9	5.04×10^{-5}	6876	27.65
52.1	1.91×10^{-6}	181,300	27.61

The ring inversion barrier of 27.6 Kcal/mol measured by this method is more than two times higher than that of corannulene and shows good agreement with the estimation from the spin polarization transfer method. Also, Table 1.2 shows very little free energy of activation ($\Delta G^{\#}$) dependence with temperature which means that the contribution of the entropy term to $\Delta G^{\#}$ is small.

1.2.3 Crystal structure of cyclopentenocorannulene

Slow crystallization of **16** from diethyl ether provided orange plates which were subjected to X-ray crystallographic analysis. A most interesting property of **16** is its crystal packing. While convex-concave stacking may be expected for the minimum energy arrangement of two bowl-shaped molecules, since it maximizes attractive Van der Waals interactions, this arrangement is not observed for corannulene where very little bowl stacking is detected.³⁰ In contrast, cyclopentacorannulene exhibits a high degree of long-range stacking in the solid state as shown in Figure 1.5.³¹

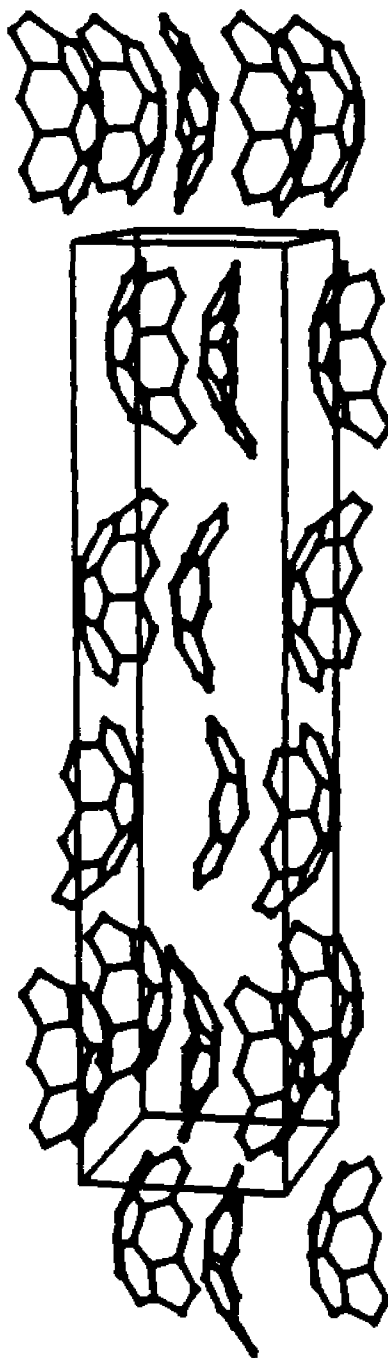


Figure 1.5 Stacked bowls of cyclopentacorannulene (16)

The structure of **16** is also interesting since it is the smallest fullerene related curved aromatic that, unlike corannulene, incorporates the pyracylene unit which is thought to be responsible for some of the chemistry of buckminsterfullerene.⁴ The five-membered ring "pulls" the corannulene system a little tighter resulting in a deeper bowl as indicated by the distance between the central five-membered ring and the rim aromatic carbons (Figure 1.6).

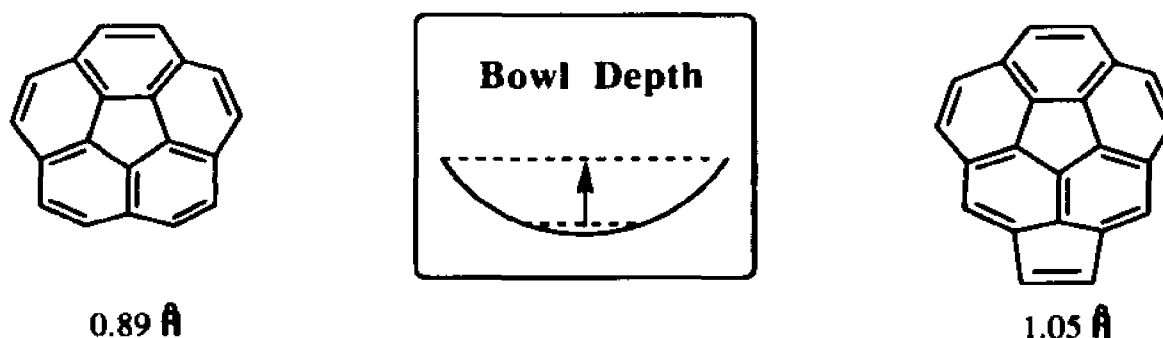


Figure 1.6 Bowl depth from X-ray diffraction as measured from the rim aromatic carbons to the best plane containing the central five-membered ring.

1.3. Conclusions

Cyclopentacorannulene was synthesized by the Scott et al. procedure for the synthesis of corannulene itself except that the starting material was 1,2-diketopyracene (**11**). The introduction of one fused, five-membered ring onto the corannulene structure is enough to effectively lock the bowl geometry of the molecule. While the barrier for the ring inversion of corannulene estimated from its derivatives is about 10 to 11 Kcal/mol (Table 1.1), the barrier for the ring inversion of the dideuterated

derivative of cyclopentacorannulene (23) is determined to be 27.6 Kcal/mol, more than twice as large. The solid state of the unsaturated cyclopentenocorannulene (16) exhibits a unique bowl stacking pattern which is not seen in the solid state of corannulene.

1.4 Experimental.

1.4.1 Materials and Methods.

Materials were obtained from commercial sources and used without further purification except for acenaphthene which was recrystallized from ethanol, and N-bromosuccinimide, recrystallized from water. $[\text{Rh}(\text{NBD})(\text{PPh}_3)_2]^+\text{BF}_4^-$ was kindly provided by Dr George G. Stanley. All reactions were performed under nitrogen atmosphere. NMR spectra were recorded with either a Bruker AC-200, AC-250 or AMX-400, using CDCl_3 as solvent unless noted otherwise. Proton chemical shifts are expressed in parts per million (ppm) downfield from internal tetramethylsilane (TMS), and coupling constants are reported in Hertz (Hz). ^{13}C chemical shifts are also expressed in ppm using residual solvent signals to scale TMS at zero. GC/MS were run on a Hewlett Packard 5971 mass spectrometer. High resolution mass spectrometry was done by the Midwest Center for Mass Spectrometry at the University of Nebraska-Lincoln, NE, and by the Mass Spectrometry Facility at Louisiana State University. Elemental analyses were performed by Oneida Research Services, Inc.. Melting points were determined using a MEL-TEMP II capillary melting point apparatus and are reported uncorrected. The silica gel used for chromatography was 60 Å (200-400 mesh) silica gel from Aldrich Chemical Company.

The Flash Vacuum Pyrolysis apparatus (Figure 1.7) was purchased from Kontes Glass, Inc.. The general pyrolysis procedure is as follow: the sample is dissolved in dichloromethane and transferred to a small glass boat filled with glass wool. The solvent is evaporated, and the boat placed in the inlet chamber wrapped with a heating mantle which allows sublimation of the substrate under vacuum and small flow of nitrogen. The pyrolysis product condenses on the side arm of the quartz tube cooled with dry ice and acetone.

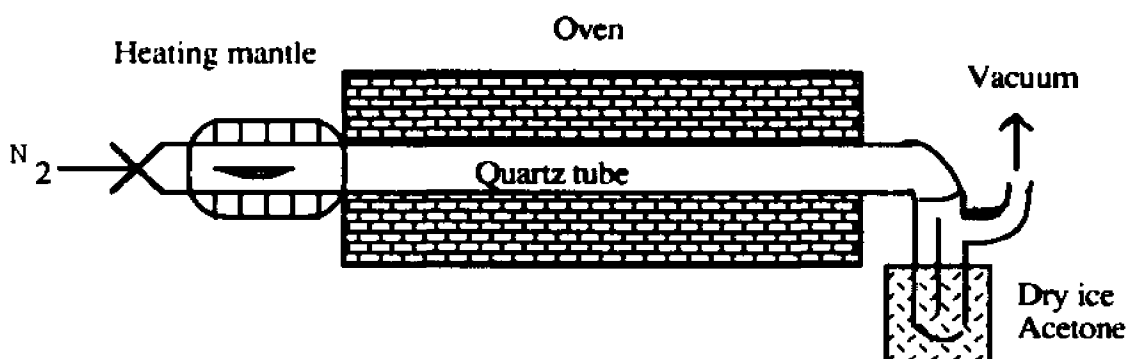
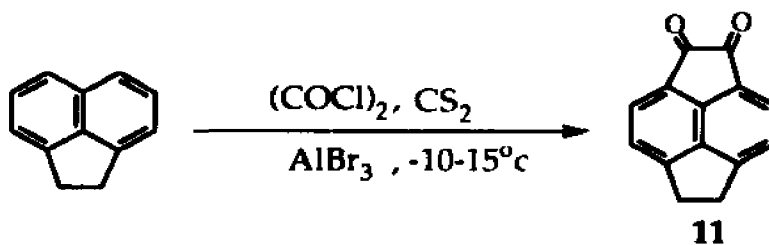


Figure 1.7 Flash vacuum pyrolysis apparatus.

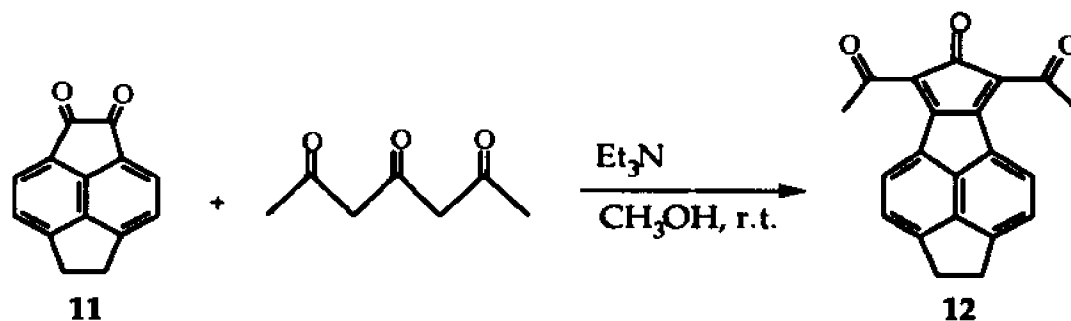
1.4.2 Synthesis of 5,6-dihydrocyclopent[*f,g*]acenaphthylene 1,2-dione, (11).²⁴



A solution of 20 g (0.13 mol) acenaphthene in 400 mL of carbon disulfide in a 1000 mL three-neck round bottom flask equipped with a mechanical stirrer was cooled in a dry ice bath to -15 °C. Then 20 mL (0.23

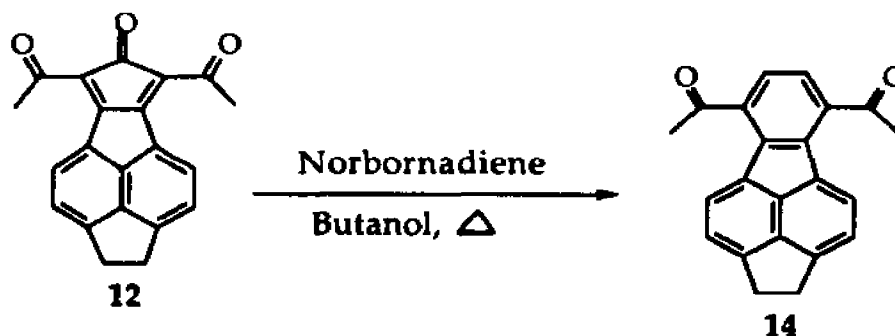
mol) of oxalyl chloride was added. The mixture was stirred vigorously and 72 g (0.27 mol) of powdered aluminum bromide was added over a period of 30 min, maintaining the temperature between -15° and -10° $^{\circ}\text{C}$. After the addition, the dry ice bath was removed and the mixture was stirred overnight (15 hrs) at room temperature. After the mixture was refluxed for 30 min, the carbon disulfide was decanted and the remaining black gum was treated with 1L of cold 10% aqueous hydrochloric acid and stirred for 30 min. The dark brown solid was filtered and thoroughly washed with water. The mixture was suspended in 800 mL of 10% aqueous sodium bisulfite and heated to 80°C for one hour. While hot, it was filtered and the filtrate was warmed to 80°C and acidified with concentrated hydrochloric acid. A fluffy yellow solid formed and was collected. This extraction process was repeated five times on the dark brown solid to yield 6.4 g (23.9% yield). Recrystallization from dimethylformamide gave 5.5 g (20.5% yield) of compound **11** as a yellow solid; mp $304\text{--}306^{\circ}\text{C}$ [Lit.²⁴: $305\text{--}306^{\circ}\text{C}$]; ^1H NMR (CDCl_3 , 200 MHz): δ 7.99 (d, $J=7.4$ Hz, 2H), 7.58 (d, $J=7.4$ Hz, 2H), 3.65 (s, 4H); GC/MS, m/z (relative intensity): 208 (58, M^+), 180 (100), 152 (80).

1.4.3 Synthesis of 5,7-diacetyl-1,2-dihydro-6H-dicyclopent[*a*,*fg*]-acenaphthylen-6-one, (12).



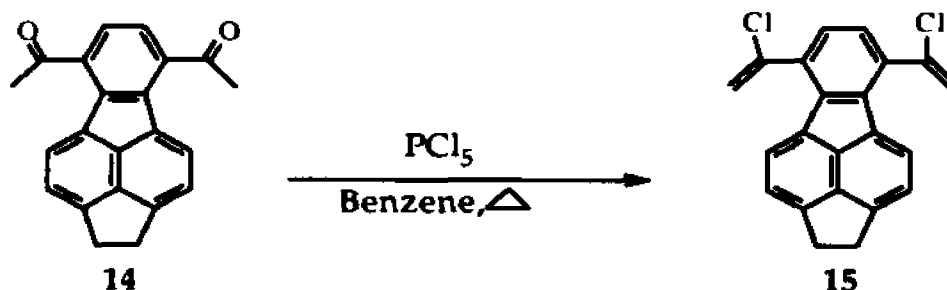
A solution of 5.8 mL (41.7 mmol) triethylamine in 20 mL of methanol was added dropwise, through a dropping funnel, to a stirred solution of 5.9 g (28.4 mmol) 1,2-diketopyracene (11) and 6.8 g (47.5 mmol) 2,4,6-heptanetrione³² in 50 mL of methanol. The mixture was stirred overnight, filtered and the dark-silver solid washed with methanol. After drying 3.56 g (40% yield) was obtained which was used without further purification. Dissolving in hot DMF, cooling and filtration gave a dark solid (12): 235-240 °C (decomp.); ¹H NMR (CDCl₃, 200 MHz): δ 8.6 (d, *J* = 7.4 Hz, 2H), 7.49 (d, *J* = 7.4 Hz, 2H), 3.58 (s, 4H), 2.64 (s, 6H); Exact mass measurement calculated for C₂₁H₁₄O₃: 314.0942, found: 314.0933.

1.4.4 Synthesis of 1,1'-(1,2-dihydrocyclopenta[cd]fluoranthene-5,8-diyl)bis-ethanone, (14).



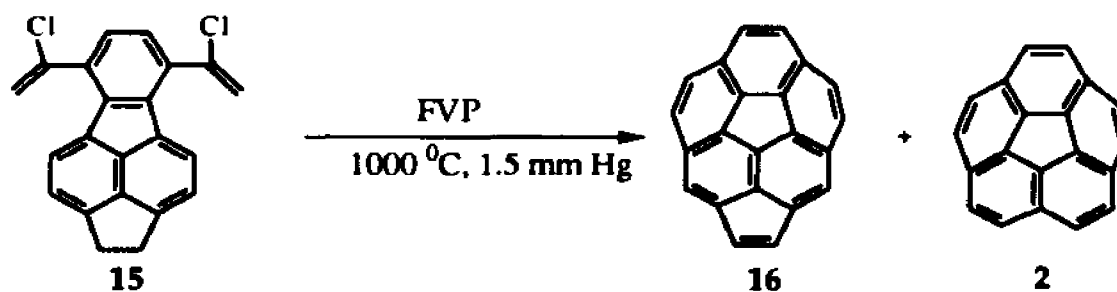
A solution of 8.6 g (28.34 mmol) of crude **12**, and 5.2 mL (48.18 mmol) of bicyclo[2.2.1]hepta-2,5-diene in 150 mL of n-butanol was refluxed overnight. After cooling, the brown solid was filtered and chromatographed on silica gel with hexane/ethyl acetate (10:1 then 5:1) or DCM to provide 5.6 g (yield: 64 %) of a yellowish product (**14**); mp 249-250 °C; ^1H NMR (CDCl_3 , 250 MHz): δ 8.49 (d, J = 7.5 Hz, 2H), 7.7 (s, 2H), 7.48 (d, J = 7.5 Hz, 2H), 3.53 (s, 4H), 2.8 (s, 6H); ^{13}C NMR (CDCl_3 , 50 MHz): δ 29.69, 32.27, 120.91, 126.03, 128.53, 129.43, 132.04, 136.31, 137.44, 138.86, 148.17, 201.45; GC/MS, m/z (relative intensity): 312 (100, M^+), 297 (100), 269 (24), 254 (19), 226 (42); analysis: calculated for $\text{C}_{22}\text{H}_{16}\text{O}_2$: C, 84.59; H, 5.16; O, 10.25. Found: C, 83.89; H, 5.13; O, 10.98. HRMS calculated for $\text{C}_{22}\text{H}_{16}\text{O}_2$: 312.1150, found: 312.1152.

1.4.5 Synthesis of 5,8-bis(1-chloroethenyl)-1,2-dihydrocyclopenta[*cd*]fluoranthene, (15).



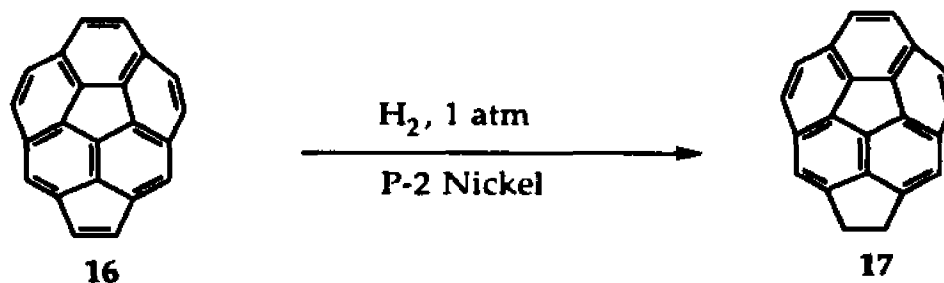
1.08 g (3.46 mmol) of **14** and 2.52 g (12.11 mmol) of PCl_5 in 40 mL of benzene was refluxed for 3 hours. After cooling, the mixture was poured onto ice and the organic layer was washed with water and sodium carbonate solution, dried over anhydrous magnesium sulfate and the solvent evaporated. After purification by column chromatography on silica gel with cyclohexane as eluant, 0.6 g of a yellow solid (**15**) was obtained (50% yield); mp 144-146 °C; ^1H NMR (CDCl_3 , 250 MHz): δ 8.3 (d, 2H, $J = 7$ Hz), 7.46 (d, 2H, $J = 7$ Hz), 7.37 (s, 2H), 5.92 (d, 2H, $J = 1.2$ Hz), 5.8 (d, 2H, $J = 1.2$ Hz), 3.51 (s, 4H); ^{13}C NMR (CDCl_3 , 250 MHz): δ 32.27, 117.02, 120.88, 126.18, 127.07, 130.14, 131.32, 135.34, 136.39, 137.31, 138.30, 147.01; GC/MS, m/z (relative intensity): 350 (44), 348 (69), M^+ , 313 (42), 276 (100), 263 (15), 250 (57), 138 (69); HRMS calculated for $\text{C}_{22}\text{H}_{14}\text{Cl}_2$: 348.0456, found: 348.0457.

1.4.6 Flash vacuum pyrolysis of 5,8-bis(1-chloroethenyl)-1,2-dihydrocyclopenta[*cd*]fluoranthene, (15).



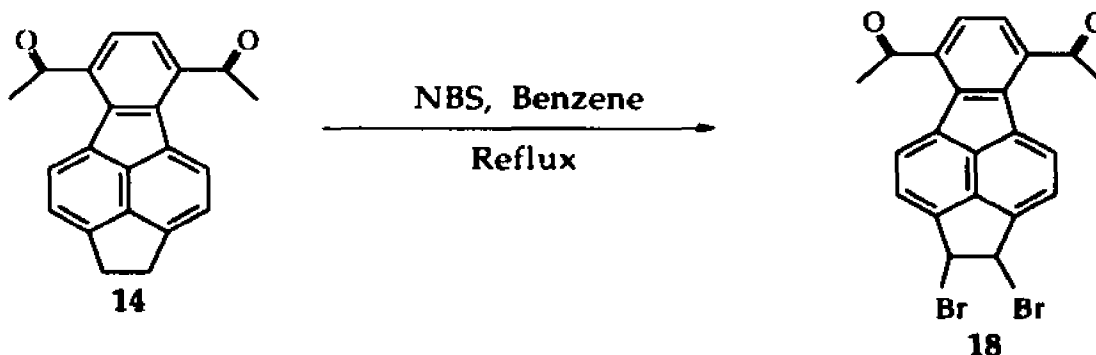
A 985 mg sample of **15** was pyrolyzed in batches of 80 mg each at 1000 °C under a slow bleed of nitrogen and 1.5 mm Hg of pressure as described in section 1.4.1. After each run (3 hrs) the pyrolysis product was washed out of the trap and the elbow with DCM and combined. The solvent was evaporated and the crude material flash chromatographed with silica gel and hexane as eluant to give a mixture of **16** and **2** (7:3, by GC/MS). Yields varied from 10 to 15%. Compound (**16**): ^1H NMR (CDCl_3 , 200.13 MHz): δ 6.49 (s, 2H), 7.31 (s, 2H), 7.38 (s, 2H), 7.44 (d, 2H, $J = 9$ Hz), 7.50 (d, 2H, $J = 9$ Hz); ^{13}C NMR (CDCl_3 , 100.614 MHz): δ 124.17, 126.46, 127.26, 128.28, 128.42, 129.73, 137.51, 137.89, 138.16; GC/MS, m/z (relative intensity): 274 (100, M^+), 272 (18), 137 (20), 136 (18). Slow crystallization from diethyl ether gave orange pellets. Crystal data and collection parameters are given in Table 1.3.

1.4.7 Selective hydrogenation of dibenzo[ghi, mno]cyclopenta[cd]-fluoranthene, (16).



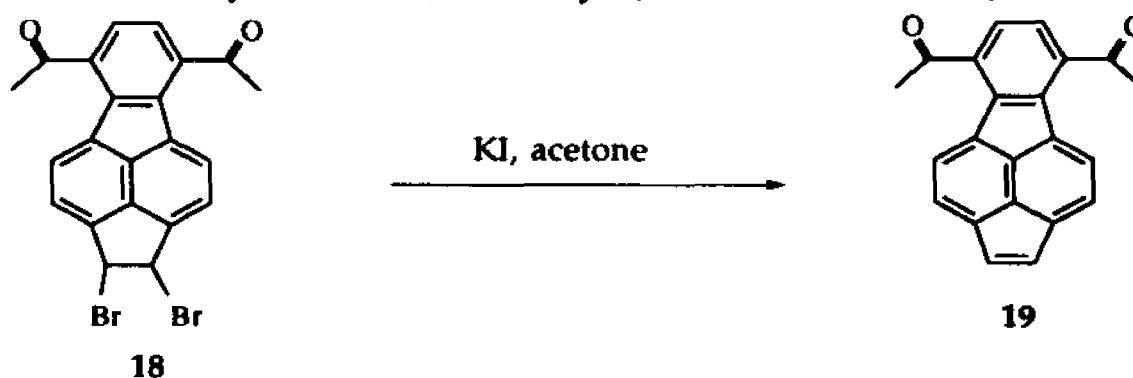
In a 50 mL three-neck round bottom flash equipped with a magnetic stirrer, 0.07 g (0.29 mmol) of nickel acetate tetrahydrate was dissolved in 3 mL of 95% ethanol. The system was purged and filled with hydrogen three times. 0.3 mL of a solution of sodium borohydride (0.25 g of NaBH_4 , 6 mL of 95% ethanol and 0.31 mL of a solution of 2N sodium hydroxide) was added, followed by the sample (16, 3 mg) dissolved in 1 mL of DCM, rinsed with another mL, and finally with 3 mL of ethanol 95%. The mixture was allowed to react for fifteen minutes. The solution was then filtered through a celite pad using DCM as solvent and evaporated. The residue was passed through a chromatographic column with silica gel and hexane as eluant. The reaction was quantitative by GC. Compound (17): ^1H NMR (CDCl_3 , 200.13 MHz): δ 2.98, 3.39 (4H), 7.34 (s, 2H), 7.70 (s, 4H), 7.72 (s, 2H); ^{13}C NMR (CDCl_3 , 100.614 MHz): δ 31.83, 121.74, 126.32, 126.96, 127.68, 130.31, 137.19, 137.53, 138.71, 139.41, 145.04, 147.51. GC/MS, m/z (relative intensity): 276 (100, M^+), 275 (21), 274 (34), 138 (27), 137 (32), 136 (18); HRMS: calculated for $\text{C}_{22}\text{H}_{12}$: 276.0939, found: 276.0937.

1.4.8 Synthesis of 7,10-diacetyl-3,4-(1,2-dibromoethano)-fluoranthene, (18).



2.52 g (8 mmol) of **14**, 3.02 g (16.96 mmol) of NBS and traces of benzoyl peroxide in 120 ml of benzene were refluxed for 6 hours. After cooling the mixture, the solvent was evaporated and the residue taken in DCM and washed with water. The solution was dried with anhydrous magnesium sulfate, and the solvent evaporated. Chromatography on silica gel with DCM as eluant gave 1.66 g (43% yield) of the dibrominated product (**18**); ^1H NMR (CDCl_3 , 250 MHz): δ 8.6 (d, $J=7.2$ Hz, 2H), 7.8 (s, 2H), 7.7 (d, $J=7.2$ Hz, 2H), 6 (s, 2H), 2.8 (s, 6H); ^{13}C NMR (CDCl_3 , 50 MHz): δ 29.8, 55.7, 124, 127, 127.4, 127.5, 129.8, 133.1, 138.2, 139.5, 142, 201.

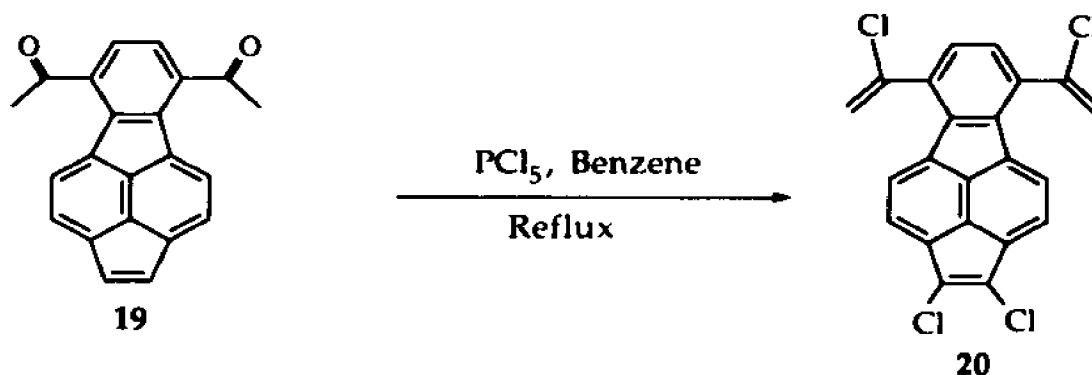
1.4.9 Synthesis of 7,10-diacetyl-3,4-ethenofluoranthene, (19).



In a nitrogen atmosphere, 1.66 g (3.5 mmol) of the dibromo compound (**18**) dissolved in 103 ml of acetone was treated with 7.73 g

(46.56 mmol) of anhydrous potassium iodide. After 20 hrs of refluxing, the mixture was cooled and poured into cold aqueous sodium thiosulfate. The aqueous mixture was extracted with DCM and dried. Evaporation of the solvent and chromatography on silica gel with DCM gave 0.84 g (77% yield) of a red solid (**19**); ^1H NMR (CDCl_3 , 250 MHz): δ 7.71 (d, $J=7.25$ Hz, 2H), 7.3 (s, 2H) 7.1 (d, $J=7.25$ Hz, 2H), 6.5 (s, 2H), 2.64 (s, 6H); ^{13}C NMR (CDCl_3 , 50 MHz): δ 29.56, 123.8, 125.9, 127.78, 128.16, 130, 132.54, 133.78, 135.88, 138.1, 142.33, 200.01. GC/MS, m/z (relative intensity): 310 (100, M^+), 295 (72), 267 (28), 224 (39). HRMS calculated for $\text{C}_{22}\text{H}_{14}\text{O}_2$: 310.0993, found: 310.0995

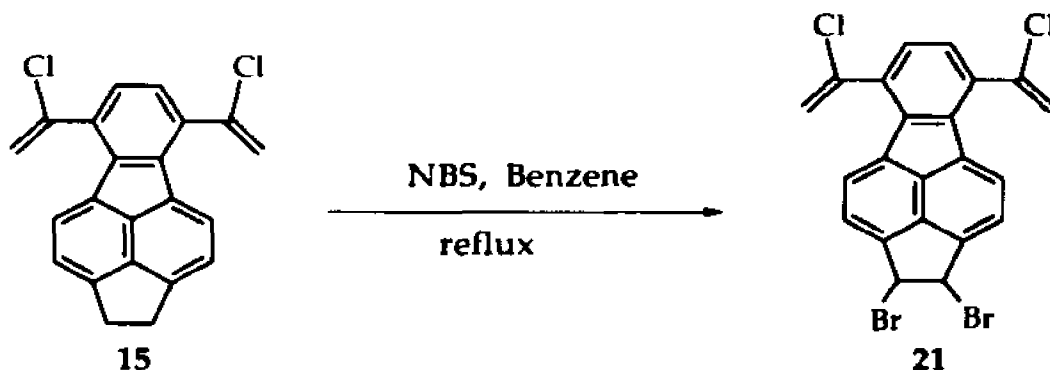
1.4.10 Attempted synthesis of 7,10-di-(1-chloroethenyl)-3,4-ethenofluoranthene (22**) from 7,10-diacetyl-3,4-ethenofluoranthene, (**19**).**



1.08 g (3.46 mmol) of **19** and 2.52 g (12.11 mmol) of PCl_5 in 40 mL of benzene was refluxed for 3 hours. After that time the mixture was cooled, poured onto ice, and then the organic layer was washed with a saturated solution of sodium carbonate and water. After drying with MgSO_4 and evaporating the solvent, it was purified by column chromatography on silica gel with hexane as eluant. GC/MS analysis showed a mixture of polychlorinated products, the major product being compound (**20**). The

reaction was repeated, this time adding a large excess of PCl_3 (8.5 g; 60.55 mmol) in order to decrease the concentration of chlorine, but the same results were obtained. Compound (20): ^1H NMR (CDCl_3 , 250 MHz): δ 7.51 (d, 2H, $J = 6.9$ Hz), 7.10 (d, 2H, $J = 6.9$ Hz), 7.03 (s, 1H), 5.78 (d, 2H, $J = 1.6$ Hz), 5.64 (d, 2H, $J = 1.6$ Hz). ^{13}C NMR (CDCl_3 , 50 MHz): δ 29.93, 117.54, 124.2, 125.55, 129.67, 131.17, 132.46, 136.43, 136.80, 137.24, 137.73, 139.88. GC/MS, m/z (relative intensity): 416 (88), 414 (68, M^+), 344 (77), 308 (59), 274 (100). HRMS calculated for $\text{C}_{22}\text{H}_{10}\text{Cl}_2$: 413.9536 found: 413.9475

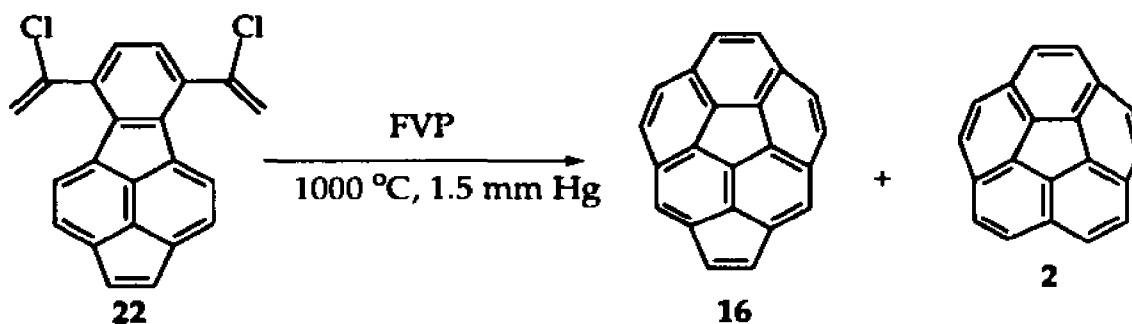
1.4.11 Synthesis of 7,10-di(1-chloroethenyl)-3,4-(dibromoethano)-fluoranthene, (21).



In a 50 mL round bottom flask equipped with a magnetic stirrer, 428 mg (1.23 mmol) of **15**, 490 mg (2.75 mmol) of NBS and traces of benzoyl peroxide in 20 mL of benzene were refluxed for 6 hours. After cooling the mixture, the solvent was evaporated and the residue taken in DCM and washed with water. The solution was dried with anhydrous magnesium sulfate, and the solvent evaporated. Chromatography on silica gel with DCM/hexane (10:1) as eluant gave 300 mg of **21** (yield: 57%). ^1H NMR (CDCl_3 , 250 MHz): δ 8.34 (d, 2H, $J = 7.5$ Hz), 7.66 (d, 2H, $J = 7.5$ Hz), 7.36 (s,

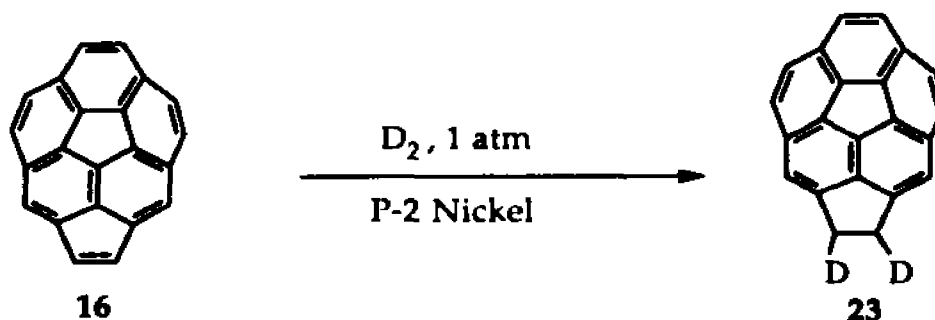
A solution of 224 mg (0.53 mmol) of **21** and 1.1 g (7 mmol) of potassium iodide in 30 mL of acetone was refluxed overnight (20 hrs). After cooling, the mixture was filtered and the residue washed with acetone. The filtrate and the washings were combined and the solvent evaporated (rotavapor). Chromatography on silica gel with hexane as eluant gave 89 mg (49% yield) of **22** as a reddish solid which decomposes over 220 °C. ¹H NMR (CDCl₃, 250 MHz): δ 5.65 (d, 2H, J= 1.33 Hz), 5.76 (d, 2H, J= 1.33 Hz), 6.52 (s, 2H), 7.11 (d, 2H, J= 7.25 Hz), 7.51 (d, 2H, J=7.25 Hz); ¹³C NMR (CDCl₃, 62.89 MHz): δ 29.92, 117.29, 125.42, 125.88, 129.08, 132.21, 136.37, 137.58, 141.53. GC/MS, m/z (relative intensity): 348 (29), 346 (44, M⁺) 311 (23), 276 (56), 275 (51), 274 (60), 250 (16), 155 (18), 137 (100), 124 (32). HRMS calculated for C₂₂H₁₂Cl₂: 346.0316 found: 346.0305

1.4.13 Flash vacuum Pyrolysis of 7,10-di(1-chloroethenyl)-3,4-ethenofluoranthene, (22).



A 247 mg sample of (22) was pyrolyzed in three batches at 1000 °C under a slowbleed of nitrogen and 1.5 mm Hg of pressure as described in section 1.4.1. After each run (3 hrs) the pyrolysis product was washed out of the trap and the elbow with DCM and combined. The solvent was evaporated and the crude material flash chromatographed on silica gel with hexane as eluant to yield 13 mg of a mixture of 16, 2 and unclosed products by GC/MS. Moreover, after each run the glass wool and the boat were recovered with tarry material suggesting that 22 polymerizes before reaching the oven.

1.4.14 Heterogeneous selective deuteration of dibenzo[ghi,mno]cyclopenta[cd]fluoranthene, (16).



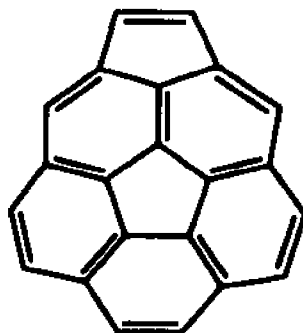
In a 50 mL three-neck round bottom flask equipped with a magnetic stirrer, 0.21 g (0.84 mmol) of nickel acetate tetrahydrate was dissolved in 9 mL of 95% ethanol. The system was purged and filled with deuterium (D_2 , 99.6% and HD, 0.4%; from Cambridge Isotope Laboratories) three times. 0.9 mL of a solution of sodium borodeuteride (0.75 g of $NaBD_4$, 18 mL of 95% ethanol and 0.93 mL of a solution of 2N sodium hydroxide) was added, followed by the sample (10 mg) dissolved in 6 mL of DCM, rinsed with another 3 mL and finally with 9 mL of ethanol 95%. The mixture was allowed to react for fifteen minutes. Afterwards the solution was filtered through a celite pad using DCM as solvent. The filtrate was evaporated and passed through a chromatographic column on silica gel with hexane as eluant. 8 mg of a yellow product (**23**) was obtained : 1H NMR ($CDCl_3$, 250 MHz): δ 2.95 (s, 2H), 7.34 (s, 2H), 7.70 (s, 4H), 7.72 (s, 2H). 1H NMR after equilibration ($DMSO-d_6$, 250 MHz): δ 2.94 (s, 2H), 3.71 (s, 2H), 7.49 (s, 2H), 7.83 (s, 4H), 7.85 (s, 2H). 1H NMR after equilibration ($Benzene-d_6$, 250 MHz): δ 2.42 (s, 2H), 3.26 (s, 2H), 7.00 (s, 2H), 7.48 (s, 4H), 7.51 (s, 2H). ^{13}C NMR ($CDCl_3$, 62.9 MHz): δ 31.43 (t, $J = 20$ Hz; DEPT 90 and 135 showed a minor peak of a CH_2 group suggesting that the sample contained traces of the monodeuterated product; probably a side product from HD contained in D_2), 121.79, 126.32, 126.94, 127.68, 130.31, 137.19, 137.53, 138.71, 139.41, 145.04, 147.51. GC/MS, m/z (relative intensity): 278 (100, M^+), 277 (67), 276 (37), 275 (24), 139 (45) 138 (54), 137 (53), 136 (18), 125 (20).

1.4.15 Homogeneous selective deuteration of dibenzo[ghi, mno]-cyclopenta[cd]fluoranthene, (16).

In a 25 ml round bottom flask, 60 mg (0.074 mmol) of $[\text{Rh}(\text{NBD})(\text{PPh}_3)_2]^+\text{BF}_4^-$ in 10 mL of dry THF was flushed with deuterium gas three times. The orange color of the solution faded in a few seconds. The solution was stirred vigorously at room temperature and at constant pressure (1 atm) for ten minutes. 20 mg (0.073 mmol) of 16 in 2 mL of THF was injected into the solution, and the reaction stirred for one hour. The solvent was removed (rotavapor) and the black residue chromatographed on silica gel with hexane to give 15 mg of the dideuterated product (23). ^1H NMR Showed identical spectrum to that obtain with the heterogeneous catalysis experiment (section 1.4.14)

1.4.16 Kinetic measurements of the equilibration of the stereo isomers of 23.

Five NMR tubes each containing approximately 4 mg of 23 in 0.5 mL of deuterated benzene were degassed and sealed under vacuum. The samples were kept in the freezer before studying the kinetics of the equilibration of the two stereoisomers at a given temperature. In a typical procedure, the sample is taken out from the freezer, warmed up to room temperature and immersed in a thermostat calibrated at 0.1 °C for a determined time, then frozen with a dry ice-acetone bath. The spectra were taken at room temperature with a 400 MHz ^1H NMR with the same parameters (relaxation time: 20 s, number of scans: 32 and receiver gain: 512).

Table 1.3 Crystal data and collection parameters for **16**.

Compound: CPC

Formula: C₂₂ H₁₀

FW: 274.3

F₀₀₀: 1136

Space Group: Pbca

Radiation: CuK α

Z: 8

a: 9.441(2)Å

b: 7.593(2)Å

c: 36.081(5)Å

 α : 90° β : 90° γ : 90°V: 2587(2)Å³D_c: 1.409 g cm⁻³D_m:m: 5.7 cm⁻¹

T: 23° C

 θ Limits: 2-75°R_{int}:

Max. Transm:

Av. Transm:

Min. Transm:

Xtal Size: 0.03x0.25x0.67mm

Color: Orange plate

Max. Decay:

Av. Decay:

Min. Decay:

R(obs. data): 0.055

R(all data): 0.084

R_w: 0.068

Unique Data: 2660

Obs Data: 1807

GOF: 2.695 Cutoff: I>3 σ (I)Max. Shift: <0.01 σ

Variables: 200

Fudge: 0.02

Max. Residual: 0.20 eÅ⁻³ Min. Residual: -0.21 eÅ⁻³ Extinction: 4.8(6)x10⁻⁷

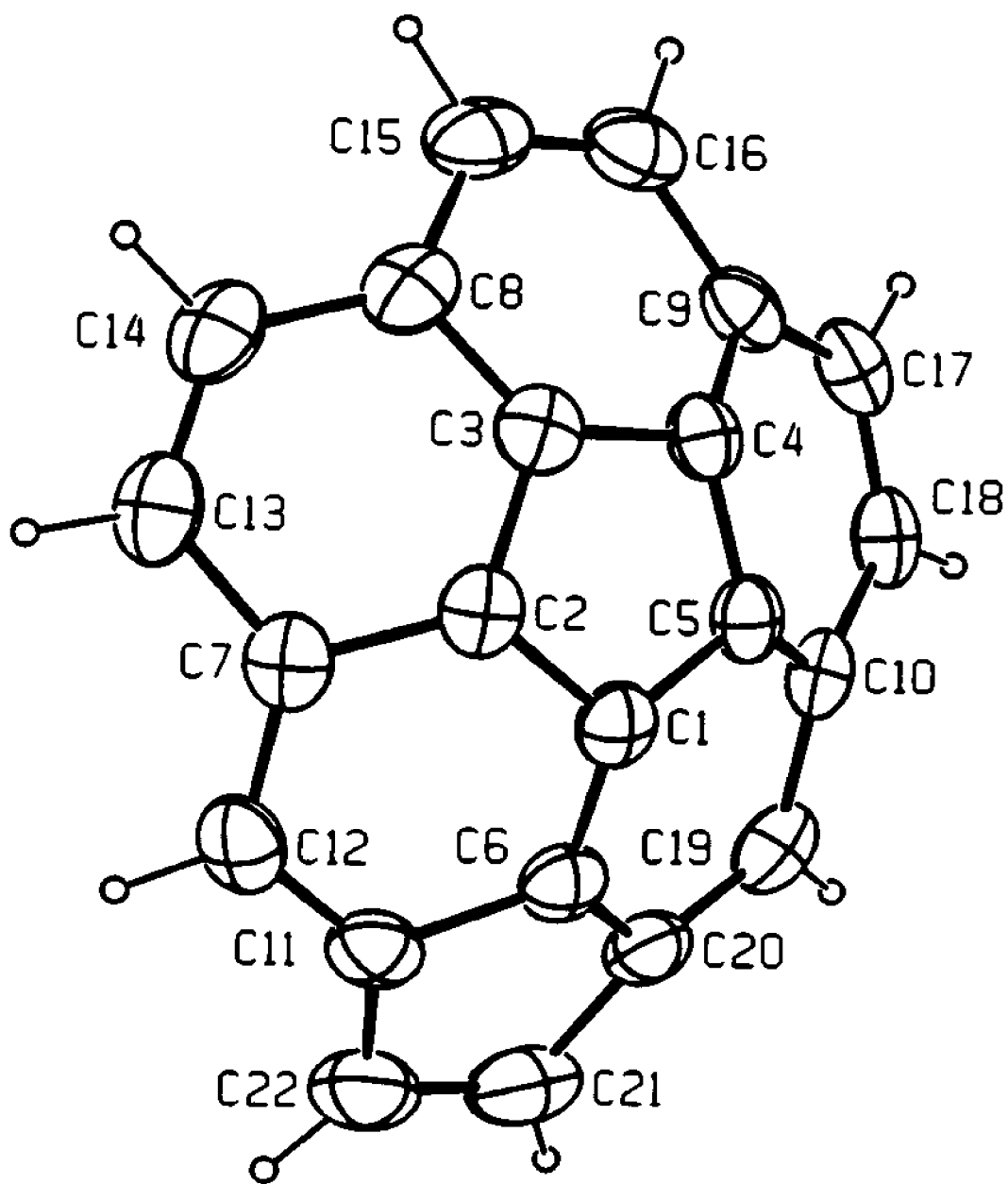


Figure 1.8 ORTEP drawing of cyclopentacorannulene (17).

Table 1.4 Coordinates and equivalent isotropic thermal parameters for 16.

atom	x	y	z	Beq(Å ²)
C1	0.5402(3)	0.5452(3)	0.14607(7)	3.39(6)
C2	0.4699(3)	0.5104(4)	0.11222(8)	3.45(6)
C3	0.5721(3)	0.5270(3)	0.08370(7)	3.55(6)
C4	0.7057(3)	0.5679(3)	0.10043(7)	3.31(5)
C5	0.6852(3)	0.5751(3)	0.13933(7)	3.28(5)
C6	0.4988(3)	0.4632(4)	0.17726(7)	3.71(6)
C7	0.3564(3)	0.3954(4)	0.11006(8)	3.83(6)
C8	0.5603(3)	0.4380(4)	0.05068(7)	4.02(6)
C9	0.8312(3)	0.5174(4)	0.08491(8)	3.79(6)
C10	0.7876(3)	0.5223(4)	0.16423(8)	3.67(6)
C11	0.3751(3)	0.3553(4)	0.17735(8)	4.04(6)
C12	0.3048(3)	0.3243(4)	0.14473(9)	4.27(7)
C13	0.3333(3)	0.3256(4)	0.07354(8)	4.64(7)
C14	0.4298(3)	0.3465(4)	0.04544(8)	4.64(7)
C15	0.6936(4)	0.4162(4)	0.03112(8)	4.76(7)
C16	0.8214(3)	0.4534(4)	0.04716(8)	4.66(7)
C17	0.9463(3)	0.4993(4)	0.11055(9)	4.29(7)
C18	0.9253(3)	0.4995(4)	0.14815(8)	4.13(6)
C19	0.7393(4)	0.4513(4)	0.19949(7)	4.36(7)
C20	0.5975(3)	0.4201(4)	0.20535(7)	4.09(6)
C21	0.5184(4)	0.2965(5)	0.22863(8)	5.79(9)
C22	0.3881(4)	0.2594(5)	0.21259(9)	5.74(8)

Table 1.5 Bond distances in angstroms for 16.

atom 1	atom 2	distance	atom 1	atom2	distance
C1	C2	1.415(4)	C8	C14	1.427(4)
C1	C5	1.408(4)	C8	C15	1.452(4)
C1	C6	1.344(4)	C9	C16	1.449(4)
C2	C3	1.416(4)	C9	C17	1.434(4)
C2	C7	1.385(4)	C10	C18	1.434(4)
C3	C4	1.432(4)	C10	C19	1.455(4)
C3	C8	1.374(4)	C11	C12	1.372(4)
C4	C5	1.418(4)	C11	C22	1.470(4)

(Table con'd.)

C4	C9	1.365(4)	C13	C14	1.373(4)
C5	C10	1.380(4)	C15	C16	1.368(5)
C6	C11	1.427(4)	C17	C18	1.371(4)
C6	C20	1.416(4)	C19	C20	1.375(5)
C7	C12	1.447(4)	C20	C21	1.464(5)
C7	C13	1.437(4)	C21	C22	1.388(5)

Table 1.6 Coordinates assigned to hydrogen atoms for 16.

atom	x	y	z	B _{iso} (Å ²)
H12	0.2209	0.2551	0.1448	5
H13	0.2482	0.2628	0.0686	6
H14	0.4091	0.2984	0.0217	6
H15	0.6919	0.3745	0.0062	6
H16	0.9057	0.4369	0.0332	6
H17	1.0398	0.4868	0.1012	5
H18	1.0044	0.4840	0.1640	5
H19	0.8058	0.4264	0.2185	5
H21	0.5514	0.2487	0.2513	7
H22	0.3181	0.1837	0.2228	7

Table 1.7 Bond angles in degrees for 16.

atom 1	atom 2	atom 3	angle	atom 1	atom 2	atom 3	angle
C2	C1	C5	109.7(2)	C14	C8	C15	128.9(3)
C2	C1	C6	120.0(3)	C4	C9	C16	115.1(3)
C5	C1	C6	120.2(3)	C4	C9	C17	114.8(3)
C1	C2	C3	106.9(2)	C16	C9	C17	128.5(3)
C1	C2	C7	122.0(3)	C5	C10	C18	114.0(2)
C3	C2	C7	122.9(3)	C5	C10	C19	117.2(3)
C2	C3	C4	108.2(2)	C18	C10	C19	126.4(3)
C2	C3	C8	122.1(3)	C6	C11	C12	119.5(3)
C4	C3	C8	122.9(3)	C6	C11	C22	102.6(2)
C3	C4	C5	107.8(2)	C12	C11	C22	134.2(3)

(Table con'd.)

C3	C4	C9	122.0(2)	C7	C12	C11	121.0(3)
C5	C4	C9	122.4(2)	C7	C13	C14	122.3(3)
C1	C5	C4	107.3(2)	C8	C14	C13	122.1(3)
C1	C5	C10	121.4(2)	C8	C15	C16	122.3(3)
C4	C5	C10	122.5(2)	C9	C16	C15	121.6(3)
C1	C6	C11	120.4(3)	C9	C17	C18	121.9(3)
C1	C6	C20	121.0(3)	C10	C18	C17	122.1(3)
C11	C6	C20	113.9(2)	C10	C19	C20	120.2(3)
C2	C7	C12	116.6(3)	C6	C20	C19	119.4(3)
C2	C7	C13	113.7(3)	C6	C20	C21	102.9(3)
C12	C7	C13	127.1(3)	C19	C20	C21	134.0(3)
C3	C8	C14	115.1(3)	C20	C21	C22	110.0(3)
C3	C8	C15	114.0(3)	C11	C22	C21	109.5(3)

Table 1.8 Torsion angles in degrees for 16.

atom 1	atom 2	atom 3	atom 4	angle
C5	C1	C2	C3	-2.67 (0.30)
C5	C1	C2	C7	146.50 (0.27)
C6	C1	C2	C3	-147.95 (0.26)
C6	C1	C2	C7	1.22 (0.42)
C2	C1	C5	C4	2.91 (0.30)
C2	C1	C5	C10	-145.34 (0.26)
C6	C1	C5	C4	148.12 (0.26)
C6	C1	C5	C10	-0.13 (0.40)
C2	C1	C6	C11	-6.61 (0.42)
C2	C1	C6	C20	147.54 (0.28)
C5	C1	C6	C11	-148.27 (0.27)
C5	C1	C6	C20	5.87 (0.41)
C1	C2	C3	C4	1.38 (0.30)
C1	C2	C3	C8	153.20 (0.26)
C7	C2	C3	C4	-147.43 (0.27)
C7	C2	C3	C8	4.39 (0.43)
C1	C2	C7	C12	5.34 (0.41)
C1	C2	C7	C13	-157.74 (0.27)
C3	C2	C7	C12	149.61 (0.27)
C3	C2	C7	C13	-13.47 (0.40)

(Table con'd.)

C2	C3	C4	C5	0.38 (0.30)
C2	C3	C4	C9	150.10 (0.26)
C8	C3	C4	C5	-151.15 (0.26)
C8	C3	C4	C9	-1.42 (0.42)
C2	C3	C8	C14	7.67 (0.41)
C3	C4	C5	C1	-2.00 (0.29)
C3	C4	C5	C10	145.84 (0.26)
C9	C4	C5	C1	-151.59 (0.26)
C9	C4	C5	C10	-3.75 (0.41)
C3	C4	C9	C16	12.31 (0.39)
C3	C4	C9	C17	-154.73 (0.26)
C5	C4	C9	C16	157.66 (0.26)
C5	C4	C9	C17	-9.39 (0.39)
C1	C5	C10	C18	157.29 (0.26)
C1	C5	C10	C19	-6.37 (0.39)
C4	C5	C10	C18	13.84 (0.38)
C4	C5	C10	C19	-149.82 (0.26)
C1	C6	C11	C12	5.14 (0.44)
C1	C6	C11	C22	166.54 (0.28)
C20	C6	C11	C12	-150.72 (0.28)
C20	C6	C11	C22	10.68 (0.33)
C1	C6	C20	C21	-165.96 (0.28)
C11	C6	C20	C19	151.05 (0.28)
C11	C6	C20	C21	-10.24 (0.33)
C2	C7	C12	C11	-6.74 (0.43)
C13	C7	C12	C11	153.73 (0.30)
C2	C7	C13	C14	11.08 (0.44)
C12	C7	C13	C14	-149.87 (0.32)
C3	C8	C14	C13	-9.96 (0.44)
C15	C8	C14	C13	153.02 (0.32)
C3	C8	C15	C16	10.78 (0.44)
C14	C8	C15	C16	-152.34 (0.32)
C4	C9	C16	C15	-11.58 (0.42)
C17	C9	C16	C15	153.35 (0.32)
C4	C9	C17	C18	11.95 (0.41)
C16	C9	C17	C18	-153.01 (0.31)
C5	C10	C18	C17	150.73 (0.30)
C5	C10	C19	C20	7.45 (0.41)
C18	C10	C19	C20	-153.93 (0.30)
C6	C11	C12	C7	1.71 (0.44)
C22	C11	C12	C7	-152.53 (0.34)
C6	C11	C22	C21	-6.63 (0.36)
C12	C11	C22	C21	150.57 (0.35)

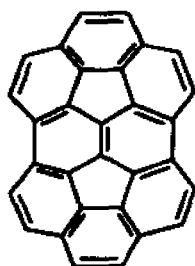
(Table con'd.)

C7	C13	C14	C8	0.46 (0.49)
C8	C15	C16	C9	-0.03 (0.57)
C9	C17	C18	C10	-1.64 (0.46)
C10	C19	C20	C6	-2.11 (0.43)
C10	C19	C20	C22	5.45 (0.36)
C19	C20	C21	C22	-151.68 (0.34)
C20	C21	C22	C11	0.80 (0.40)

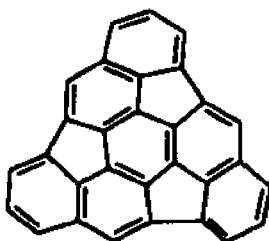
CHAPTER TWO. BUCKYBOWLS! SYNTHESIS AND CHARACTERIZATION OF SEMIBUCKMINSTERFULLERENES ($C_{30}H_{12}$)

2.1 Introduction.

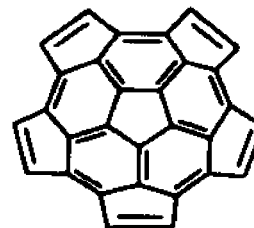
As we progress in the generation of hydrocarbons whose carbon frameworks are represented on the buckminsterfullerene surface, we encounter a new class of polynuclear aromatic hydrocarbons called semibuckminsterfullerenes (or "buckybowls"). These $C_{30}H_{12}$ hydrocarbons represent half of the buckminsterfullerene C_{60} surface, and share several common characteristics including 30 sp^2 carbon frameworks consisting of multiple fused five and six-membered rings, and bowl-shaped geometries. Among the buckybowls, the ones that are the most hemispherical and have the highest symmetry, are **24**, **25** and **26**.



24



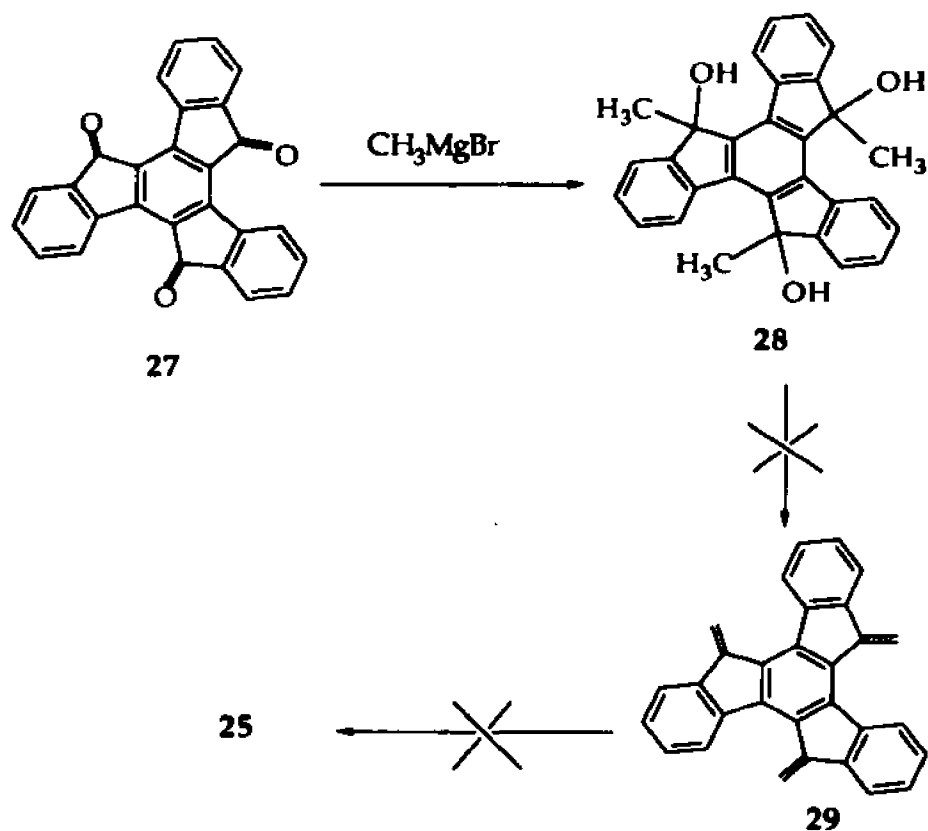
25



26

One of the reasons behind the interest in this subclass of polynuclear aromatic hydrocarbons is that they are attractive synthetic targets as potential intermediates in a "classical" total synthesis of C_{60} ; a goal for a number of research groups.³³⁻³⁸ Among them, Orville Chapman and his team at the University of California at Los Angeles, explored the chemistry of the truxenone (**27**) to obtain **25** in an attempt to

dimerize it to C_{60} , but failed at the step of dehydration of the mixture of syn and anti triols (28) to 5,10,15-trimethylenetribenzo[*a,f,k*]trindene or truxenene (29) (Scheme 2.1).³⁸



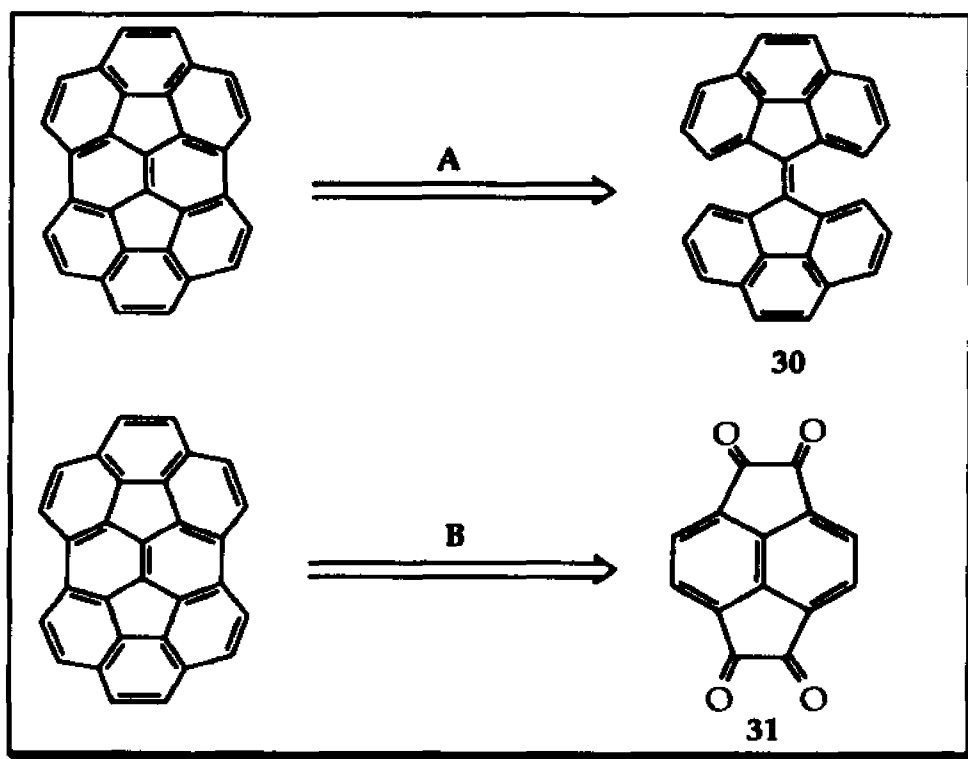
Scheme 2.1 Chapman et al. attempts to 25.

Truxenene (29) has been recently synthesized from the truxenone via the triols (28) by a team of Italian researchers.³⁹ However, neither flash vacuum thermolysis nor photochemical irradiation of 29 gave the product of ring closure. So, despite all the efforts towards the synthesis of 25,^{33,34,38,39} semibuckminsterfullerenes have remained elusive. This chapter presents the synthesis and characterization of the first two semibuckminsterfullerenes 24 and 25.

2.2 Results and discussion.

2.2.1 Synthesis and characterization of diacenaphtho[3,2,1,8-*cdefg*:-3',2',1',8'-*lmnop*]chrysene, (24).

2.2.1.1 Attempted synthesis of 24 from bis(4H-cyclopenta[*def*]-phenanthren-4-ylidene), (30).



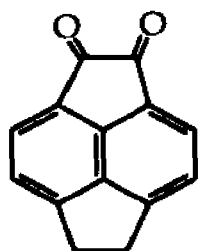
Scheme 2.2 Retrosynthetic routes proposed for 24.

One of the designed routes to prepare 24 was by dehydrocyclization of the known stilbene-type hydrocarbon 30 (route A). However, in our hands, both thermal and photochemical dehydrocyclization of 30 to produce 24 were unsuccessful. Also, researchers at the Department of High Temperature Reactions at the University of Leipzig (Germany) recently reported the failure of thermal dehydrocyclization of 30 to get

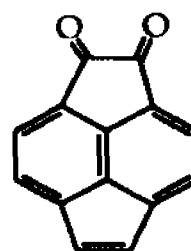
24.³⁸ Thus, this approach was abandoned, and instead we turned our attention to the synthetic route which has been used for the synthesis of corannulene and cyclopentacorannulene (route B). The crucial starting material for that type of chemistry is the 1,2,5,6-tetraketopyracene (31).

2.2.1.2 Synthesis of cyclopent[fg]acenaphthylene-1,2,5,6-tetrone, (31).

Although the synthesis of 31 seemed rather simple, classical methods of oxidation of 11 and 32 were unsuccessful. For example, oxidation of 11 with potassium dichromate cleaved the diketone part to give an anhydride. Also, oxidation of 32 with potassium permanganate, chromyl chloride, palladium dichloride or palladium nitrate did not produce the desired product.

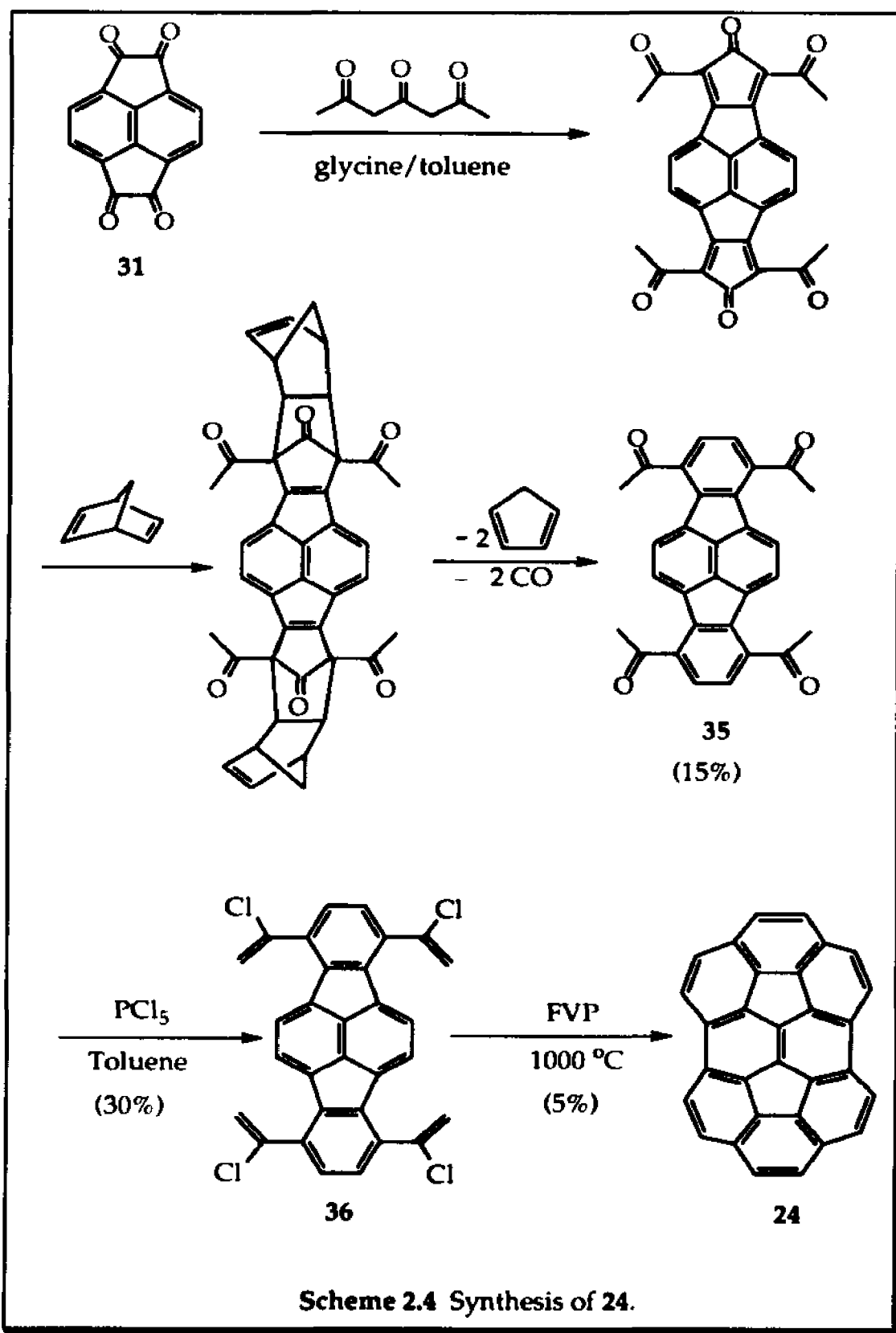


11



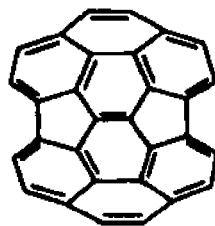
32

We finally succeeded in obtaining 31 first by bromination of 1,2-diketopyracene (11) at the benzylic positions with NBS,⁴¹ then conversion of the dibromo compound to the nitrate ester derivative (34) with silver nitrate in acetonitrile. Treatment of the nitrate ester with a catalytic amount of a sodium acetate solution in dimethylsulfoxide afforded 1,2,5,6-tetraketopyracene in yields of 55-70% (Scheme 2.3).⁴²



As expected from its structure, the ^1H NMR spectrum of **24** exhibited an AB multiplet at 7.91 and 7.55 ppm, and a singlet at 7.42 ppm (in CDCl_3 , ratio 2:1). The ^{13}C NMR spectrum showed three methine carbons and five quaternary carbons. The assignment of the structure of **24** was also supported by its mass spectrum as well as by exact mass measurement.

There is a formal possibility that under the high temperature conditions used in the FVP, compound **24** may rearrange itself into **24'** by Stone-Wales transformation.⁴⁴ The rearranged product (**24'**) would exhibit the same symmetry pattern as compound **24** in its ^1H and ^{13}C NMR spectra.



24'

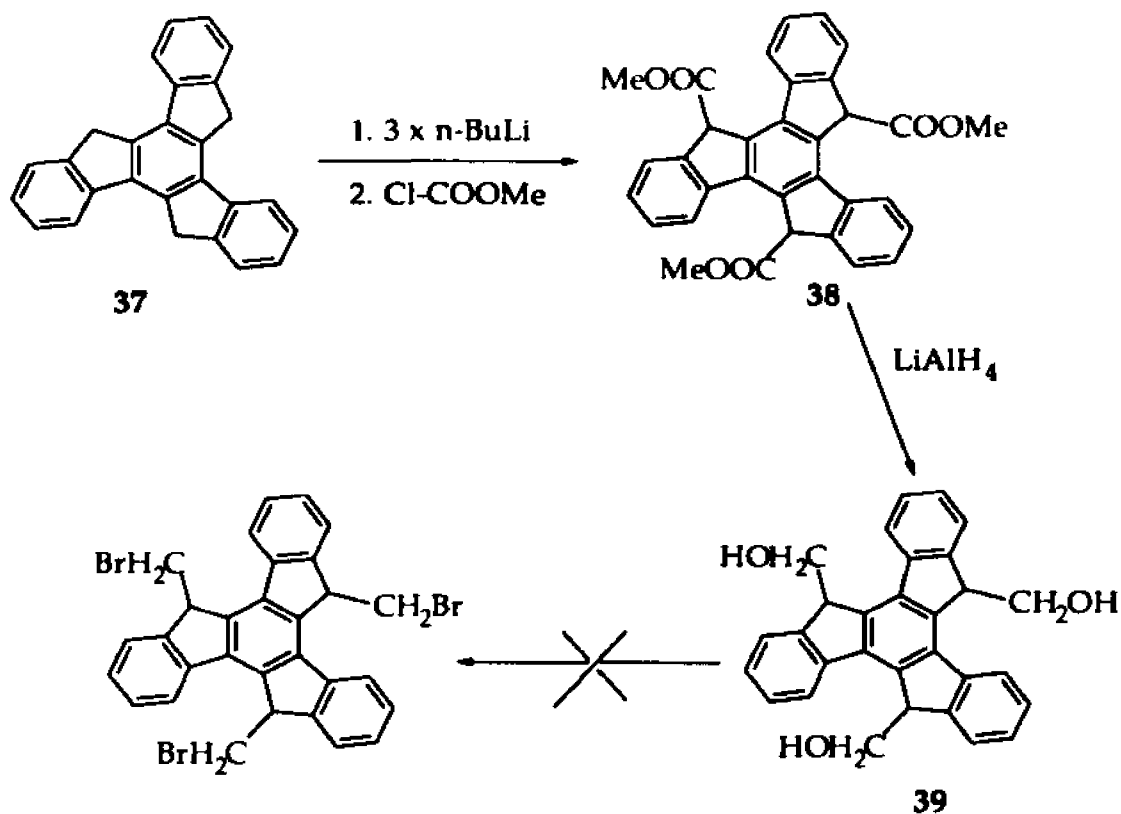
However, such process is rather unlikely in our case since recent studies show that the barrier for this rearrangement is very high for fullerenes. For example, no racemization for the optically active C_{84} isomer was observed even for two hours at 700 °C which sets a limit for the activation energy of the Stone-Wales transformation higher than 83 Kcal/mol.⁴⁵ Recent calculations show that the activation barrier for this process in C_{60} is about 143 Kcal/mol.⁴⁶ Moreover, no isotope scrambling was observed under FVP for ^{13}C labeled pyracylene.⁴⁷

Even though **24** is expected to have a bowl-shape geometry, it does not represent a symmetrical half of buckminsterfullerene. That is, when the carbon framework of **24** is removed from C_{60} , the remaining C_{30} structure is not identical with it. This makes the possibility of dimerization to buckminsterfullerene unlikely from **24**, or at least not possible without some bond reorganization of the carbon framework.

Inspired by our success with the pyrolytic, multiple ring closures required for the synthesis of **24**, we undertook the synthesis of the symmetrical half of buckminsterfullerene: benz[5,6]-*as*-indaceno[3,2,1,8,7-*mno**pqr*]indeno[4,3,2,1-*cdef*]chrysene or triindenotriphenylene (**25**).

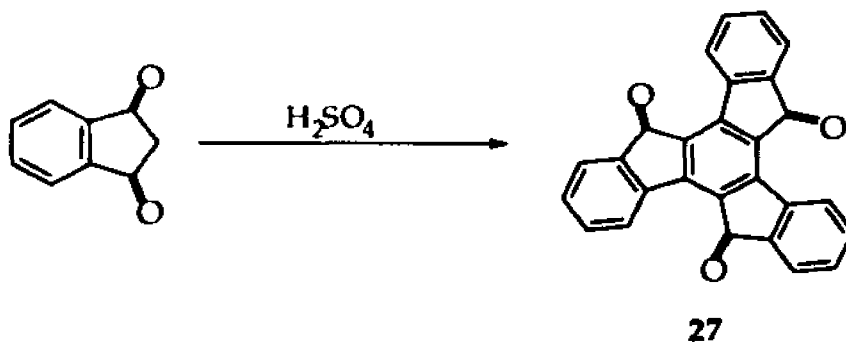
2.2.2 Synthesis of benz[5,6]-*as*-indaceno[3,2,1,8,7-*mno**pqr*]indeno[4,3,2,1-*cdef*]chrysene, (**25**).

To synthesize **25** our group has been exploring the chemistry of truxine (**37**). The trianion of **37** reacted with methylchloroformate produced the tricarboxylic ester (**38**) and reduction with lithium aluminum hydride gave a mixture of syn and anti triols (**39**). Conversion of the triols to the tribromides for pyrolysis was not achieved and this route was later abandoned (Scheme 2.5).⁴⁸

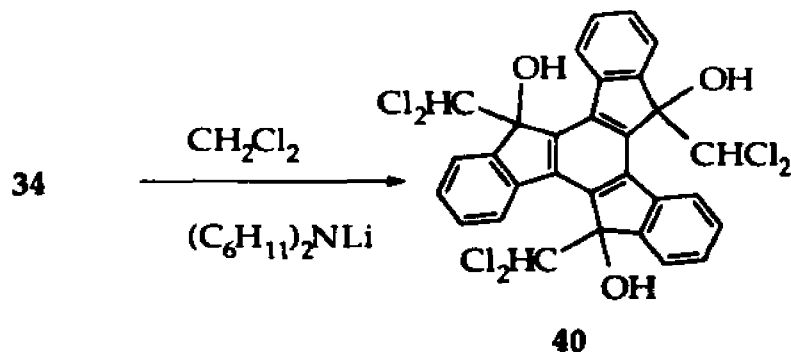


Scheme 2.5 Previous attempts to 25 by our group.

We finally synthesized **25** from the truxenone (**27**) obtained by trimerization of 1,3-indanedione with sulfuric acid.⁴⁹

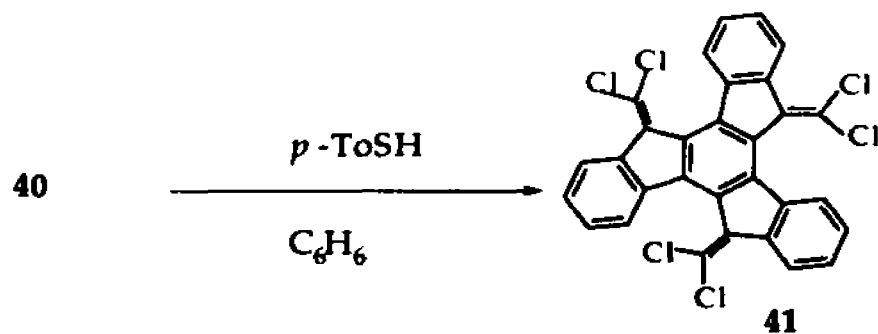


Generation of dichloromethyl lithium from dichloromethane and lithium dicyclohexylamide in the presence of **27** afforded a mixture of syn and anti hexachlorotriols (**40**) (1: 6 by NMR, 80% yield).

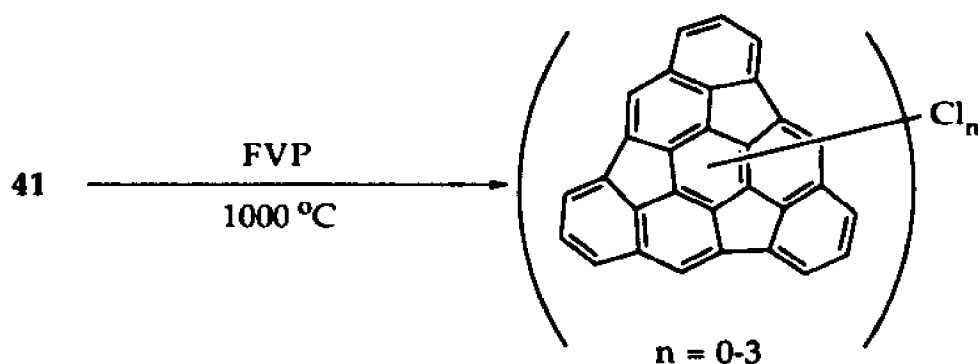


Crystals of syn-40 suitable for X-ray diffraction were grown from DCM:hexane. The structural features of bond angles, bond distances, coordinates and equivalent isotropic thermal parameters, the coordinates assigned to hydrogens and the torsion angles are included in Tables 2.7 through 2.11, respectively.

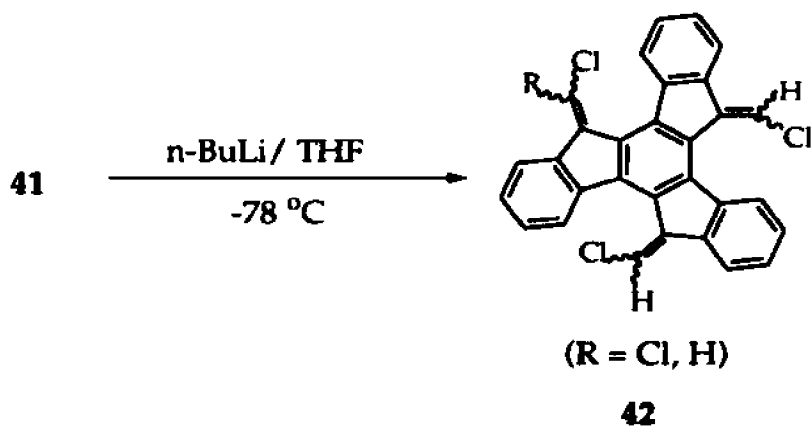
We tried to dehydrohalogenate 40 to the tris(chlorovinyl) derivatives but without success. Dehydration with para-toluene sulfonic acid in refluxing benzene gave the corresponding hexachlorovinyl 41 in 60% yield. We were also able to get crystals of 41 suitable for X-ray diffraction. The structural features of bond distances, bond angles, coordinates assigned to hydrogens, coordinates and equivalent isotropic thermal parameters and torsion angles are given in Tables 2.13 through 2.17, respectively.



Flash vacuum pyrolysis of **41** at 1000 °C gave a mixture of products corresponding to the tri, di and monochlorinated **25** by mass spectrometry; the $C_{30}H_{12}$ hydrocarbon was detected only as a very minor product. Attempts to separate the mixture were unsuccessful. Also, several dechlorination methods were tried, but no significant amount of **25** was formed.



Thus, we decided to decrease the number of chlorines before the pyrolytic step. Compound **41** was treated with three equivalents of *n*-butyllithium to give a mixture of isomeric tetra and trichlorovinyl derivatives (**42**). Complete conversion of **41** to the trichlorovinyl derivatives was never possible for reasons beyond our understanding.



Pyrolysis of the mixture of tetra and trichlorovinyl derivatives yielded **25**, some incomplete ring closure products, and a number of smaller hydrocarbons. The desired product (**25**) was isolated by column chromatography on silica gel and hexane: DCM (25:1). Crystallization from petroleum ether gave **25** as an orange solid that darkened, softened and sublimed over 250 °C in a sealed tube, but did not melt below 340 °C.

The structural assignment of **25** was made by NMR spectroscopy. ¹H NMR exhibited a doublet of doublets at 7.39 ppm, two doublets at 7.62 and 7.67 ppm, and a singlet at 7.85 ppm. ¹³C NMR showed four methine carbons and six quaternary carbons. The structure of **25** was also supported by GC/MS as well as by HRMS.

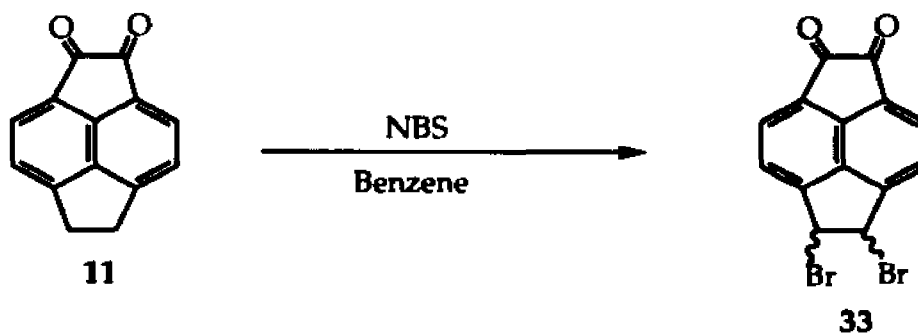
2.3 Conclusions.

The synthesis of the first two semibuckminsterfullerenes was successfully achieved using high temperature pyrolysis method developed for the synthesis of corannulene. The chemistry of these molecules, and that of polynuclear aromatic hydrocarbons with curved surfaces in general, holds great promise and has yet to be explored. Of special interest, of course, is their dimerization to fullerenes which will lead to the development of a synthetic route which would allow things not possible via the vaporization of graphite such as selective ¹³C labelling, the incorporation of heteroatoms or the capture of suitable atoms within the sphere. However, improvements are still necessary in the synthetic method of these molecules since the overall yields are low. The importance of our work on polynuclear aromatic hydrocarbons with curved surfaces has been recognized by the chemical community.⁵⁰⁻⁵⁵

2.4 Experimental.

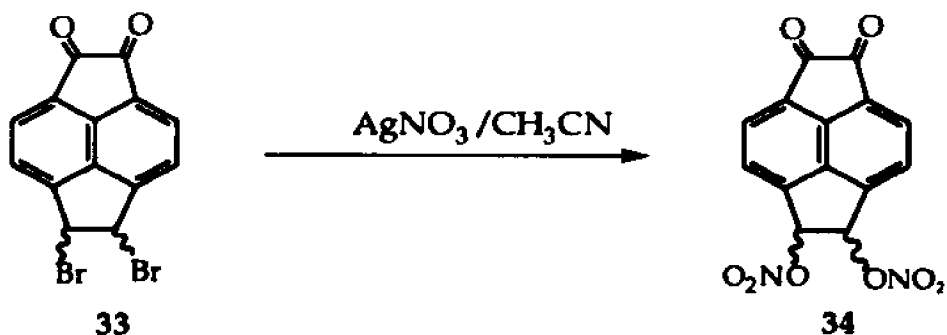
2.4.1 Synthesis of diacenaphtho[3,2,1,8-*cdefg*:3',2',1',8'-*lmnop*]chrysene, (24).

2.4.1.1 Synthesis of 5,6-dibromo-5,6-dihydrocyclopent[fg]-acenaphthylene-1,2-dione, (33).³⁹



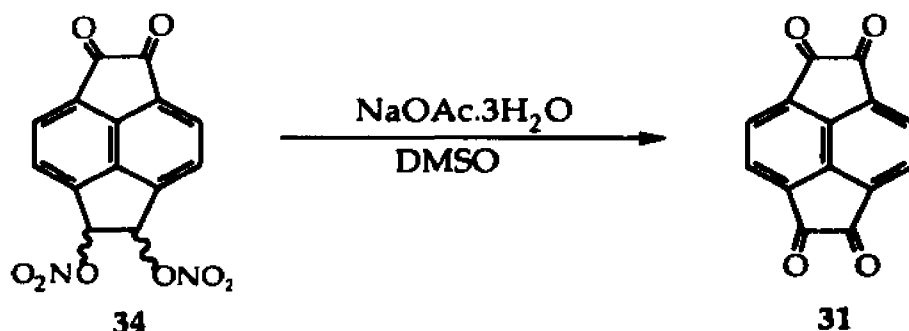
A solution of 6.858 g (32.97 mmol) 1,2-diketopyracene (11), 12.44 g (69.9 mmol) of NBS and traces of benzoyl peroxide in 520 mL of benzene was refluxed for 6 hours. The solution was cooled, filtered and the solvent evaporated. The solid was taken in DCM and washed with water. Chromatography on silica gel with DCM as eluant gave 10.4 g of a yellow solid (33) (yield: 60%). ¹H NMR (CDCl₃, 200 MHz): δ 6.09 (s, 2H), 7.9 (d, 2H, J= 7 Hz), 8.2 (d, 2H, J= 7 HZ) [Lit:³⁹ 6.09 (s, 2H), 7.91 (d, 2H), 8.25 (d, 2H)]; GC/MS, m/z (relative intensity): 366 (16, M⁺), 364 (34), 362 (16), 338 (50), 336 (100), 334 (50), 310 (29), 308 (65), 306 (29), 281 (10), 258 (14), 256 (14), 230 (19), 228 (19), 207 (66).

2.4.1.2 Synthesis of 5,6-dihydro-5,6-bis(nitrooxy)-cyclopent[fg]-acenaphthylene-1,2-dione, (34).



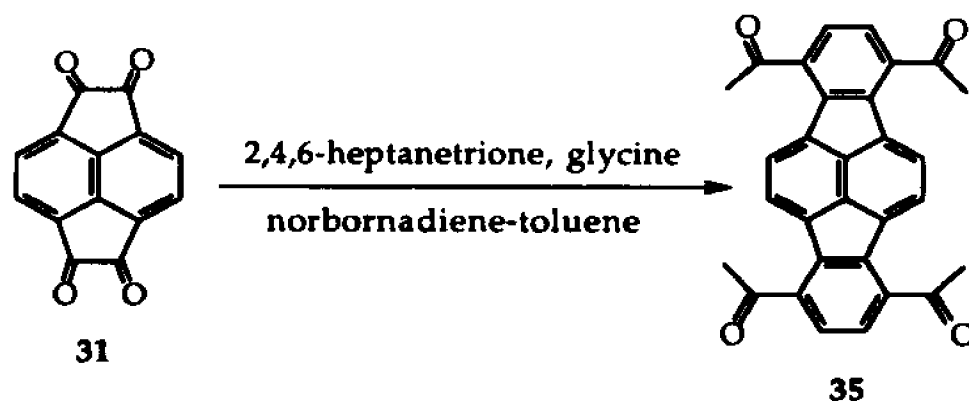
5,6-Dibromo-5,6-dihydrocyclopent[fg]acenaphthylene-1,2-dione (**33**) (5.19 g; 14.18 mmol) was dissolved in 300 mL of acetonitrile. To this solution was added 6.02 g of silver nitrate trihydrate in 100 mL of acetonitrile. After refluxing for one hour, it was filtered and the solid silver bromide washed with diethyl ether. The combined filtrate and washings were evaporated (rotavapor). The residue was taken in DCM, washed with water and dried with anhydrous magnesium sulfate. Chromatography on silica gel with DCM:hexane (4:1) yielded 3.74 g (80% yield) of two isomers of (**34**). Separation of the two isomers was not attempted. ^1H NMR (CDCl_3 , 250.13 MHz): δ 8.23 (d, 2H), 7.98 (d, 2H), 7.10 (s, 2H), 6.96 (s, 2H).

2.4.1.3 Synthesis of cyclopent[fg]acenaphthylene-1,2,5,6-tetrone, (31).



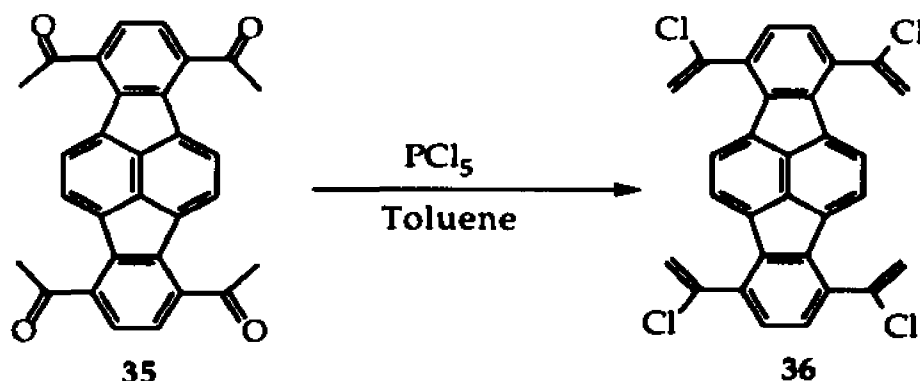
Sodium acetate trihydrate (0.118 g; 0.872 mmol) was added to the stirred solution of the mixture of nitrate esters (**34**) (1.44 g; 4.36 mmol) dissolved in 40 mL of DMSO. After thirty minutes, the reaction mixture was poured onto 400 mL of ice-water saturated with sodium chloride, filtered, washed thoroughly with water and dried. Recrystallization from dimethylformamide gave 0.81 g of orange plates (79% yield). Crystal data and collection parameters are given in Table 2.1. Compound (**31**): mp > 350 °C; ¹H NMR (DMSO-d₆, 400.13 MHz): δ 8.29 (s, 4H); ¹³C NMR (DMSO-d₆, 100.61 MHz): δ 122.8, 131.7, 141.8, 185.4. GC/MS, m/z (relative intensity): 236 (41, M⁺), 208 (82), 180 (89), 152 (100), 124 (64); HRMS calculated for C₁₄H₄O₄: 236.0110, found: 236.0102

2.4.1.4 Synthesis of 1,4,7,10-tetraethanone-indeno[1,2,3-*cd*]-fluoranthene, (35).



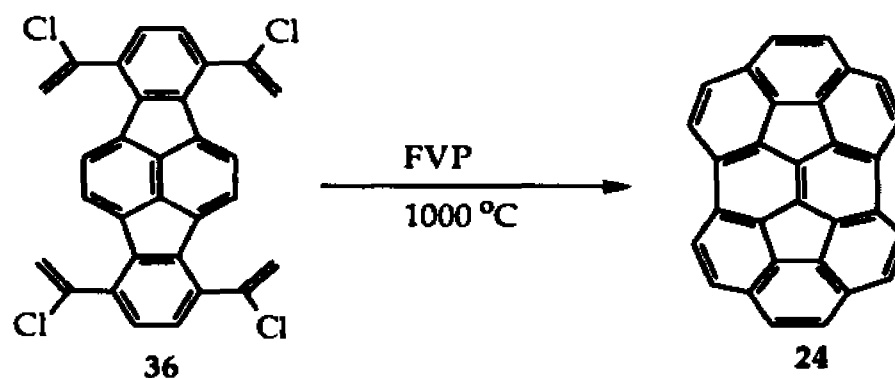
In a 250 mL three-neck round bottom flask equipped with a thermometer, a magnetic stirrer and a Dean-Stark receiver fitted with a condenser, 1.87 g (7.92 mmol) of the tetraketone (31) and 1.48 g (19.81 mmol) of glycine in 48 mL of toluene were refluxed for 30 min. After this time, 3.33 g (23.4 mmol) of 2,4,6-heptanetrione was added to the mixture and stirred. After 30 min, 50 mL of norbornadiene was added and the mixture was refluxed for 24 hours. At the end of this period, another 2.5 g (17.58 mmol) of 2,4,6-heptanetrione was added and the brown solution was refluxed for a total of 72 hours. The mixture was cooled and diluted with 20 mL of DCM and washed with water. The organic layer was dried over magnesium sulfate. After evaporating the solvent, chromatography on silica gel with ethyl acetate gave 0.553 g (15% yields) of (35): ^1H NMR (CDCl_3 , 250.13 MHz): δ 8.10 (s, 4H), 7.53 (s, 4H), 2.74 (s, 12H). GC/MS, m/z (relative intensity): 444 (100, M^+), 429 (66), 393 (33), 367 (33), 344 (16), 313 (66), 281 (50), 264 (66), 239 (83).

2.4.1.5 Synthesis of 1,4,7,10-tetrakis(1-chloroethenyl)-indeno[1,2,3-*cd*]fluoranthene, (36).



240 mg (0.54 mmol) of **35** and 670 mg (3.24 mmol) of PCl_5 in 20 mL of toluene were refluxed for 3 hours. The solvent was evaporated and the residue chromatographed on silica gel with hexane; 85 mg (30% yield) of a yellow solid (**36**) was obtained. ^1H NMR (CDCl_3 , 250.13 MHz): δ 5.71 (d, 4H, $J = 1.5$ Hz), 5.83 (d, 4H, $J = 1.5$ Hz), 7.15 (s, 4H), 7.89 (s, 4H). ^{13}C NMR (CDCl_3 , 62.9 MHz): δ 171.47, 126.05, 129.03, 132.96, 136.21, 136.50, 137.73, 139.40. GC/MS, m/z (relative intensity): 520 (28), 518 (57), 516 (46, M^+), 445 (18), 410 (21), 374 (82), 372 (78), 348 (75), 281 (100). HRMS calculated for $\text{C}_{30}\text{H}_{16}\text{Cl}_4$: 516.0006, found: 515.9976.

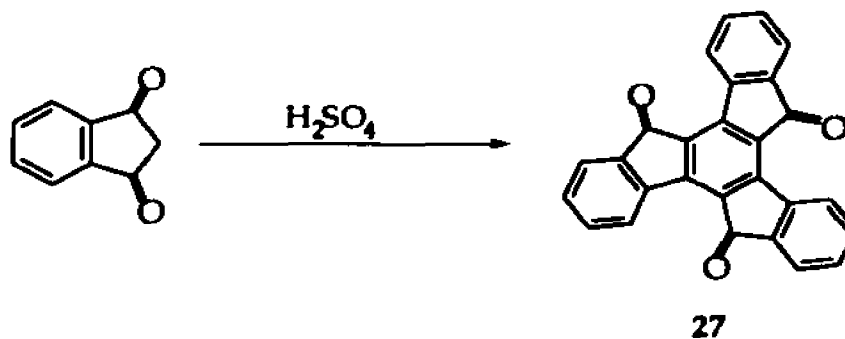
2.4.1.6 Flash vacuum pyrolysis of 1,4,7,10-tetrakis(1-chloroethenyl)-indeno[1,2,3-*cd*]fluoranthene, (36).



Flash vacuum pyrolysis of 270 mg of **36** in runs of 90 mg each at 1000 °C under a flow of nitrogen and a pressure of 1.5 mm of Hg gave 23 mg of crude product. Chromatography on silica gel with hexane:DCM (50:1) provided 12 mg of the desired product (**24**). Crystallization from benzene gave yellow needles which decompose over 300 °C. ^1H NMR (CDCl_3 , 400.13 MHz): δ 7.42 (s, 4H), 7.55 (d, 4H, $J = 9$ Hz), 7.91 (d, 4H, $J = \text{Hz}$); ^{13}C NMR (CDCl_3 , 100.61 MHz): δ 125.5, 126.8, 127.3, (all three CH by DEPT experiment); 128.2, 128.6, 136.8, 137.3, 142.0 (quaternary). GC/MS, m/z (relative intensity): 372 (M^+ , 100), 186 (30). HRMS calculated for $\text{C}_{30}\text{H}_{12}$: 372.0939, found 372.0929.

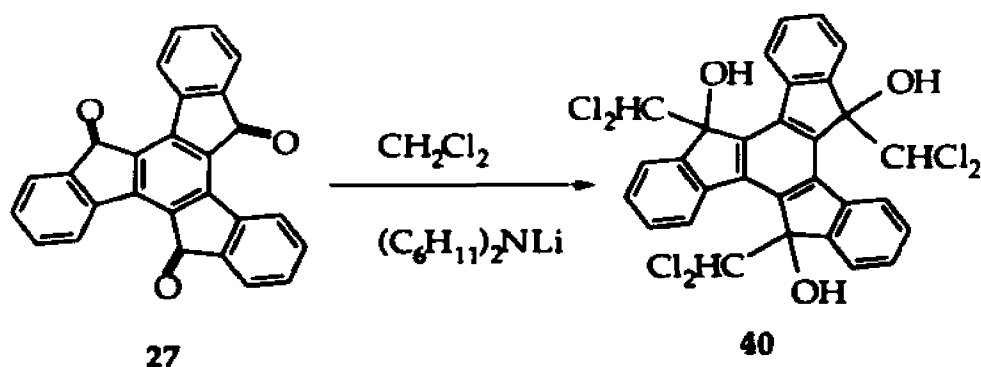
2.4.2 Synthesis of benz[5,6]-as-indaceno[3,2,1,8,7-mnopqr]indeno[4,3,2,1-cdef]chrysene, (25).

2.4.2.1 Synthesis of 5H-diindeno[1,2-a:1',2'-c]fluorene-5,10,15-trione (27).⁴³



In a 500 mL three-neck round bottom flask equipped with a magnetic stirrer, 27 g of 1,3-indanedione was added to 192 mL of concentrated sulfuric acid under nitrogen over a period of 8 hours, and the reaction was allowed to stir overnight. The reaction mixture was then poured over crushed ice, filtered, and washed with water until the water was no longer acidic. The remaining solid was then washed with methanol and chloroform. Extraction with chloroform for two days in a soxhlet gave 10.5 g (44% yield) of 27 as a yellow solid. Prior to use, compound 27 was heated in N,N-dimethylformamide, filtered and washed with methanol: mp > 360 °C; ^1H NMR (CDCl_3 , 250.13 MHz): δ 9.31 (d, 3H, J = 8 Hz), 7.88 (d, 3H, J = 8 Hz), 7.78-7.71 (m, 3H), 7.62-7.54 (m, 3H).

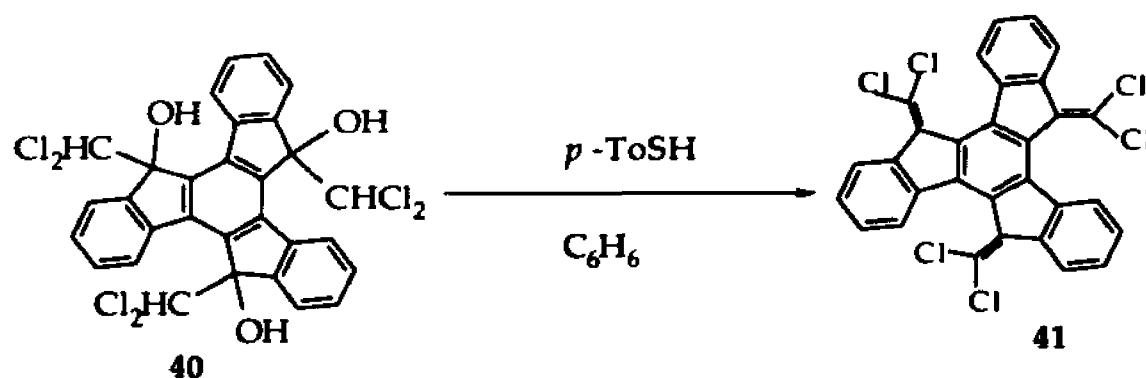
2.4.2.2 Synthesis of 5,10,15-tris(dichloromethyl)-5,10,15-trihydroxy-5H-diindeno[1,2-*a*:1',2'-*c*]fluorene, (40).



A solution of lithium dicyclohexylamide, prepared from dicyclohexylamine (17 mL, 93.6 mmol) and *n*-butyllithium (51 mL of 1.6 M solution in hexanes, 93.6 mmol) in 75 mL of dry THF, was added dropwise over a period of one hour to a well stirred suspension of 5H-diindeno[1,2-*a*:1',2'-*c*]fluorene-5,10,15-trione (27) (2.8 g, 7.3 mmol) in 100 mL of THF and 6 mL of dichloromethane at 0 °C. The mixture was stirred for another 30 min at the same temperature, and subsequently quenched with aqueous ammonium chloride. THF was removed under reduced pressure, and the resulting mixture extracted with DCM. The organic layer was washed with aqueous citric acid solution, dried and evaporated. Flash chromatography on silica gel with DCM provided a mixture of syn and anti triols (40) (ca. 1:6 by ¹H NMR) which can be subsequently used without further purification. Yield 80%. Additional chromatography on silica gel with DCM:hexane (3:1) provided samples of the anti and syn triols. Anti-40: colorless crystals (from CHCl₃), decomposing over 285 °C. ¹H NMR (CDCl₃, 250.13 MHz): δ 3.33 (s, 1H), 3.40 (s, 2H), 6.69 (s, 1H), 6.76 (s, 1H), 6.86 (s, 1H), 7.42-7.58 (m, 6H), 7.94-8.04 (m, 3H), 8.48-8.54 (m, 3H);

^{13}C NMR (CDCl_3 , 62.90 MHz): δ 74.34, 84.45, 84.82, 85.40, 125.09, 125.21, 125.37, 125.60, 128.74, 128.80, 130.84, 137.92, 138.44, 138.53, 139.05, 139.95, 143.96, 144.02. Some of the peaks are broad, apparently due to overlapping. FAB/MS, (m/z): 640, 638, 636. LC/MS: no molecular ion detected, loss of CHCl_2 produces $\text{C}_{29}\text{H}_{17}\text{Cl}_4\text{O}_3$ fragment: m/z , (relative intensity) 553(59), 555(100), 557(60). Syn-40: yellowish crystals (from DCM:hexane), decomposing over 240 °C. Crystal data and collection parameters are given in Table 2.6. ^1H NMR (CDCl_3 , 250.13 MHz): δ 3.84 (s, 3H), 6.41 (s, 3H), 7.35 - 7.38 (m, 6H), 7.75 - 7.79 (m, 3H), 8.11 - 8.14 (m, 3H). ^{13}C NMR (CDCl_3 , 62.90 MHz): δ 74.04, 84.78, 124.87, 125.10, 128.58, 130.85, 138.40, 138.50, 139.96, 143.07.

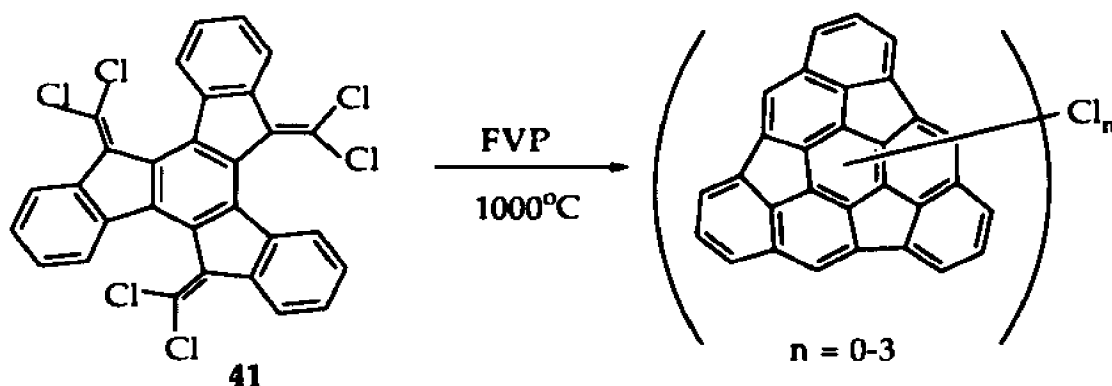
2.4.2.3 Synthesis of 5,10,15-tris(dichloromethylene)-5H-diindeno[1,2-a:1',2'-c]fluorene (41).



A mixture of triols **40** (2.1g, 3.28 mmol) and *p*-toluene sulfonic acid (3.8 g, 20 mmol) in 140 mL of benzene was refluxed for 20 hours. Benzene was then evaporated and the resulting mixture extracted with DCM, washed with aqueous sodium carbonate, and chromatographed on silica

gel with hexane:DCM (25:1). Yield 60% of yellow crystals (**41**), decomposing over 380 °C. Crystal data and collection parameters are given in Table 2.12. ^1H NMR (CDCl_3 , 400.13 MHz): δ 7.36 (t, $J = 7.0$ Hz, 3H), 7.43 (t, $J = 7.3$ Hz, 3H), 7.62 (d, $J = 7.7$ Hz, 3H), 8.17 (d, $J = 7.6$ Hz, 3H). ^{13}C NMR (CDCl_3 , 100.61 MHz): δ 120.28, 124.42, 125.76, 127.53, 128.12, 133.84, 136.26, 137.270, 138.98, 139.18. PD/MS, m/z : 585. LC/MS, m/z (relative intensity): 588(36), 586(79), 584(100), 582(51).

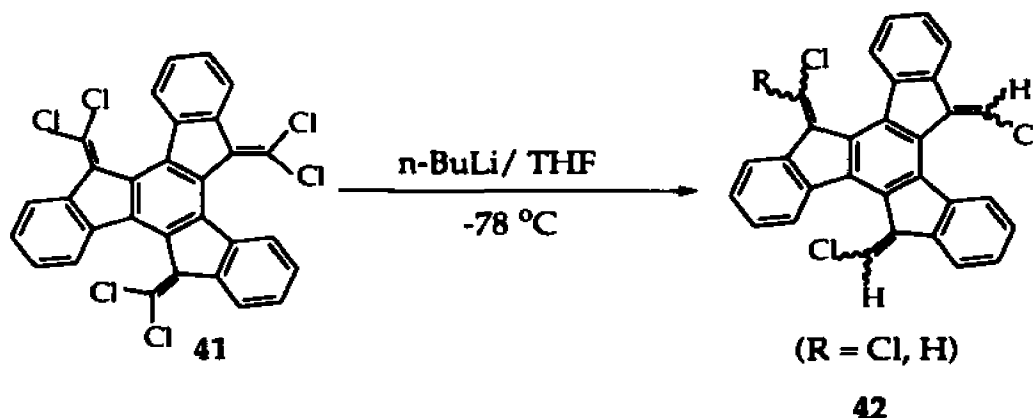
2.4.2.4 Flash vacuum pyrolysis of 5,10,15-tris(dichloromethylene)-5H-diindeno[1,2-*a*:1',2'-*c*]fluorene (**41**).



Flash Vacuum pyrolysis of 1.15 g of **41** at 1000 °C under a flow of nitrogen and a pressure of 1.5 mm of Hg gave 71 mg of a reddish product after chromatography on silica gel with hexane:DCM (1:2). Some polymerization and/or decomposition of the substrate in the evaporation zone occurred, as evidenced by the presence of black, tarry material in the sublimation boat. LC/MS showed three major peaks with masses of 476, 442 and 406 corresponding to the tri, di and monochlorinated **25**, respectively. A minor peak of mass 372 (molecular peak of **25**) was also

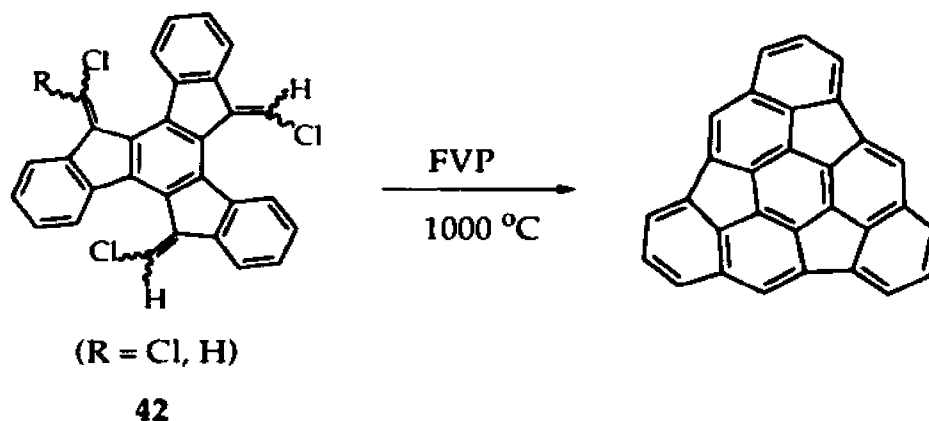
observed by LC/MS as well by GC/MS and PD/MS, but no significant amount of **25** could be produced. Several attempts to separate the mixture were unsuccessful. Also, methods for removing the chlorines were without success.

2.4.2.5 Synthesis of 5,10-bis(chloromethylene)-15-dichloromethylene -5H-diindeno[1,2-a:1',2'-c]fluorenes, (**42**).



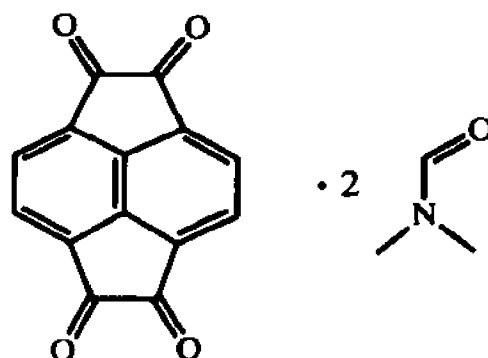
(relative intensity): 484(25), 482(100), 480(98). The separation of the above mixture was not attempted.

2.4.2.6 Flash vacuum pyrolysis of 5,10-bis(chloromethylene)-15-dichloromethylene-5H-diindeno[1,2-*a*:1',2'-*c*]fluorenes, (42).



The mixture of tetrachlo and trichlorinated material was flash vacuum pyrolysed in a stream of nitrogen as a carrier gas under the total pressure of 1.5 torr. In a typical run ca. 80 mg of the substrate was slowly sublimed during two hours and the dark pyrolisate (10-15 mg) was washed out from the cold trap with DCM. Some polymerization and/or decomposition of the substrate in the evaporation zone occurred, as evidenced by the presence of black, tarry material in the sublimation boat. Combined pyrolisates from several runs (typically 80-90 mg) were chromatographed on silica gel with hexane:DCM (25:1), and the less polar fractions were collected. Subsequent chromatography on silica gel with cyclohexane or recrystallization from petroleum ether provided ca. 5 mg of pure **25** as an orange solid that darkens, softens and sublimes over 250 °C, but does not melt below 340 °C. ¹H NMR (CDCl₃, 400.13 MHz): δ 7.39

(dd, 3H), 7.62 (d, 3H, $J = 8.0$ Hz), 7.67 (d, 3H, $J = 6.9$ Hz), 7.85 (s, 3H); ^{13}C NMR (CDCl_3 , 100.61 MHz): δ 120.7, 125.0, 127.4, 128.3, (all four CH by DEPT-90 experiment), 135.4, 138.2, 138.6, 144.9, 148.3, 153.1. GC/MS, m/z (relative intensity): 373 ($M+1$, 22), 372 (M^+ , 74), 186 (100), 185 (85), 184 (50), 172 (20), 171 (15). HRMS calculated for $\text{C}_{30}\text{H}_{12}$: 372.0939, found 372.0936.

Table 2.1 Crystal data and collection parameters for 31.

Formula: C ₂₀ H ₁₈ N ₂ O ₆	FW: 382.4	F ₀₀₀ : 800
Space Group: C2/c	Radiation: Mo K α	Z: 4
a: 19.963(9)Å	b: 6.193(2)Å	c: 14.316(7)Å
α :	β : 94.85(4)°	γ :
V: 1763(2)Å ³	D _c : 1.426 gcm ⁻³	D _m :
μ : 1.0 cm ⁻¹	T: 115 K	θ Limits: 1-25°
R _{int} : 0.047	Max. Transm:	Av. Transm:
Min. Transm:	XtalSize:0.88x0.62x0.01m m	Color: Yellow plate
Max. Decay:	Av. Decay:	Min. Decay:
R(obs. data): 0.055	R(all data): 0.088	R _w : 0.057
Unique Data: 1565	Obs Data: 1045	GOF: 2.450 Cutoff: I>3 σ (I)
Max. Shift: 0.03 σ	Variables: 152	Fudge: 0.02
Max. Residual: 0.28eÅ ⁻³	Min. Residual:-0.32 eÅ ⁻³	Extinction: 1.9(2)x10 ⁻⁶

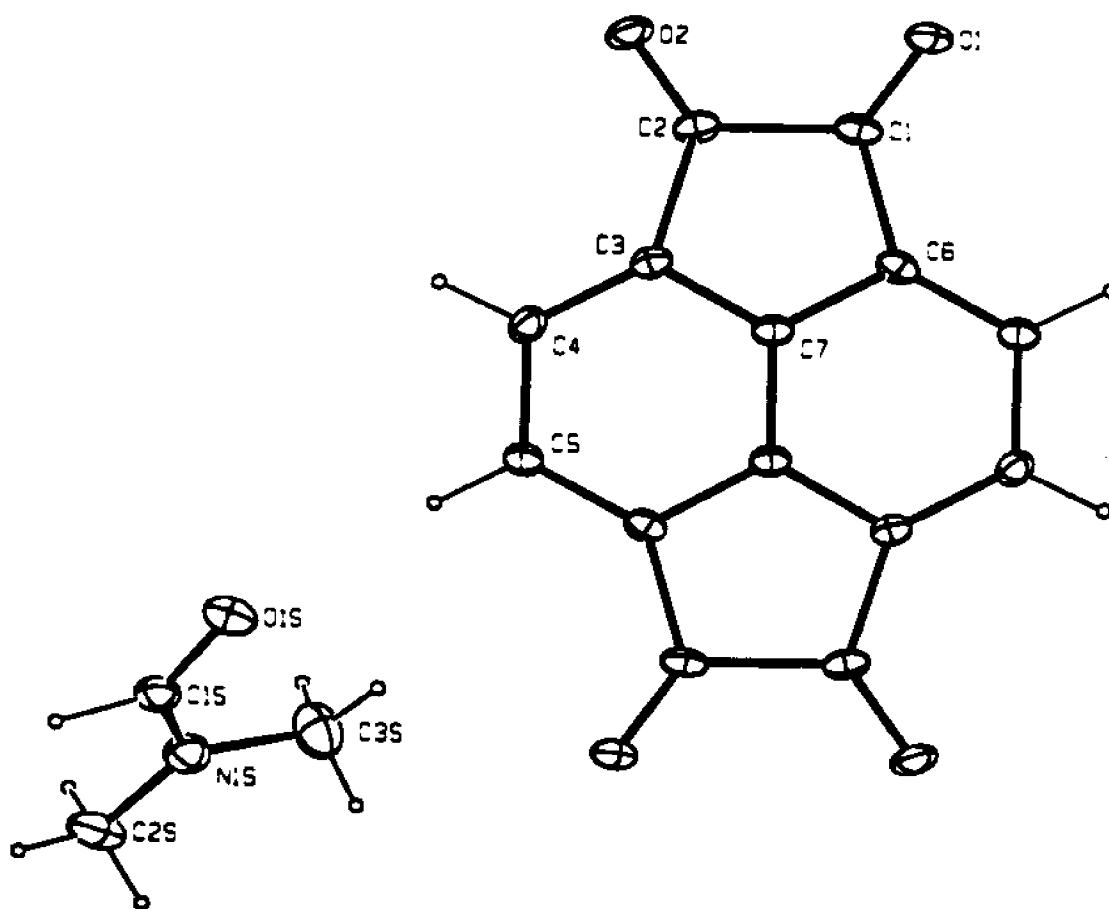


Figure 2.1 ORTEP drawing of cyclopent[fg]acenaphthylene-1,2,5,6-tetrone, (31) and DMF.

Table 2.2 Bond distances in angstroms for **31**.

atom 1	atom 2	distance	atom 1	atom 2	distance
O1	C1	1.203(4)	C5	C6	1.379(5)
O2	C2	1.208(4)	C6	C7	1.398(5)
C1	C2	1.579(5)	C7	C7	1.385(5)
C1	C6	1.504(5)	O1S	C1S	1.230(5)
C2	C3	1.497(5)	N1S	C1S	1.298(5)
C3	C4	1.373(5)	N1S	C2S	1.433(5)
C3	C7	1.392(5)	N1S	C3S	1.479(6)
C4	C5	1.433(5)			

Table 2.3 Coordinates and equivalent isotropic thermal parameters for **31**.

atom	x	y	z	B _{eq} (Å ²)
O1	0.1293(1)	0.1008(4)	0.7097(2)	1.76(5)
O2	0.2109(1)	0.4841(4)	0.7584(2)	1.72(5)
C1	0.1697(2)	0.1756(6)	0.6610(2)	1.50(7)
C2	0.2121(2)	0.3864(6)	0.6854(2)	1.31(7)
C3	0.2520(2)	0.4284(6)	0.6034(2)	1.28(7)
C4	0.2971(2)	0.5824(6)	0.5795(2)	1.42(7)
C5	0.3269(2)	0.5686(6)	0.4922(2)	1.40(7)
C6	0.1891(2)	0.1036(6)	0.5666(2)	1.28(6)
C7	0.2357(2)	0.2580(6)	0.5423(2)	1.19(6)
O1S	0.4116(1)	0.9784(4)	0.4126(2)	2.05(5)
N1S	0.5163(1)	0.8965(6)	0.3731(2)	1.92(6)
C1S	0.4666(2)	1.0254(8)	0.3856(3)	1.73(9)#
C2S	0.5819(2)	0.9618(9)	0.3505(3)	2.5(1)*
C3S	0.5097(2)	0.6633(8)	0.3926(3)	2.9(1)*
C1S'	0.458(1)	0.852(4)	0.391(2)	2.0(5)*
C3S'	0.529(1)	1.144(5)	0.358(2)	2.8(6)*
C2S'	0.573(2)	0.754(6)	0.358(2)	4.4(7)*

Populated 0.85

* Populated 0.15 and refined isotropically.

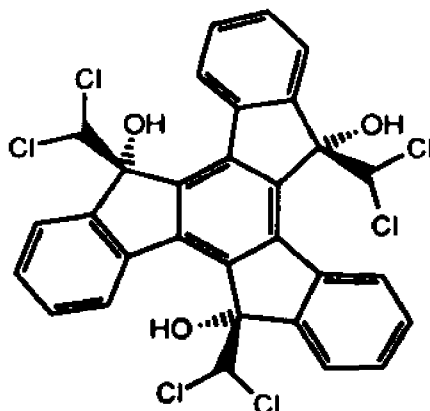
Table 2.4 Coordinates assigned to hydrogen atoms for **31**.

Atom	x	y	z	B _{iso} (Å ²)
H4	0.310(1)	0.707(5)	0.619(2)	0.3(6)
H5	0.363(1)	0.673(6)	0.479(2)	2.1(8)
H1S	0.475(2)	1.195(7)	0.365(3)	3(1)*
H21S	0.5963	0.8736	0.3024	3*
H31S	0.5354	0.6299	0.4497	3*
H22S	0.6128	0.9484	0.4051	3*
H23S	0.5805	1.1083	0.3310	3*
H32S	0.5256	0.5820	0.3431	3*
H33S	0.4638	0.6291	0.3983	3*

* Population = 0.85

Table 2.5 Bond angles in degrees for **31**.

atom 1	atom 2	atom 3	angle	atom 1	atom 2	atom 3	angle
O1	C1	C2	124.2(3)	C1	C6	C5	135.5(3)
O1	C1	C6	130.1(3)	C1	C6	C7	104.4(3)
C2	C1	C6	105.7(3)	C5	C6	C7	120.1(3)
O2	C2	C1	123.8(3)	C3	C7	C6	119.2(3)
O2	C2	C3	129.9(3)	C3	C7	C7	120.8(3)
C1	C2	C3	106.3(3)	C6	C7	C7	120.1(3)
C2	C3	C4	136.0(3)	C1S	N1S	C2S	125.5(4)
C2	C3	C7	104.4(3)	C1S	N1S	C3S	119.5(3)
C4	C3	C7	119.6(3)	C2S	N1S	C3S	114.6(3)
C3	C4	C5	120.4(3)	O1S	C1S	N1S	127.7(4)
C4	C5	C6	119.1(3)				

Table 2.6 Crystal data and collection parameters for syn-40.

Compound : syn-40

Formula: $C_{30}H_{18}Cl_6O_3 \cdot CH_2Cl_2$	FW: 724.1	F_{000} : 732
Space Group: $P\bar{1}$	Radiation: Cu $K\alpha$	Z: 2
a: 11.1328(11)Å	b: 11.6731(9)Å	c: 14.0665(11)Å
α : 71.202(7)°	β : 85.681(8)°	γ : 68.283(8)°
V: 1605.7(2)Å ³	D_c : 1.498 gcm ⁻³	D_m :
μ : 68.4 cm ⁻¹	T: 24°C	θ Limits: 2-75°
R _{int} :	Max. Transm: 99.88%	Av. Transm: 87.64%
Min. Transm: 60.49%	Xtal Size: 0.50x0.12x0.04mm	Color: Yellow lath
Max. Decay:	Av. Decay:	Min. Decay:
R(obs. data): 0.066	R(all data): 0.097	R_w : 0.083
Unique Data: 6599	Obs Data: 4330	GOF: 3.181 Cutoff: $1 > 3\sigma(I)$
Max. Shift: 0.14σ	Variables: 398	Fudge: 0.02
Max. Residual: 0.71 eÅ ⁻³	Min. Residual: -0.11 eÅ ⁻³	Extinction: $2.8(6) \times 10^{-7}$

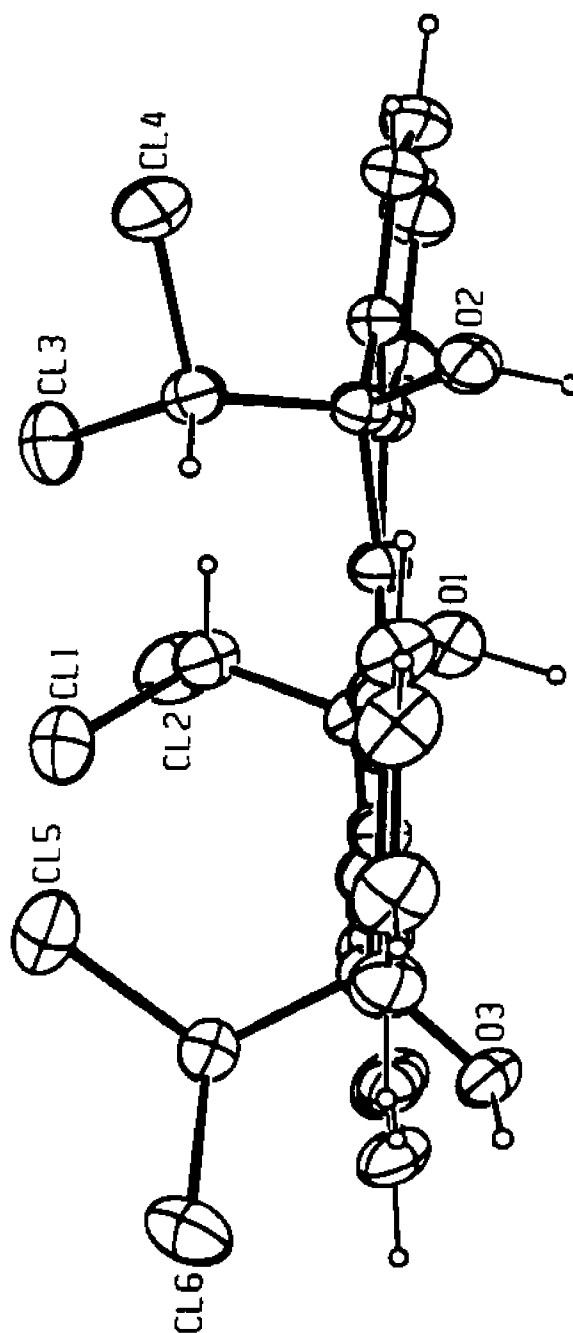


Figure 2.2 ORTEP side view 5,10,15-tris(dichloromethyl)-5,10,15-trihydroxy-5H-diindeno[1,2-a,1',2'-c]fluorene, (syn-40).

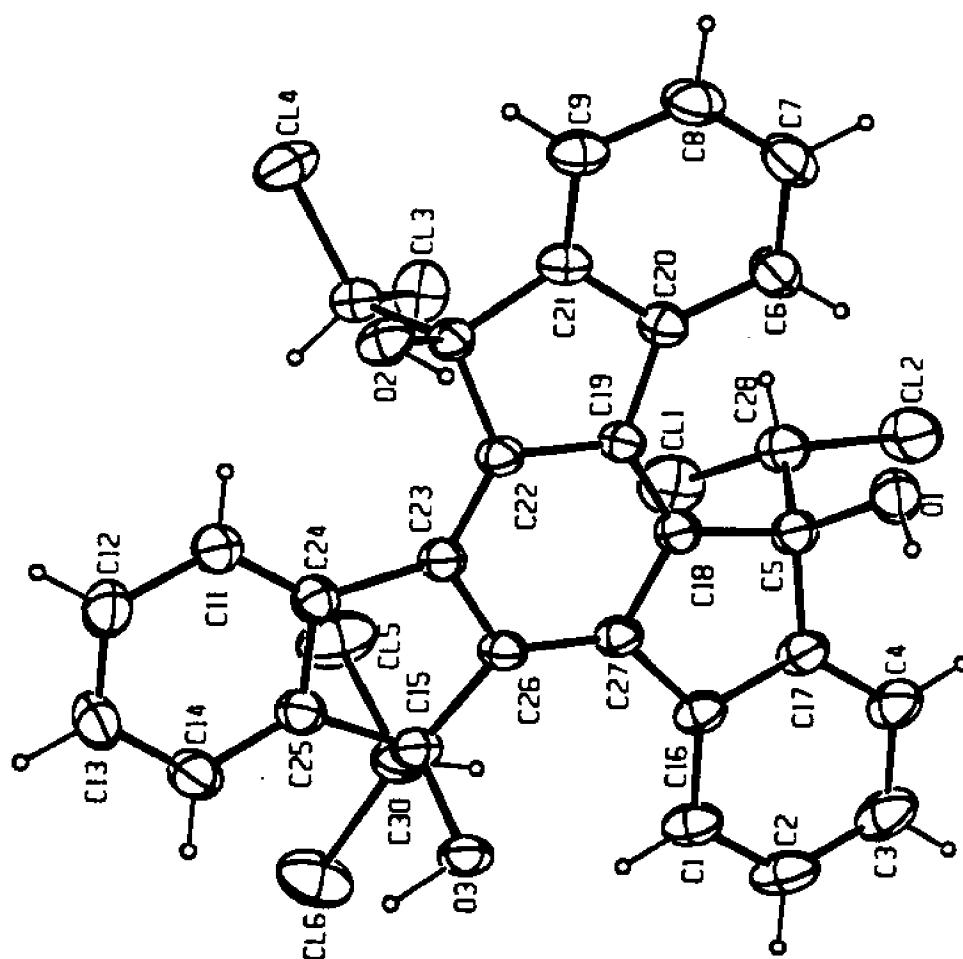


Figure 2.3 ORTEP top view of 5,10,15-tris(dichloromethyl)-5,10,15-trihydroxy-5H-diindeno[1, 2-a, 1',2'-c]fluorene, (syn-40).

Table 2.7 Bond angles in degrees for syn-40.

atom 1	atom 2	atom 3	angle	atom 1	atom 2	atom 3	angle
C2	C1	C16	119.9(5)	C12	C13	C14	120.9(5)
C1	C2	C3	120.8(5)	C13	C14	C25	117.8(5)
C2	C3	C4	120.1(6)	O3	C15	C25	113.1(4)
C3	C4	C17	119.3(5)	O3	C15	C26	111.0(4)
O1	C5	C17	113.2(5)	O3	C15	C30	107.2(4)
O1	C5	C18	115.4(3)	C25	C15	C26	103.3(4)
O1	C5	C28	104.6(4)	C25	C15	C30	113.5(4)
C17	C5	C18	102.3(4)	C26	C15	C30	108.6(4)
C17	C5	C28	114.1(3)	C1	C16	C17	119.0(5)
C18	C5	C28	107.4(5)	C1	C16	C27	133.1(4)
C7	C6	C20	118.3(5)	C17	C16	C27	107.9(4)
C6	C7	C8	121.2(5)	C4	C17	C5	128.0(5)
C7	C8	C9	121.4(5)	C4	C17	C16	120.9(5)
C8	C9	C21	117.9(5)	C5	C17	C16	111.1(4)
O2	C10	C21	113.4(3)	C5	C18	C19	129.5(4)
O2	C10	C22	114.7(4)	C5	C18	C27	109.6(4)
O2	C10	C29	105.6(4)	C19	C18	C27	120.6(4)
C21	C10	C22	102.7(4)	C18	C19	C20	132.2(4)
C21	C10	C29	113.1(4)	C18	C19	C22	119.4(4)
C22	C10	C29	107.3(3)	C20	C19	C22	108.4(4)
C12	C11	C24	119.8(5)	C6	C20	C19	132.2(5)
C11	C12	C13	120.6(5)	C6	C20	C21	119.6(4)
C19	C20	C21	108.0(4)	C15	C26	C23	109.6(4)
C9	C21	C10	127.7(4)	C15	C26	C27	129.7(4)
C9	C21	C20	121.5(4)	C23	C26	C27	120.5(4)
C10	C21	C20	110.6(4)	C16	C27	C18	108.5(4)
C10	C22	C19	109.3(4)	C16	C27	C26	132.2(4)
C10	C22	C23	130.2(4)	C18	C27	C26	119.3(4)
C19	C22	C23	120.2(4)	CL1	C28	CL2	109.0(2)
C22	C23	C24	131.9(4)	CL1	C28	C5	111.8(3)
C22	C23	C26	119.9(4)	CL2	C28	C5	112.7(4)
C24	C23	C26	108.2(4)	CL3	C29	CL4	109.4(3)
C11	C24	C23	132.5(4)	CL3	C29	C10	111.8(3)
C11	C24	C25	118.6(4)	CL4	C29	C10	112.4(3)
C23	C24	C25	108.8(4)	CL5	C30	CL6	109.9(3)
C14	C25	C15	128.1(5)	CL5	C30	C15	111.7(4)
C14	C25	C24	122.2(5)	CL6	C30	C15	111.4(4)
C15	C25	C24	109.7(4)				

Table 2.8 Bond distances in angstroms for syn-40.

atom 1	atom 2	distance	atom 1	atom 2	distance
C1	C2	1.375(8)	C10	C22	1.519(7)
C1	C16	1.389(7)	C10	C29	1.547(7)
C2	C1	1.375(8)	C11	C12	1.378(8)
C2	C3	1.392(8)	C11	C24	1.382(7)
C3	C2	1.392(8)	C12	C11	1.378(8)
C3	C4	1.379(8)	C12	C13	1.377(9)
C4	C3	1.379(8)	C13	C12	1.377(9)
C4	C17	1.385(8)	C13	C14	1.396(8)
C5	O1	1.412(5)	C14	C13	1.396(8)
C5	C17	1.511(7)	C14	C25	1.368(7)
C5	C18	1.520(6)	C15	O3	1.432(7)
C5	C28	1.541(8)	C15	C25	1.523(7)
C6	C7	1.398(8)	C15	C26	1.515(6)
C6	C20	1.384(7)	C15	C30	1.549(6)
C7	C6	1.398(8)	C16	C1	1.389(7)
C7	C8	1.370(8)	C16	C17	1.403(7)
C8	C7	1.370(8)	C16	C27	1.480(7)
C8	C9	1.383(8)	C17	C4	1.385(8)
C9	C8	1.383(8)	C17	C5	1.511(7)
C9	C21	1.378(7)	C17	C16	1.403(7)
C10	O2	1.417(5)	C18	C5	1.520(6)
C10	C21	1.512(6)	C18	C19	1.388(6)
C18	C27	1.417(6)	C25	C14	1.368(7)
C19	C18	1.388(6)	C25	C15	1.523(7)
C19	C20	1.478(6)	C25	C24	1.405(7)
C19	C22	1.426(6)	C26	C15	1.515(6)
C20	C6	1.384(7)	C26	C23	1.420(6)
C20	C19	1.478(6)	C26	C27	1.384(6)
C20	C21	1.411(7)	C27	C16	1.480(7)
C21	C9	1.378(7)	C27	C18	1.417(6)
C21	C10	1.512(6)	C27	C26	1.384(6)
C21	C20	1.411(7)	C28	CL1	1.763(5)
C22	C10	1.519(7)	C28	CL2	1.775(5)
C22	C19	1.426(6)	C28	C5	1.541(8)
C22	C23	1.376(6)	C29	CL3	1.757(5)
C23	C22	1.376(6)	C29	CL4	1.774(5)
C23	C24	1.486(6)	C29	C10	1.547(7)

(Table con'd.)

C23	C26	1.420(6)	C30	CL5	1.761(7)
C24	C11	1.382(7)	C30	CL6	1.775(5)
C24	C23	1.486(6)	C30	C15	1.549(6)
C24	C25	1.405(7)			

Table 2.9 Coordinates and equivalent isotropic thermal parameters for syn-40.

atom	x	y	z	Beq(Å ²)
CL1	0.6510(2)	0.3043(2)	0.9345(1)	6.48(4)
CL2	0.4062(2)	0.3495(2)	1.0285(1)	6.55(4)
CL3	0.7485(1)	0.6177(1)	0.7527(1)	5.20(4)
CL4	0.7339(1)	0.8551(1)	0.5972(1)	5.56(3)
CL5	0.9369(2)	0.2299(2)	0.7078(1)	7.59(4)
CL6	0.9648(2)	0.0328(2)	0.6159(1)	7.34(5)
O1	0.2910(3)	0.4550(3)	0.8242(3)	4.8(1)
O2	0.5700(3)	0.7885(3)	0.4831(2)	3.89(8)
O3	0.6936(3)	0.1908(3)	0.5372(2)	4.06(8)
C1	0.5823(5)	0.0906(4)	0.7461(4)	4.5(1)
C2	0.5352(6)	0.0010(5)	0.8090(4)	5.5(1)
C3	0.4447(6)	0.0342(5)	0.8788(4)	6.0(2)
C4	0.4062(6)	0.1561(5)	0.8892(4)	5.3(1)
C5	0.4250(5)	0.3842(4)	0.8248(3)	3.7(1)
C6	0.3217(5)	0.7211(5)	0.7670(4)	4.5(1)
C7	0.2664(5)	0.8521(5)	0.7610(4)	5.2(2)
C8	0.3120(5)	0.9423(5)	0.6980(4)	5.1(1)
C9	0.4166(5)	0.9068(4)	0.6400(4)	4.3(1)
C10	0.5832(4)	0.7168(4)	0.5870(3)	3.1(1)
C11	0.7893(5)	0.5684(5)	0.4262(4)	4.4(1)
C12	0.8806(5)	0.5343(5)	0.3584(4)	5.2(1)
C13	0.9314(5)	0.4082(5)	0.3562(4)	5.3(1)
C14	0.8931(5)	0.3118(5)	0.4234(4)	4.7(1)
C15	0.7515(4)	0.2597(4)	0.5747(3)	3.5(1)
C16	0.5427(5)	0.2145(4)	0.7542(3)	3.7(1)
C17	0.4557(5)	0.2457(4)	0.8276(4)	4.1(1)
C18	0.4929(4)	0.4358(4)	0.7323(3)	3.3(1)
C19	0.4967(4)	0.5593(4)	0.6893(3)	3.1(1)
C20	0.4251(4)	0.6839(4)	0.7083(3)	3.5(1)
C21	0.4735(4)	0.7775(4)	0.6466(3)	3.5(1)
C22	0.5825(4)	0.5805(4)	0.6108(3)	3.2(1)

(Table con'd.)

C23	0.6569(4)	0.4805(4)	0.5754(3)	3.3(1)
C24	0.7521(4)	0.4745(4)	0.4954(3)	3.6(1)
C25	0.8061(4)	0.3461(4)	0.4927(4)	3.8(1)
C26	0.6513(4)	0.3548(4)	0.6193(3)	3.3(1)
C27	0.5701(4)	0.3322(4)	0.6968(3)	3.3(1)
C28	0.4835(5)	0.3961(5)	0.9154(4)	4.3(1)
C29	0.7170(5)	0.7027(4)	0.6235(4)	3.7(1)
C30	0.8532(5)	0.1577(5)	0.6589(4)	4.5(1)
CL1S	0.9892(6)	0.6984(7)	0.0764(4)	19.2(3)*
CL2S	0.9100(7)	0.7876(6)	-0.1381(4)	21.2(2)*
CL3S	0.908(1)	0.9128(8)	-0.0318(8)	21.8(5)*
CL4S	1.0668(8)	0.628(1)	-0.0639(8)	22.3(4)*
C1S	0.913(1)	0.770(2)	-0.0385(9)	38.6(7)

* CL1S and CL2S are populated 0.65; CL3S and CL4S 0.35.

Table 2.10 Coordinates assigned to hydrogen atoms for syn-40.

atom	x	y	z	B _{iso} (Å ²)
H1	0.6417	0.0676	0.6972	5
H2	0.5647	-0.0846	0.8047	7
H3	0.4094	-0.0270	0.9194	7
H4	0.3462	0.1783	0.9380	6
H6	0.2891	0.6591	0.8103	5
H7	0.1958	0.8792	0.8012	6
H8	0.2709	1.0310	0.6942	6
H9	0.4482	0.9696	0.5968	5
H11	0.7520	0.6562	0.4253	5
H12	0.9086	0.5983	0.3127	6
H13	0.9933	0.3865	0.3084	6
H14	0.9263	0.2252	0.4210	6
H28	0.4695	0.4858	0.8989	5
H29	0.7786	0.6542	0.5869	4
H30	0.8070	0.1200	0.7114	5
H1OH	0.2425	0.4530	0.7651	8
H2OH	0.4915	0.7867	0.4612	8
H3OH	0.7534	0.1662	0.4838	8

Table 2.11 Torsion angles in degrees for syn-40.

atom 1	atom 2	atom 3	atom 4	angle
C16	C1	C2	C3	2.10 (0.89)
C2	C1	C16	C17	0.59 (0.81)
C2	C1	C16	C27	-177.05 (0.55)
C1	C2	C3	C4	-3.31 (0.94)
C2	C3	C4	C17	1.76 (0.91)
C3	C4	C17	C5	178.72 (0.54)
C3	C4	C17	C16	0.93 (0.85)
O1	C5	C17	C4	-46.81 (0.70)
O1	C5	C17	C16	131.16 (0.44)
C18	C5	C17	C4	171.66 (0.53)
C18	C5	C17	C16	6.30 (0.55)
C28	C5	C17	C4	72.73 (0.72)
C28	C5	C17	C16	-109.31 (0.50)
O1	C5	C18	C19	54.70 (0.69)
O1	C5	C18	C27	-131.76 (0.43)
C17	C5	C18	C19	178.04 (0.49)
C17	C5	C18	C27	-8.42 (0.52)
C28	C5	C18	C19	-61.52 (0.64)
C28	C5	C18	C27	112.02 (0.45)
O1	C5	C28	CL1	176.13 (0.32)
O1	C5	C28	CL2	52.88 (0.45)
C17	C5	C28	CL1	51.89 (0.53)
C17	C5	C28	CL2	71.35 (0.51)
C18	C5	C28	CL1	-60.73 (0.45)
C18	C5	C28	CL2	176.03 (0.33)
C20	C6	C7	C8	0.56 (0.85)
C7	C6	C20	C19	-173.41 (0.52)
C7	C6	C20	C21	1.69 (0.76)
C6	C7	C8	C9	-1.68 (0.92)
C7	C8	C9	C21	0.46 (0.86)
C8	C9	C21	C10	176.34 (0.50)
C8	C9	C21	C20	1.84 (0.78)
O2	C10	C21	C9	-43.76 (0.69)
O2	C10	C21	C20	131.23 (0.42)
C22	C10	C21	C9	-168.17 (0.50)

(Table con'd.)

C22	C10	C21	C20	6.82 (0.50)
C29	C10	C21	C9	76.48 (0.62)
C29	C10	C21	C20	-108.53 (0.46)
O2	C10	C22	C19	-132.75 (0.41)
O2	C10	C22	C23	53.52 (0.68)
C21	C10	C22	C19	-9.19 (0.49)
C21	C10	C22	C23	177.07 (0.48)
C29	C10	C22	C19	110.28 (0.42)
C29	C10	C22	C23	-63.46 (0.60)
O2	C10	C29	CL3	178.96 (0.29)
O2	C10	C29	CL4	55.45 (0.41)
C21	C10	C29	CL3	54.35 (0.45)
C21	C10	C29	CL4	-69.16 (0.44)
C22	C10	C29	CL3	-58.24 (0.42)
C22	C10	C29	CL4	178.26 (0.30)
C24	C11	C12	C13	2.60 (0.85)
C12	C11	C24	C23	-178.94 (0.53)
C12	C11	C24	C25	-1.87 (0.78)
C11	C12	C13	C14	-0.86 (0.89)
C12	C13	C14	C25	-1.56 (0.85)
C13	C14	C25	C15	-178.69 (0.50)
C13	C14	C25	C24	2.29 (0.81)
O3	C15	C25	C14	-54.42 (0.69)
O3	C15	C25	C24	124.70 (0.43)
C26	C15	C25	C14	-174.48 (0.52)
C26	C15	C25	C24	4.65 (0.52)
C30	C15	C25	C14	68.09 (0.67)
C30	C15	C25	C24	-112.79 (0.47)
O3	C15	C26	C23	-127.17 (0.41)
O3	C15	C26	C27	58.36 (0.64)
C25	C15	C26	C23	-5.64 (0.51)
C25	C15	C26	C27	179.88 (0.50)
C30	C15	C26	C23	115.20 (0.44)
C30	C15	C26	C27	-59.28 (0.66)
O3	C15	C30	CL5	177.32 (0.31)
O3	C15	C30	CL6	53.97 (0.46)
C25	C15	C30	CL5	51.63 (0.49)
C25	C15	C30	CL6	-71.73 (0.47)
C26	C15	C30	CL5	-62.70 (0.47)
C26	C15	C30	CL6	173.94 (0.34)
C1	C16	C17	C4	-2.12 (0.79)
C1	C16	C17	C5	179.75 (0.46)
C27	C16	C17	C4	176.07 (0.49)

(Table con'd.)

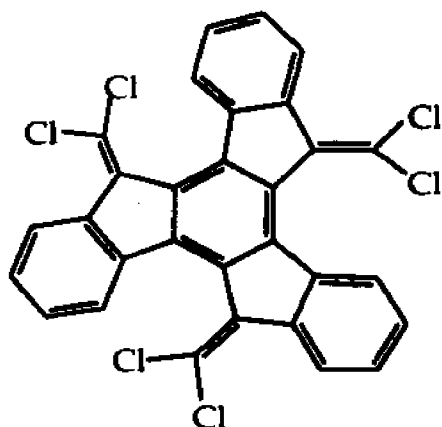
C27	C16	C17	C5	-2.06 (0.57)
C1	C16	C27	C18	174.32 (0.56)
C1	C16	C27	C26	-4.64 (0.97)
C17	C16	C27	C18	-3.51 (0.56)
C17	C16	C27	C26	177.54 (0.52)
C5	C18	C19	C20	-9.48 (0.88)
C5	C18	C19	C22	170.83 (0.47)
C27	C18	C19	C20	177.60 (0.48)
C27	C18	C19	C22	-2.09 (0.69)
C5	C18	C27	C16	7.65 (0.54)
C5	C18	C27	C26	-173.24 (0.43)
C19	C18	C27	C16	-178.14 (0.43)
C19	C18	C27	C26	0.96 (0.70)
C18	C19	C20	C6	-8.14 (0.92)
C18	C19	C20	C21	176.34 (0.50)
C22	C19	C20	C6	171.58 (0.53)
C22	C19	C20	C21	-3.94 (0.53)
C18	C19	C22	C10	-171.85 (0.41)
C18	C19	C22	C23	2.62 (0.69)
C20	C19	C22	C10	8.39 (0.52)
C20	C19	C22	C23	-177.14 (0.43)
C6	C20	C21	C9	-2.95 (0.75)
C6	C20	C21	C10	-178.30 (0.44)
C19	C20	C21	C9	173.24 (0.46)
C19	C20	C21	C10	-2.11 (0.54)
C10	C22	C23	C24	-7.37 (0.87)
C10	C22	C23	C26	171.17 (0.46)
C19	C22	C23	C24	179.46 (0.47)
C19	C22	C23	C26	-1.99 (0.70)
C22	C23	C24	C11	-5.65 (0.94)
C22	C23	C24	C25	177.06 (0.51)
C26	C23	C24	C11	175.68 (0.54)
C26	C23	C24	C25	-1.61 (0.55)
C22	C23	C26	C15	-174.21 (0.43)
C22	C23	C26	C27	0.85 (0.71)
C24	C23	C26	C15	4.64 (0.53)
C24	C23	C26	C27	179.71 (0.43)
C11	C24	C25	C14	-0.61 (0.77)
C11	C24	C25	C15	-179.79 (0.45)
C23	C24	C25	C14	177.11 (0.48)
C23	C24	C25	C15	-2.07 (0.55)
C15	C26	C27	C16	-7.50 (0.89)
C15	C26	C27	C18	173.64 (0.46)

(Table con'd.)

C23	C26	C27	C16	178.54 (0.49)
C23	C26	C27	C18	-0.32 (0.70)
CL4S	CL1S	CL3S	C1S	40.45 (0.91)
CL3S	CL1S	CL4S	CL2S	-30.58 (0.52)
CL3S	CL1S	CL4S	C1S	-34.07 (0.85)
C1S	CL1S	CL4S	CL2S	3.49 (0.78)
CL3S	CL1S	C1S	CL2S	117.42 (3.21)
CL3S	CL1S	C1S	CL4S	128.61 (1.04)
CL4S	CL1S	C1S	CL2S	-11.19 (2.56)
CL4S	CL1S	C1S	CL3S	-128.61 (1.04)
C1S	CL2S	CL4S	CL1S	-3.89 (0.88)
CL4S	CL2S	C1S	CL1S	11.51 (2.63)
CL4S	CL2S	C1S	CL3S	125.28 (1.19)
CL1S	CL3S	C1S	CL2S	-154.30 (1.54)
CL1S	CL3S	C1S	CL4S	-75.16 (1.08)
CL1S	CL4S	C1S	CL2S	174.48 (1.25)
CL1S	CL4S	C1S	CL3S	79.45 (1.09)
CL2S	CL4S	C1S	CL1S	-174.48 (1.25)
CL2S	CL4S	C1S	CL3S	-95.04 (1.22)

.....

Table 2.12 Crystal data and collection parameters for 41.



Compound : 41

Formula: C ₃₀ H ₁₂ Cl ₆	FW: 585.15	F ₀₀₀ : 1176
Space Group: P2 ₁ /n	Radiation: Cu K α	Z: 4
a: 12.460(1)Å	b: 11.897(1)Å	c: 16.819(1)Å
α : 90°	β : 106.385(5)°	γ : 90°
V: 2392(2)Å ³	D _c : 1.625gcm ⁻³	D _m :
μ : 68.738 cm ⁻¹	T: 23°C	θ Limits: 2-75°
R _{int} :	Max. Transm: 99.546%	Av. Transm: 80.748%
Min. Transm: 48.052%	Xtal Size: 0.50x0.25x0.25mm	Color: Brown-orange
Max. Decay: 1.000	Av. Decay: 1.000	Min. Decay: 1.000
R(obs. data): 0.086	R(all data): 0.097	R _w : 0.124
Unique Data: 4929	Obs Data: 4133	GOF: 6.023 Cutoff: I > 3 σ (I)
Max. Shift: 0.00 σ	Variables: 326	Fudge: 0.02
Max. Residual: 0.809eÅ ⁻³	Min. Residual: -0.19eÅ ⁻³	Extinction: 1.1(2)x10 ⁻⁶

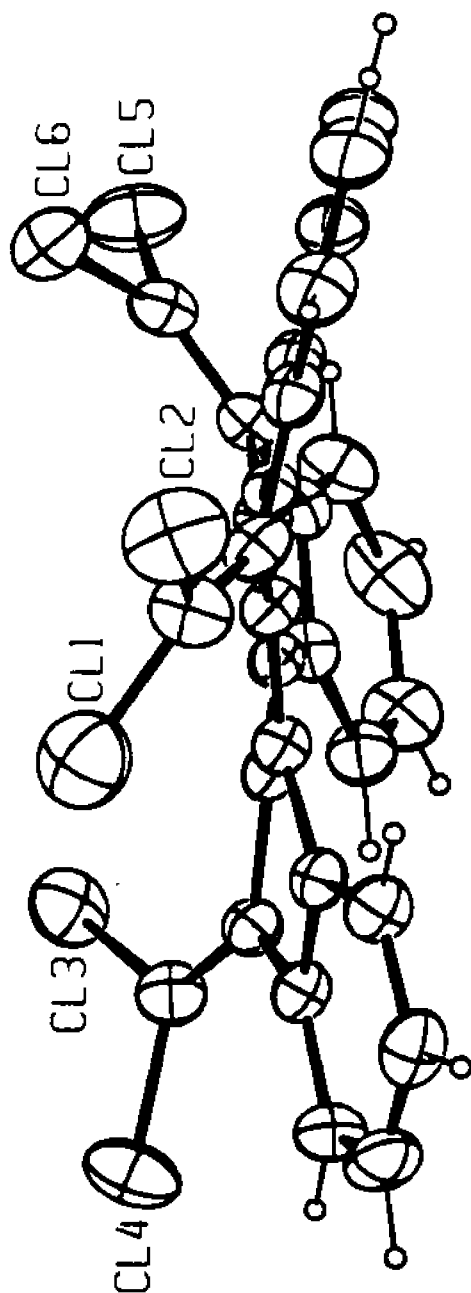


Figure 2.4 ORTEP side view of 5,10,15-tris(dichloromethylene)-5H-diindeno[1,2-a:1',2'-c]fluorene, (41).

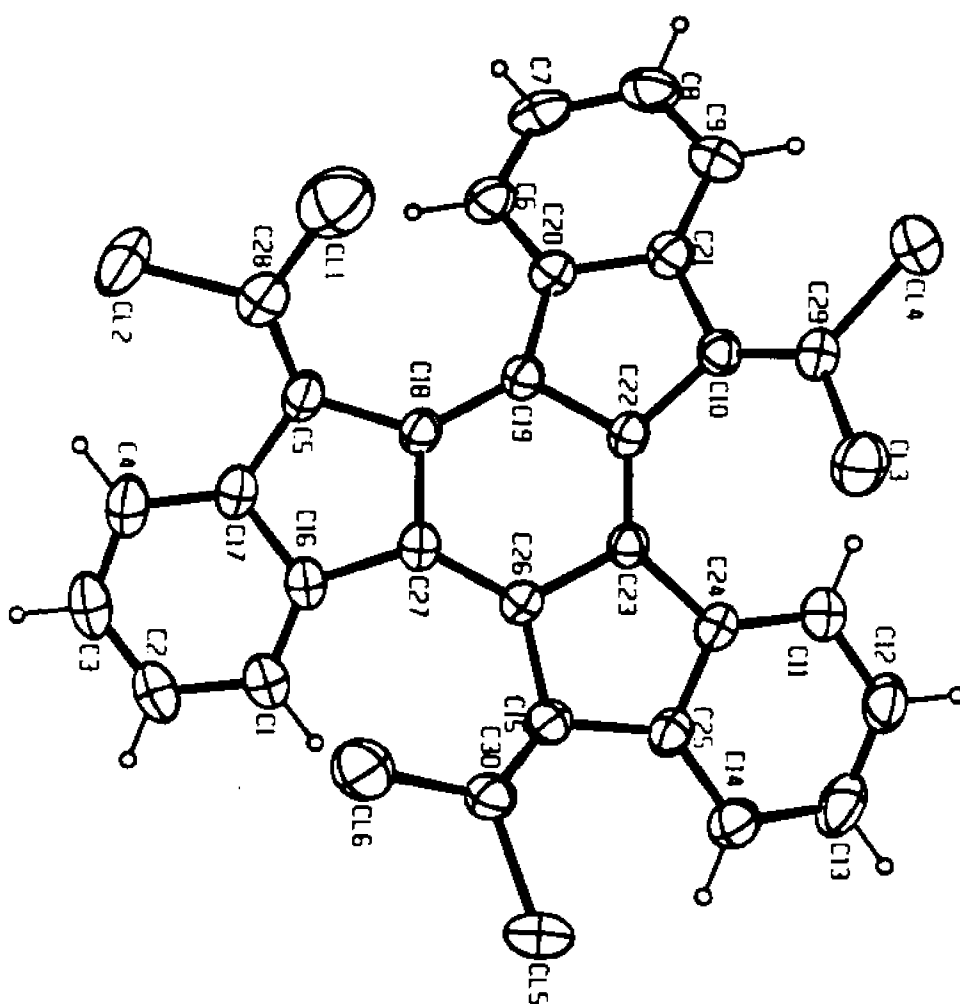


Figure 2.5 ORTEP top view of 5,10,15-tris(dichloromethylene)-5H-diindeno[1,2-a:1',2'-c]fluorene, (41).

Table 2.13 Bond angles in degrees for 41.

atom 1	atom 2	atom 3	angle	atom 1	atom 2	atom 3	angle
C2	C1	C16	119.5(5)	C1	C16	C27	131.2(5)
C1	C2	C3	119.9(6)	C17	C16	C27	108.2(5)
C2	C3	C4	121.3(6)	C4	C17	C5	132.7(5)
C3	C4	C17	119.3(5)	C4	C17	C16	119.5(5)
C17	C5	C18	106.6(4)	C5	C17	C16	107.8(4)
C17	C5	C28	126.0(5)	C5	C18	C19	132.9(4)
C18	C5	C28	125.5(5)	C5	C18	C27	107.2(5)
C7	C6	C20	119.0(5)	C19	C18	C27	119.9(4)
C6	C7	C8	120.6(5)	C18	C19	C20	133.0(4)
C7	C8	C9	121.0(6)	C18	C19	C22	119.2(4)
C8	C9	C21	119.4(6)	C20	C19	C22	107.5(4)
C21	C10	C22	105.9(4)	C6	C20	C19	130.9(5)
C21	C10	C29	124.7(5)	C6	C20	C21	119.6(5)
C22	C10	C29	126.8(4)	C19	C20	C21	109.1(4)
C12	C11	C24	119.1(5)	C9	C21	C10	132.5(5)
C11	C12	C13	120.1(6)	C9	C21	C20	119.8(4)
C12	C13	C14	122.2(6)	C10	C21	C20	107.7(4)
C13	C14	C25	117.6(6)	C10	C22	C19	106.7(4)
C25	C15	C26	104.9(4)	C10	C22	C23	133.5(4)
C25	C15	C30	125.2(4)	C19	C22	C23	119.9(5)
C26	C15	C30	126.8(5)	C22	C23	C24	133.1(5)
C1	C16	C17	120.2(5)	C22	C23	C26	119.7(4)
C24	C23	C26	106.8(4)	C16	C27	C26	132.2(5)
C11	C24	C23	130.0(5)	C18	C27	C26	119.5(5)
C11	C24	C25	120.3(5)	CL1	C28	CL2	109.6(4)
C23	C24	C25	109.4(5)	CL1	C28	C5	125.3(5)
C14	C25	C15	131.2(5)	CL2	C28	C5	124.2(5)
C14	C25	C24	120.6(5)	CL3	C29	CL4	109.8(3)
C15	C25	C24	108.2(4)	CL3	C29	C10	124.2(5)
C15	C26	C23	107.5(4)	CL4	C29	C10	125.3(4)
C15	C26	C27	132.4(5)	CL5	C30	CL6	111.3(3)
C23	C26	C27	120.1(4)	CL5	C30	C15	123.0(4)
C16	C27	C18	108.0(4)	CL6	C30	C15	125.3(4)

Table 2.14 Bond distances in angstroms for **41**.

atom 1	atom 2	distance	atom 1	atom 2	distance
CL1	C28	1.702(7)	C10	C29	1.329(7)
CL2	C28	1.708(7)	C11	C12	1.384(8)
CL3	C29	1.723(5)	C11	C24	1.380(8)
CL4	C29	1.717(6)	C12	C13	1.38(1)
CL5	C30	1.704(5)	C13	C14	1.38(1)
CL6	C30	1.711(6)	C14	C25	1.392(8)
C1	C2	1.409(9)	C15	C25	1.484(8)
C1	C16	1.359(8)	C15	C26	1.496(6)
C2	C3	1.370(8)	C15	C30	1.324(8)
C3	C4	1.38(1)	C16	C17	1.423(7)
C4	C17	1.384(8)	C16	C27	1.467(7)
C5	C17	1.477(8)	C18	C19	1.391(8)
C5	C18	1.466(7)	C18	C27	1.434(7)
C5	C28	1.357(9)	C19	C20	1.448(7)
C6	C7	1.384(8)	C19	C22	1.447(6)
C7	C8	1.40(1)	C22	C23	1.370(7)
C8	C9	1.363(8)	C23	C24	1.471(7)
C9	C21	1.396(8)	C23	C26	1.434(7)
C10	C22	1.481(7)	C26	C27	1.390(6)

Table 2.15 Coordinates assigned to hydrogen atoms for **41**.

atom	x	y	z	Beq(Å ²)
H1	0.5091	-0.0947	0.2658	5.0*
H2	0.6833	-0.1298	0.2361	6.0*
H3	0.8354	-0.0154	0.2912	6.2*
H4	0.8240	0.1389	0.3779	5.9*
H6	0.6536	0.2631	0.6046	4.5*
H7	0.6600	0.3395	0.7341	5.2*
H8	0.4925	0.3975	0.7626	5.5*
H9	0.3187	0.3411	0.6766	4.8*
H11	0.1299	0.0265	0.4853	4.7*
H12	-0.0010	-0.1220	0.4461	5.6*
H13	-0.0080	-0.2284	0.3284	6.5*
H14	0.1173	-0.1982	0.2496	5.4*

Starred atoms were assigned as the calculated position.

Table 2.16 Coordinates and equivalent isotropic thermal parameters for **41**.

atom	x	y	z	Beq(Å ²)
CL1	0.6083(2)	0.4146(2)	0.4668(2)	7.33(6)
CL2	0.8031(1)	0.3345(2)	0.4363(1)	6.94(5)
CL3	0.0833(1)	0.2384(2)	0.4097(1)	4.78(3)
CL4	0.1317(1)	0.3545(2)	0.5615(1)	5.34(4)
CL5	0.1896(2)	-0.1067(2)	0.1363(1)	5.65(4)
CL6	0.3647(1)	0.0513(2)	0.16288(9)	4.92(4)
C1	0.5735(4)	-0.0462(5)	0.2883(3)	3.8(1)
C2	0.6758(5)	-0.0672(6)	0.2708(4)	4.4(1)
C3	0.7663(5)	0.0003(6)	0.3043(4)	4.9(1)
C4	0.7599(5)	0.0896(6)	0.3551(4)	4.5(1)
C5	0.6268(4)	0.1956(5)	0.4259(3)	3.3(1)
C6	0.5848(4)	0.2777(5)	0.6191(3)	3.6(1)
C7	0.5880(5)	0.3266(5)	0.6944(4)	4.2(1)
C8	0.4888(5)	0.3547(5)	0.7134(3)	4.3(1)
C9	0.3872(5)	0.3260(5)	0.6616(3)	3.7(1)
C10	0.2870(4)	0.2240(4)	0.5212(3)	2.85(9)
C11	0.1278(4)	-0.0197(5)	0.4378(3)	3.6(1)
C12	0.0508(4)	-0.1059(6)	0.4144(4)	4.4(1)
C13	0.0467(5)	-0.1692(5)	0.3446(5)	5.1(2)
C14	0.1203(5)	-0.1524(5)	0.2978(4)	4.1(1)
C15	0.2904(4)	-0.0294(4)	0.2879(3)	2.8(1)
C16	0.5649(4)	0.0429(5)	0.3367(3)	3.0(1)
C17	0.6604(4)	0.1099(5)	0.3740(3)	3.3(1)
C18	0.5161(4)	0.1625(4)	0.4319(3)	2.80(9)
C19	0.4533(4)	0.1944(4)	0.4847(3)	2.69(9)
C20	0.4813(4)	0.2515(4)	0.5639(3)	2.8(1)
C21	0.3816(4)	0.2709(4)	0.5873(3)	3.0(1)
C22	0.3381(4)	0.1582(4)	0.4665(3)	2.58(9)
C23	0.2984(4)	0.0766(4)	0.4082(3)	2.52(9)
C24	0.2022(4)	-0.0003(4)	0.3921(3)	2.75(9)
C25	0.1992(4)	-0.0671(5)	0.3224(3)	3.0(1)
C26	0.3628(4)	0.0442(4)	0.3535(3)	2.66(9)
C27	0.4727(4)	0.0807(4)	0.3684(3)	2.76(9)
C28	0.6747(5)	0.2981(6)	0.4458(4)	4.5(1)
C29	0.1823(4)	0.2611(5)	0.5030(3)	3.4(1)
C30	0.2867(4)	-0.0317(5)	0.2084(3)	3.3(1)

Table 2.17 Torsion angles in degrees for **41**.

atom 1	atom 2	atom 3	atom 4	angle
C16	C1	C2	C3	1.64 (0.89)
C2	C1	C16	C17	-4.21 (0.82)
C2	C1	C16	C27	-176.19 (0.54)
C1	C2	C3	C4	-0.11 (0.97)
C2	C3	C4	C17	1.24 (0.98)
C3	C4	C17	C5	179.30 (0.60)
C3	C4	C17	C16	-3.77 (0.89)
C18	C5	C17	C4	-171.24 (0.61)
C18	C5	C17	C16	11.56 (0.57)
C28	C5	C17	C4	24.03 (1.00)
C28	C5	C17	C16	-153.16 (0.56)
C17	C5	C18	C19	164.02 (0.55)
C17	C5	C18	C27	-15.40 (0.56)
C28	C5	C18	C19	-31.14 (0.93)
C28	C5	C18	C27	149.43 (0.55)
C17	C5	C28	CL1	151.52 (0.49)
C17	C5	C28	CL2	-16.83 (0.89)
C18	C5	C28	CL1	-10.42 (0.89)
C18	C5	C28	CL2	-178.77 (0.43)
C20	C6	C7	C8	-3.27 (0.88)
C7	C6	C20	C19	-175.42 (0.55)
C7	C6	C20	C21	-2.67 (0.82)
C6	C7	C8	C9	5.81 (0.94)
C7	C8	C9	C21	-2.13 (0.91)
C8	C9	C21	C10	176.28 (0.57)
C8	C9	C21	C20	-3.84 (0.83)
C22	C10	C21	C9	-169.83 (0.57)
C22	C10	C21	C20	10.27 (0.55)
C29	C10	C21	C9	27.52 (0.92)
C29	C10	C21	C20	-152.37 (0.52)
C21	C10	C22	C19	-17.02 (0.52)
C21	C10	C22	C23	162.37 (0.54)
C29	C10	C22	C19	145.15 (0.54)
C29	C10	C22	C23	-35.46 (0.91)
C21	C10	C29	CL3	159.31 (0.43)
C21	C10	C29	CL4	-10.63 (0.81)
C22	C10	C29	CL3	0.29 (0.83)
C22	C10	C29	CL4	-169.65 (0.42)

(Table con'd.)

C24	C11	C12	C13	-1.98 (0.90)
C12	C11	C24	C23	-172.84 (0.54)
C12	C11	C24	C25	0.34 (0.80)
C11	C12	C13	C14	2.38 (1.01)
C12	C13	C14	C25	-1.03 (0.97)
C13	C14	C25	C15	178.30 (0.57)
C13	C14	C25	C24	-0.64 (0.85)
C26	C15	C25	C14	-165.87 (0.57)
C26	C15	C25	C24	13.18 (0.54)
C30	C15	C25	C14	33.20 (0.92)
C30	C15	C25	C24	-147.75 (0.53)
C25	C15	C26	C23	-17.98 (0.52)
C25	C15	C26	C27	160.90 (0.53)
C30	C15	C26	C23	142.55 (0.54)
C30	C15	C26	C27	-38.57 (0.89)
C25	C15	C30	CL5	-15.18 (0.79)
C25	C15	C30	CL6	156.41 (0.44)
C26	C15	C30	CL5	-171.97 (0.41)
C26	C15	C30	CL6	-0.39 (0.83)
C1	C16	C17	C4	5.33 (0.81)
C1	C16	C17	C5	-177.04 (0.49)
C27	C16	C17	C4	178.99 (0.51)
C27	C16	C17	C5	-3.38 (0.58)
C1	C16	C27	C18	166.39 (0.56)
C1	C16	C27	C26	-6.55 (0.97)
C17	C16	C27	C18	-6.32 (0.57)
C17	C16	C27	C26	-179.26 (0.53)
C5	C18	C19	C20	-16.23 (1.01)
C5	C18	C19	C22	170.76 (0.53)
C27	C18	C19	C20	163.14 (0.53)
C27	C18	C19	C22	-9.88 (0.73)
C5	C18	C27	C16	13.49 (0.56)
C5	C18	C27	C26	-172.52 (0.46)
C19	C18	C27	C16	-166.03 (0.46)
C19	C18	C27	C26	7.96 (0.73)
C18	C19	C20	C6	-11.51 (1.00)
C18	C19	C20	C21	175.15 (0.55)
C22	C19	C20	C6	162.10 (0.56)
C22	C19	C20	C21	-11.24 (0.57)
C18	C19	C22	C10	-167.88 (0.45)
C18	C19	C22	C23	12.63 (0.72)
C20	C19	C22	C10	17.47 (0.54)
C20	C19	C22	C23	-162.02 (0.45)

(Table con'd.)

C6	C20	C21	C9	6.27 (0.78)
C6	C20	C21	C10	-173.83 (0.48)
C19	C20	C21	C9	-179.52 (0.49)
C19	C20	C21	C10	0.39 (0.57)
C10	C22	C23	C24	-20.00 (0.96)
C10	C22	C23	C26	167.62 (0.50)
C19	C22	C23	C24	159.32 (0.51)
C19	C22	C23	C26	-13.06 (0.70)
C22	C23	C24	C11	-7.09 (0.95)
C22	C23	C24	C25	179.15 (0.53)
C26	C23	C24	C11	166.00 (0.53)
C26	C23	C24	C25	-7.76 (0.55)
C22	C23	C26	C15	-169.85 (0.44)
C22	C23	C26	C27	11.11 (0.72)
C24	C23	C26	C15	15.95 (0.52)
C24	C23	C26	C27	-163.09 (0.45)
C11	C24	C25	C14	0.98 (0.79)
C11	C24	C25	C15	-178.18 (0.47)
C23	C24	C25	C14	175.45 (0.49)
C23	C24	C25	C15	-3.72 (0.57)
C15	C26	C27	C16	-14.82 (0.94)
C15	C26	C27	C18	172.90 (0.50)
C23	C26	C27	C16	163.94 (0.51)
C23	C26	C27	C18	-8.34 (0.72)

BIBLIOGRAPHY

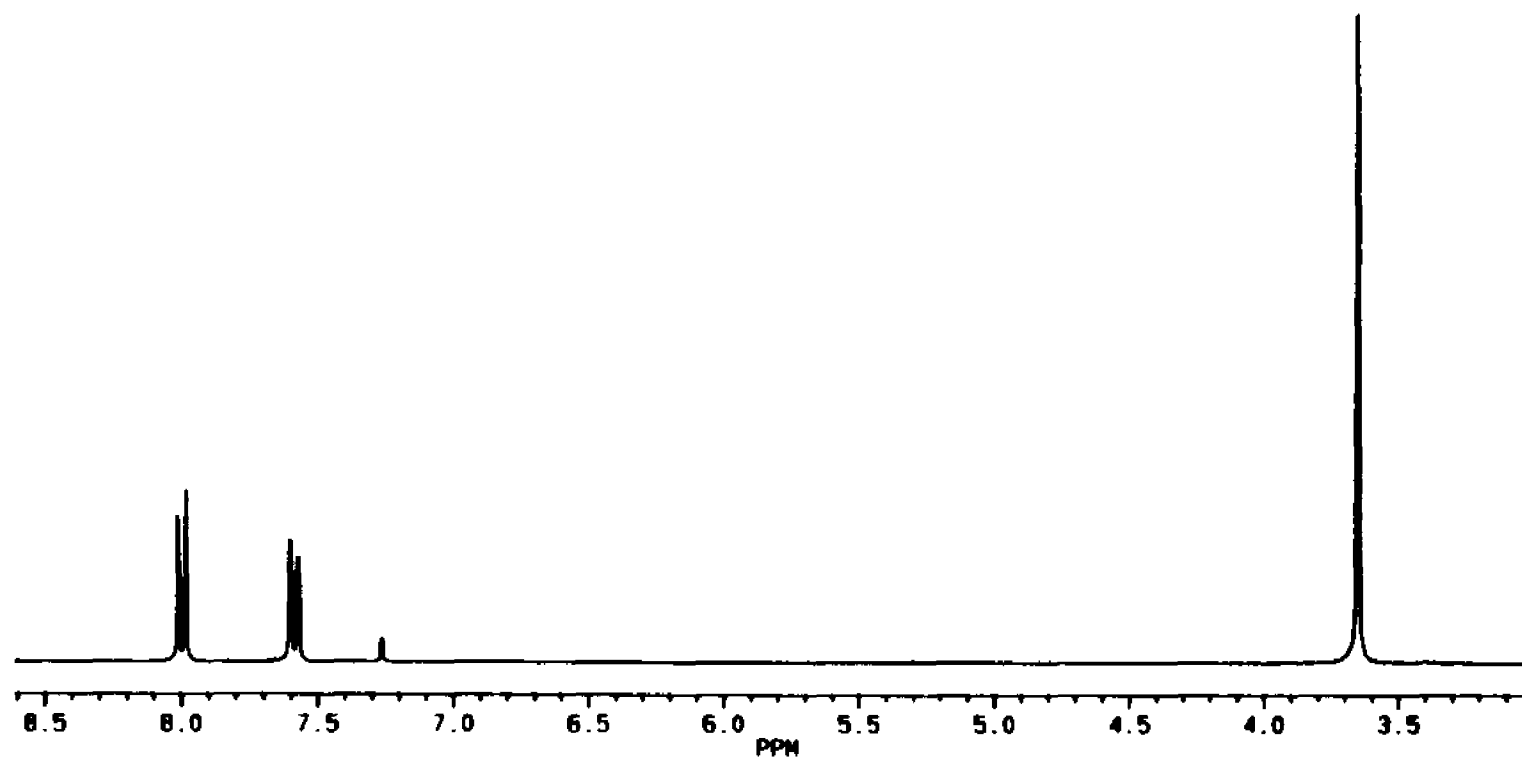
- 1 (a) Kroto, H. W.; Heath, J. R.; O'Brien, S. C.; Curl, R. F.; Smalley, R. E. *Nature*, **1985**, *318*, 162. (b) Kratschmer, W.; Lamb, L. D.; Fostiropoulos, K.; Huffman, D. R. *Nature*, **1990**, *347*, 354. (c) Kroto, H. W.; Allaf, A. W.; Balm, S. P.; *Chem. Rev.*, **1991**, *91*, 1213. (d) Hammond, G. S.; Kuck, V. J., Ed., "Fullerenes," ACS Symposium Series 481, Washington, D. C., 1992. (e) *Acc. Chem. Res.* (special issue), **1992**, *25*, 97.
- 2 Hirsch, A.; Khemani, K. C.; Susuki, T.; Allerman, P. M.; Kolch, A.; Srdanov, G.; Wudl, F. In *Large Carbon Clusters*; ACS Symposium Series; American Chemical Society: Washington, DC, 1991.
- 3 Howard, J. B.; McKinnon, J. T.; Makarovskiy, Y.; Lafleur, A. L.; Johnson, E. *Nature* **1991**, *352*, 139.
- 4 Wudl, F. *Acc. Chem. Res.* **1992**, *25*, 157.
- 5 Braun, T. *Angew. Chem. Int. Ed. Engl.* **1992**, *31*, 588.
- 6 Coustel, N.; Bernier, P.; Aznar, R.; Zahad, A.; Lambert, L. M.; Lyard, P. *J. Chem. Soc., chem. Comm.* **1992**, 1462.
- 7 Scribevens, W. A.; Bedworth, P. V.; Tour, J. M. *J. Am. Chem. Soc.* **1992**, *114*, 7917.
- 8 Khemani, K. C.; Prato, M.; Wudl, F. *J. Org. Chem.* **1992**, *57*, 3254.
- 9 Schwarz, H. *Angew. Chem. Int. Ed. Engl.* **1992**, *31*, 293.
- 10 Hoke, S. H., II; Molstad, J.; Dilletato, D.; Jay, M. J.; Carlson, D.; Kahr, B.; Cookes, R. G. *J. Org. Chem.* **1992**, *57*, 5069.
- 11 Barth, W. E.; Lawton, R. G. *J. Am. Chem. Soc.* **1966**, *88*, 380.
- 12 Baum, R. M. *C & EN*, March 16, **1992**, p 27.
- 13 Craig, J. T.; Robins, M. D. W. *Aust. J. Chem.* **1968**, *21*, 2237.
- 14 Davy, J. R.; Iskander, M. N.; Reiss, J. A. *Aust. J. Chem.* **1979**, *32*, 1067.
- 15 Scott, L. T.; Hashemi, M. M.; Meyer, D. T.; Warren, H. B. *J. Am. Chem. Soc.* **1991**, *113*, 7082.

- 16 Borchardt, A.; Fuchichello, A.; Kilway, K.V.; Baldrige, K. K.; Siegel, J. S. *J. Am. Chem. Soc.* **1992**, *114*, 1921.
- 17 Zimmerman, G.; Nuechter, U.; Hagen, S.; Nuechter, M. *Tett. Lett.* **1994**, *27*, 4747.
- 18 Scott, L. T., personal communication. Scott, L. T.; Cheng, P.-C.; Brachter, M. S. *Seventh International Symposium on Novel Aromatic Compounds*, Victoria, Canada, July, 1992, Abstract 64. See also: Cheng, P.-C. M.S.Thesis, University of Nevada, Reno, NV, December, 1992.
- 19 Clar, E. *Polycyclic Hydrocarbons*; Academic Press, New York, NY 1964.
- 20 Scott, L. T.; Hashemi, M. M.; Brachter, M. S. *J. Am. Chem. Soc.* **1992**, *114*, 1920.
- 21 Anet, F. A. L.; Ahmad, M.; Hall, L. D. *Proc. Chem. Soc.* **1964**, 145.
- 22 Anet, F. A. L.; Bourn, A. J. R.; Lin, Y. S. *J. Am. Chem. Soc.* **1964**, *86*, 3576.
- 23 Sygula, A.; Rabideau, P. W. unpublished results.
- 24 Trost, B. A. *J. Am. Chem. Soc.* **1969**, *91*, 918.
- 25 Newman, M. S.; Wood, L. L. Jr. *J. Am. Chem. Soc.* **1959**, *81*, 4300.
- 26 Brown, C. A.; Ahuja, Y. K. *J. Org. Chem.* **1973**, *38*, 2276.
- 27 Dahlquist, F. W.; Longmuir, K. J.; Du Vernet, R. B. *J. Magn. Reson.* **1975**, *17*, 406.
- 28 Eliel, E. L.; *Stereochemistry of Carbon Compounds*; McGraw-Hill, 1962, p 31-86.
- 29 Oki, M. *Applications of Dynamic NMR Spectroscopy to Organic Chemistry*; VCH, Florida, 1985, p 407.
- 30 Hanson, J. C.; Nordman, C. E. *Acta Crystallogr., Sect. B*, **1976**, *32*, 1147.
- 31 Sygula, A.; Folsom, H. E.; Sygula, R.; Abdourazak, A. H.; Marcinow, Z.; Fronczek, F. R.; Rabideau, P. W. *J. Chem. Soc., Chem. Comm.*, **1994**, *22*, 2571.
- 32 Feist, F.; Belart, H. *Chem. Berichte*, **1895**, *28*, 1823.

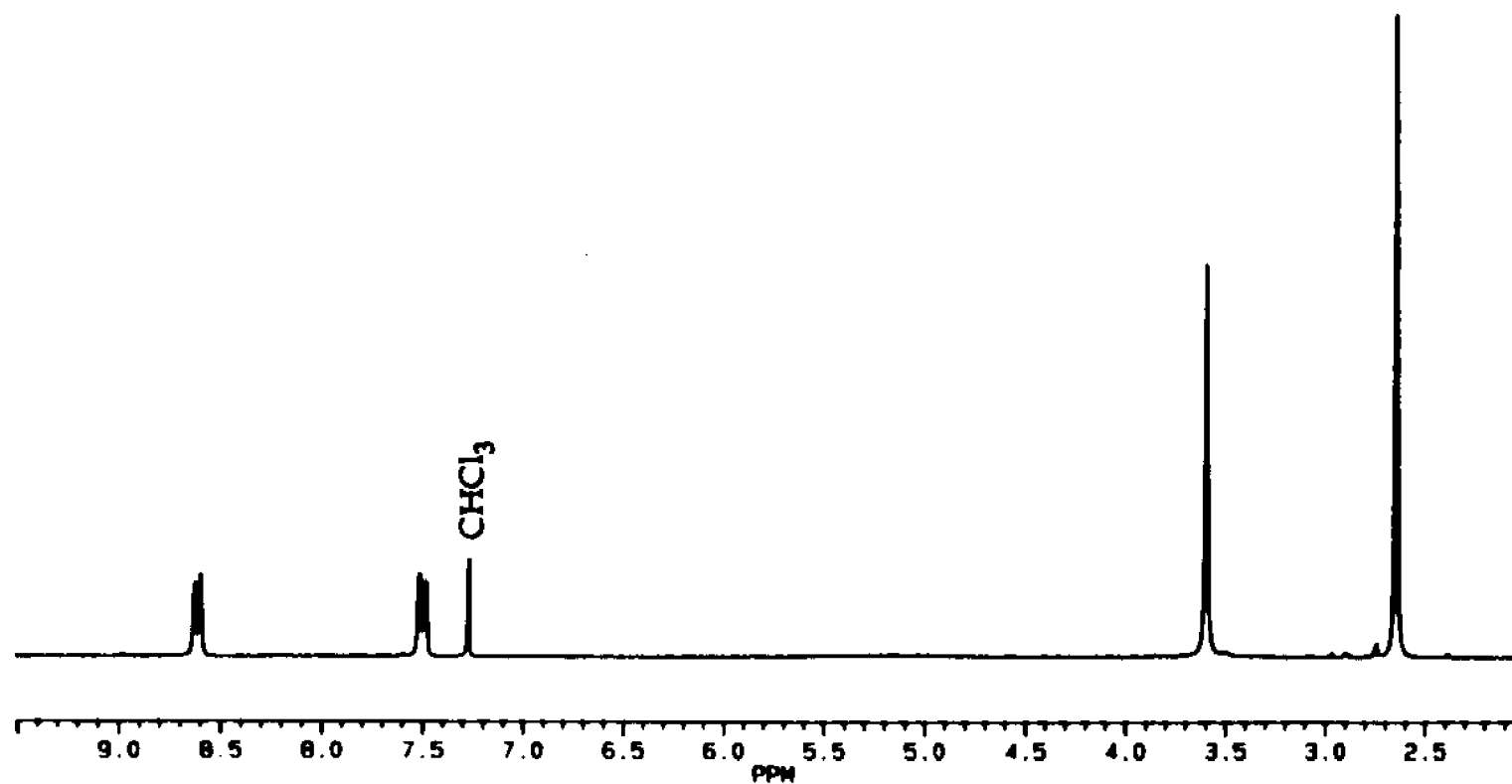
- 33 Diederich, F.; Rubin, Y. *Angew. Chem. Internat. Ed. Engl.* **1992**, *31*, 1101.
- 34 McElvany, S. W.; Ross, M. M.; Goroff, N. S.; Diederich, F. *Science*, **1993**, *259*, 1594.
- 35 Faust, R.; Volhardt, K. P. C. *J. Chem. Soc. Chem. Commun.* **1993**, 1471.
- 36 Mehta, G.; Shah, R. S.; Ravikumar, K. *J. Chem. Soc., Chem. Comm.* **1993**, 1006.
- 37 Sastry, G. N.; Jemmis, E. D.; Mehta, G.; Shah, S. R. *J. Chem. Soc., Perkin Trans. 2*, **1993**, 1867.
- 38 Loguercio, D., PhD. Thesis, UCLA, Los Angeles, CA, **1988**.
- 39 Sbrogio, F.; Fabris, F.; De Lucchi, O. *Synlett.*, **1994**, *9*, 761.
- 40 Zimmerman, G.; Nuechter, U.; Hagen, S.; Nuechter, M. *Tetrahedron Lett.* **1994**, *35*, 7013.
- 41 Trost, B. M. *J. Am. Chem. Soc.*, **1966**, *88*, 853.
- 42 Abdourazak, A. H.; Marcinow, Z.; Folsom, H. E.; Fronczek, F. R.; Sygula, R.; Sygula, A.; Rabideau, P. R. *Tetrahedron Lett.* **1994**, *35*, 3857.
- 43 Rabideau, P. W.; Abdourazak, A. H.; Folsom, F. E.; Marcinow, Z.; Sygula, A.; Sygula, R. *J. Am. Chem. Soc.* **1994**, *116*, 7891.
- 44 Stone, A. J.; Wales, D. J. *Chem. Phys. Lett.* **1986**, *128*, 501.
- 45 Hawkins, J. M.; Nambu, M.; Meyer, A. *J. Am. Chem. Soc.* **1994**, *116*, 7642.
- 46 Heggie, M. I.; Latham, C. D.; Jones, R.; Briddon, P. R. in *Recent Advances in the Chemistry and Physics of Fullerenes and Related Materials*: Vol. 2, Ed. K. M. Kadish, R. S. Ruoff, The Electrochemical Society, Pennigton, **1995**.
- 47 Scott, L. T. Summaries of FY 1994, Research in Chemical Sciences; U.S. Department of Energy, Office of Energy Research, Division of Chemical Sciences
- 48 Dhar, R. J.; Marcinow, Z.; Rabideau, P. W. unpublished results.

- 49 Jonescu, M. *Ber. Dtsch. Chem. Ges.* **1927**, 60, 1228.
- 50 *C&E News*, April 19, **1993**, 32.
- 51 *C & E News*, August 22, **1994**, 7.
- 52 *New Scientist*(U.K.), January 7, **1995**, 14.
- 53 *Office of Energy Research News*, August **1994**, 4 (4), 1.
- 54 *C&E News*, June 19, **1995**, 22.
- 55 *Science Magazine*, July 21,**1995**, 269, 305-307.

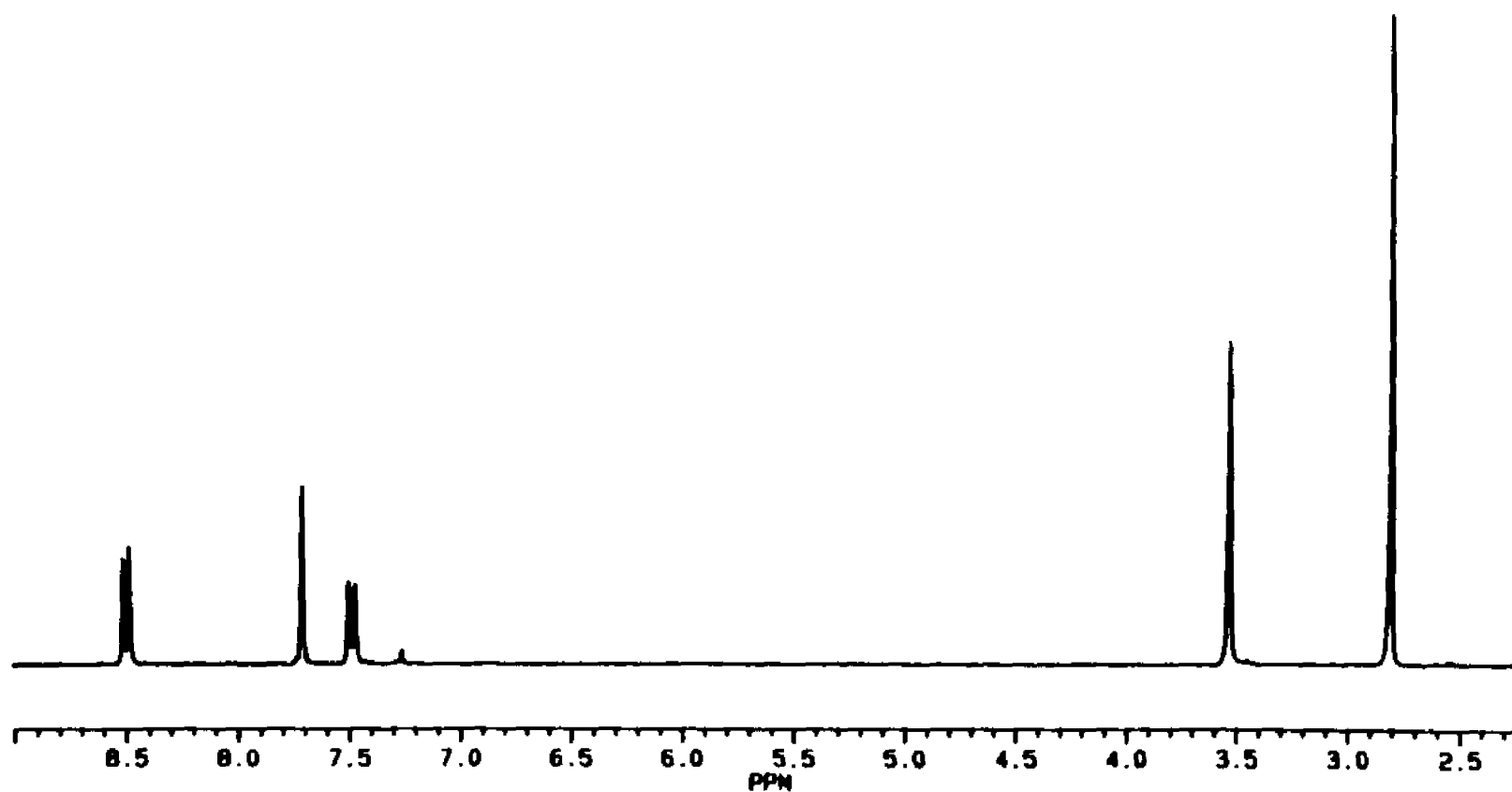
APPENDIXES



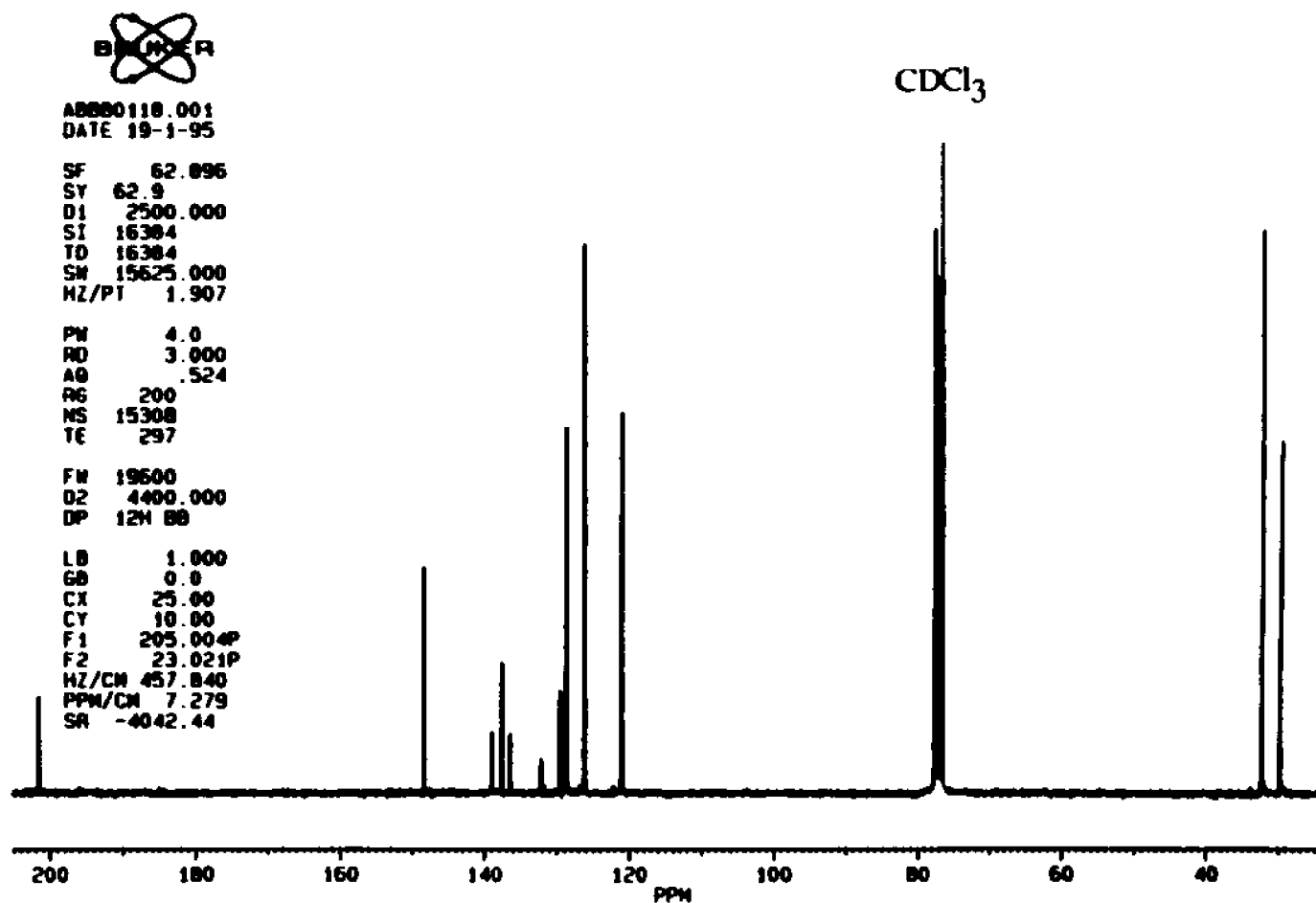
Appendix 1: ^1H NMR spectrum of 5,6-dihydrocyclopenta[f,g]acenaphthylene-1,2-dione, (11).



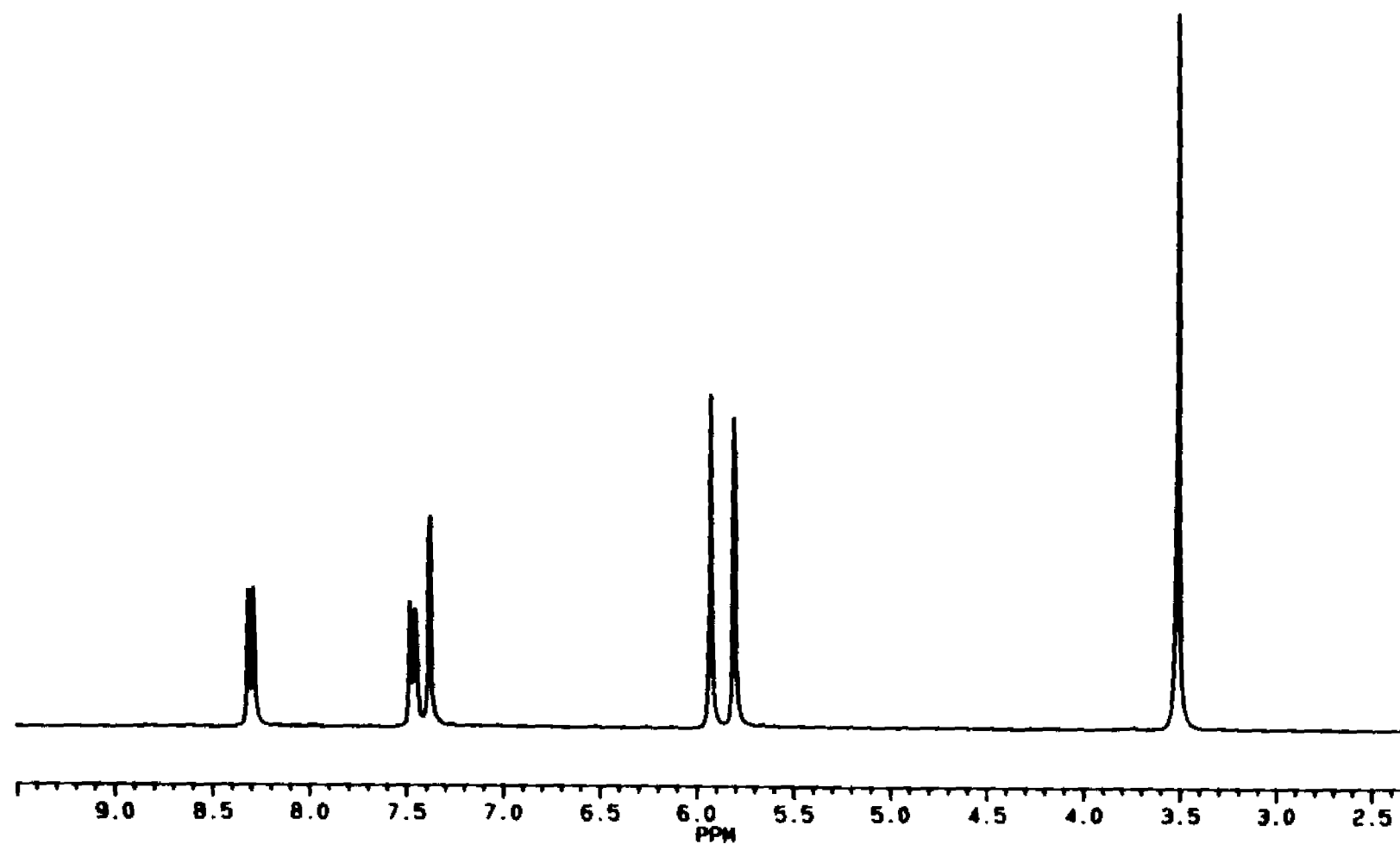
Appendix 2: ^1H NMR spectrum of 5,7-diacetyl-1,2-dihydro-6H-dicyclopenta[a,f]acenaphthylen-6-one, (12).



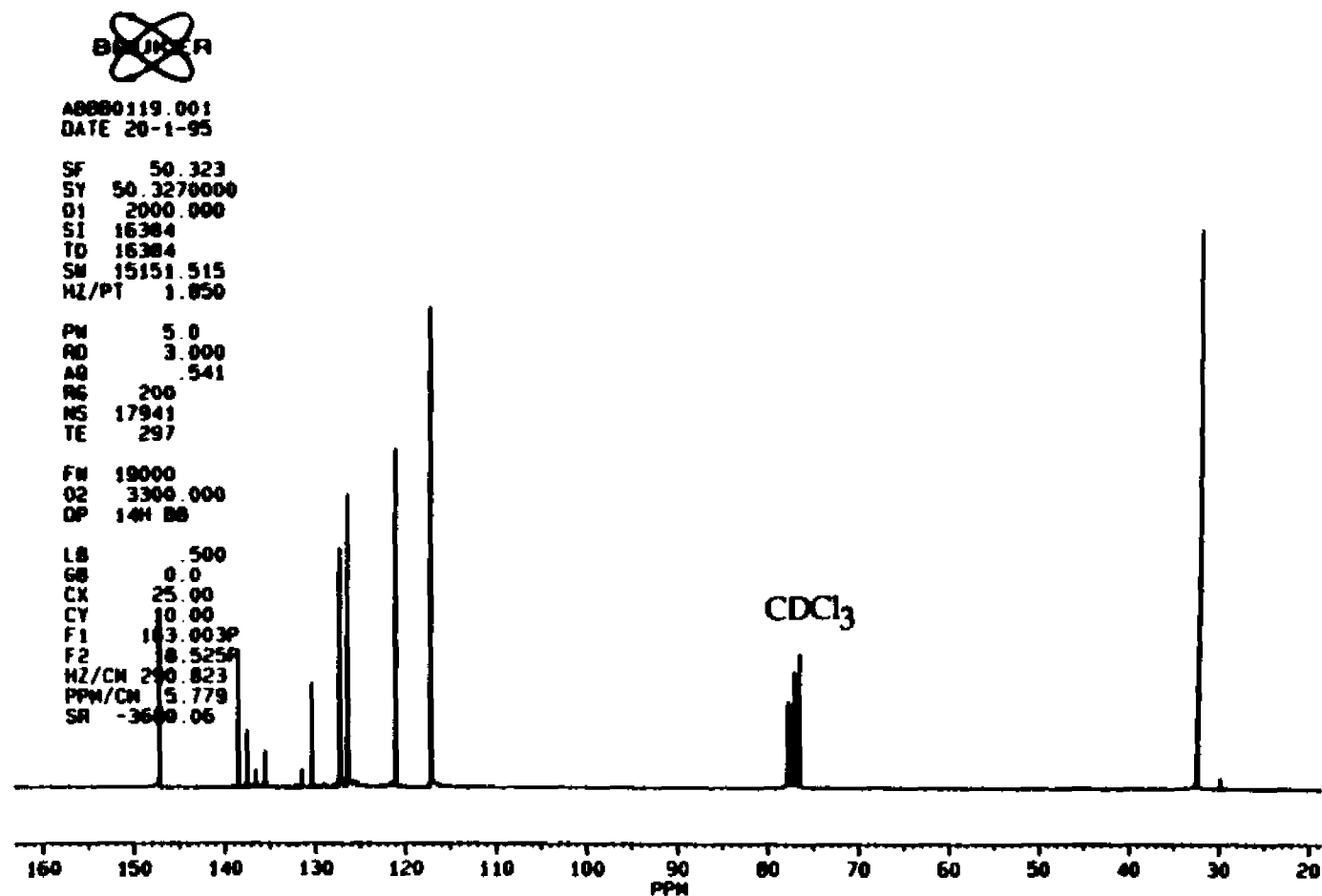
Appendix 3: ^1H NMR spectrum of 1,1'-(1,2-dihydrocyclopenta[*cd*]fluoranthene-5,8-diyl)bis-ethanone, (14).



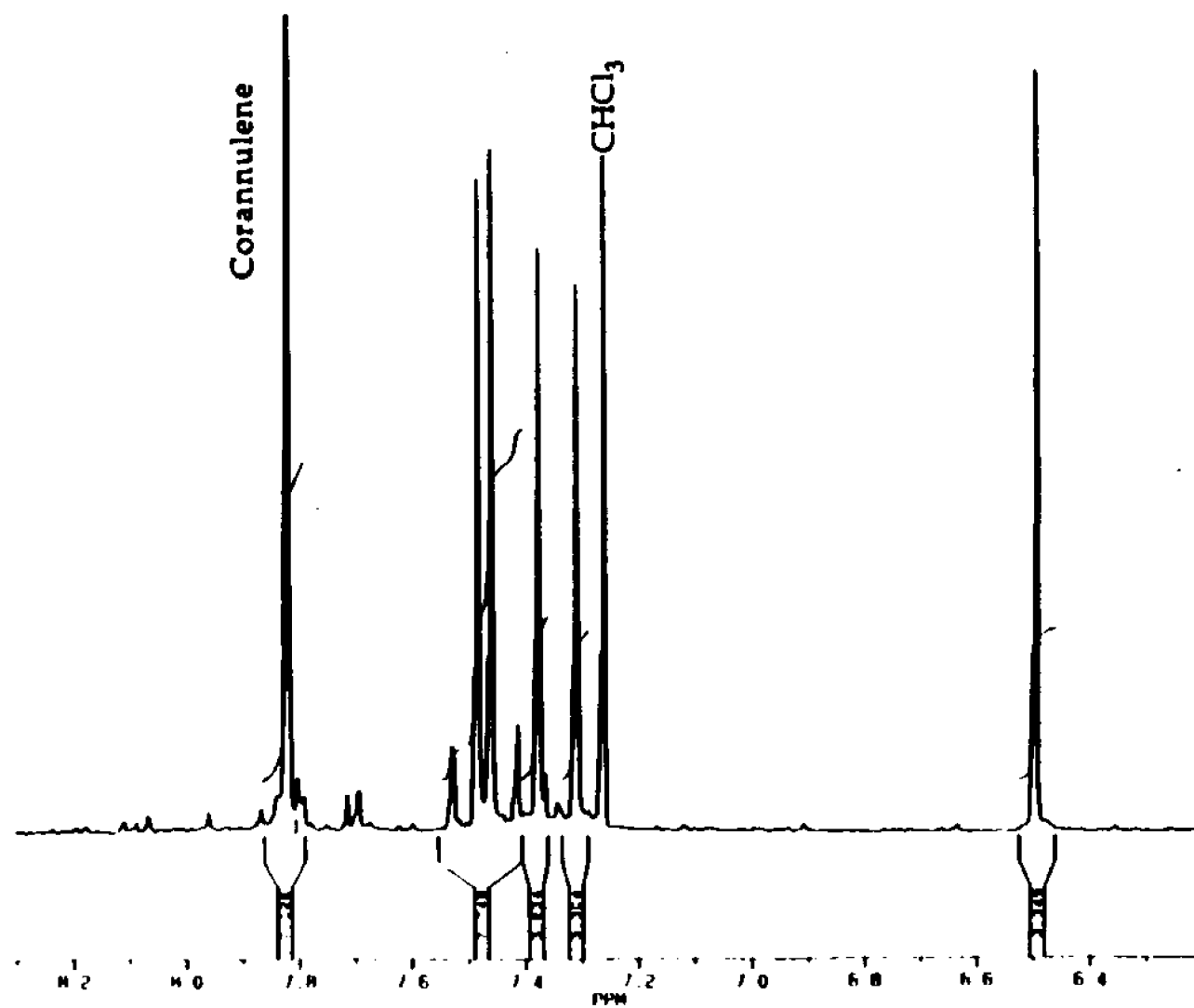
Appendix 4: ¹³C NMR spectrum of 1,1'-(1,2-dihydrocyclopenta[cd]fluoranthene-5,8-diyl)bis-ethanone, (14).



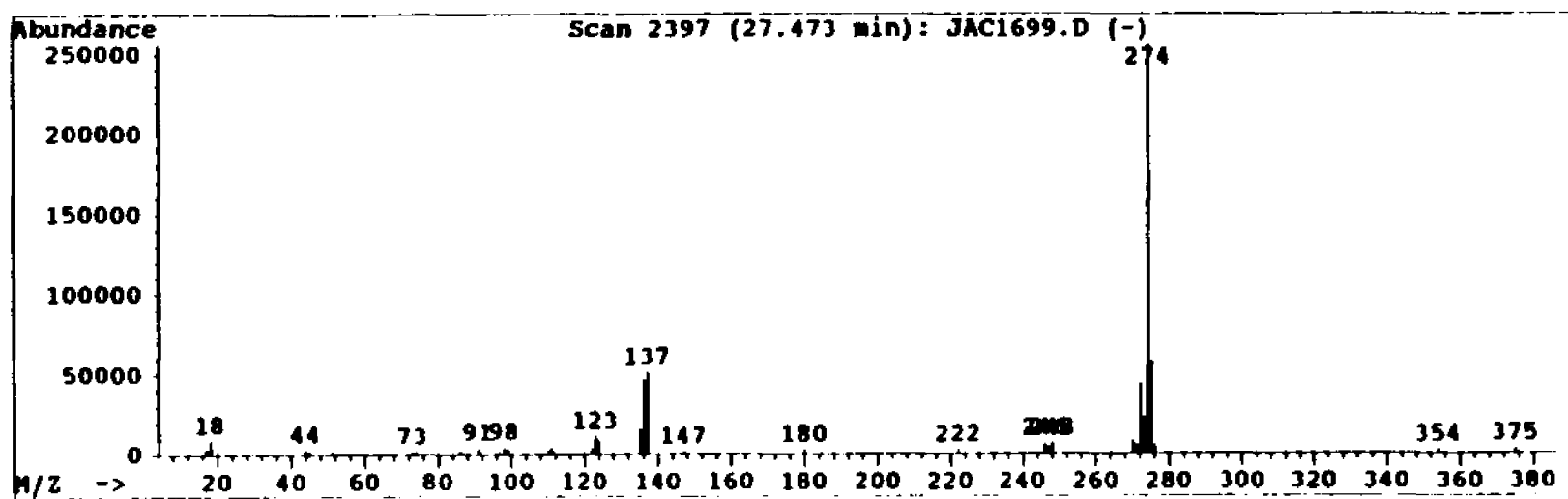
Appendix 5: ^1H NMR spectrum of 5,8-bis(1-chloroethenyl)-1,2-dihydrocyclopenta[cd]fluoranthene, (15).



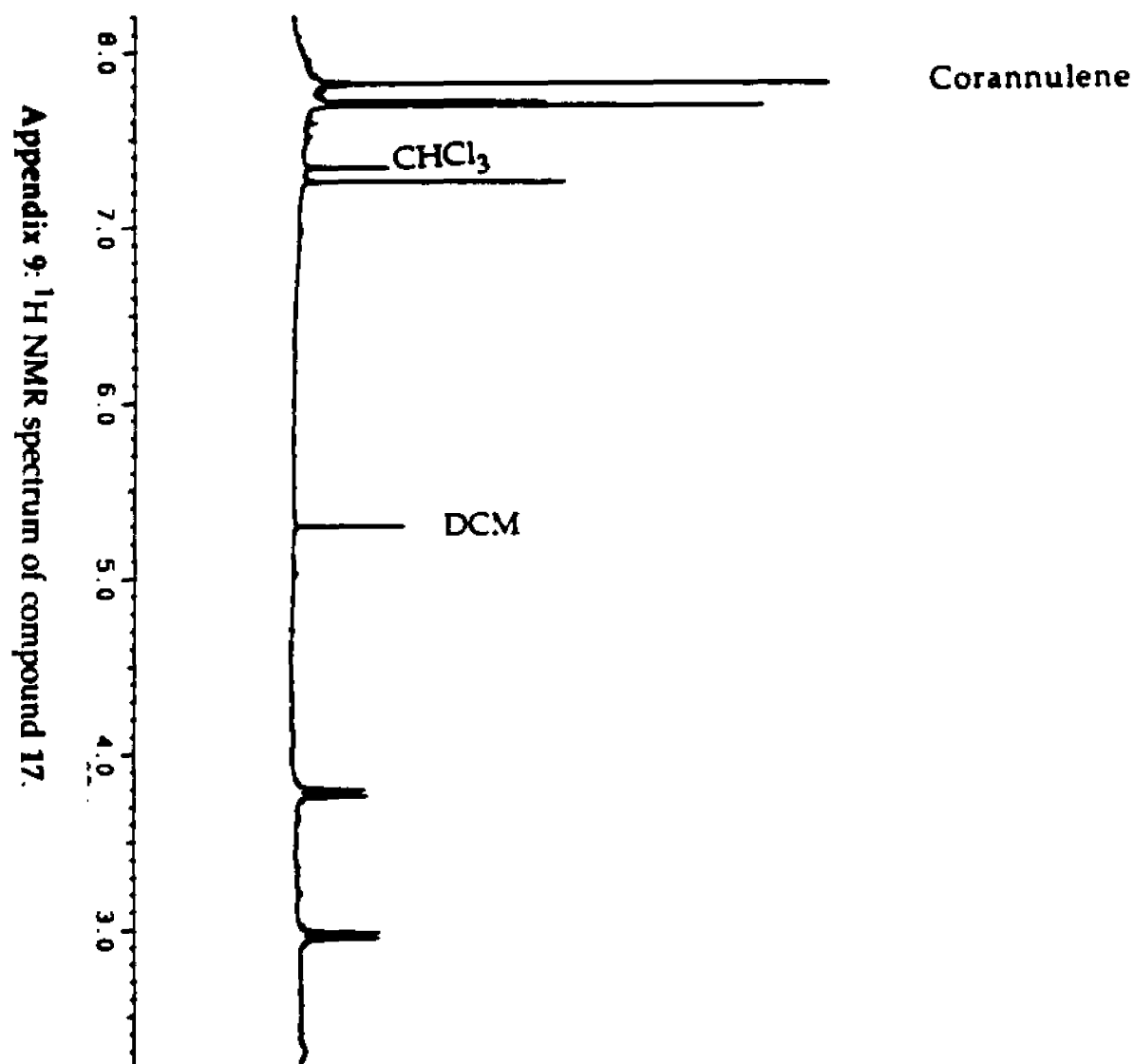
Appendix 6: ¹³C NMR spectrum of 5,8-bis(1-chloro-ethenyl)-1,2-dihydrocyclopenta[cd]fluoranthene, (15).



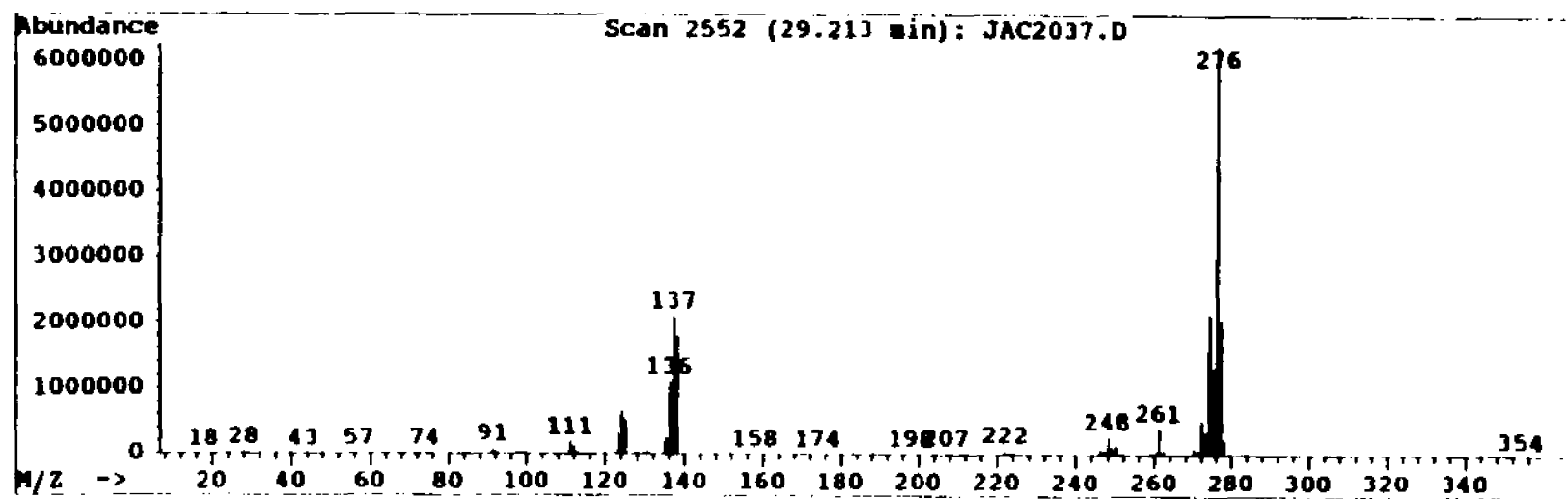
Appendix 7: ^1H NMR spectrum of dibenzo[ghi, mno]cyclopenta[cd]fluoranthene, (16).



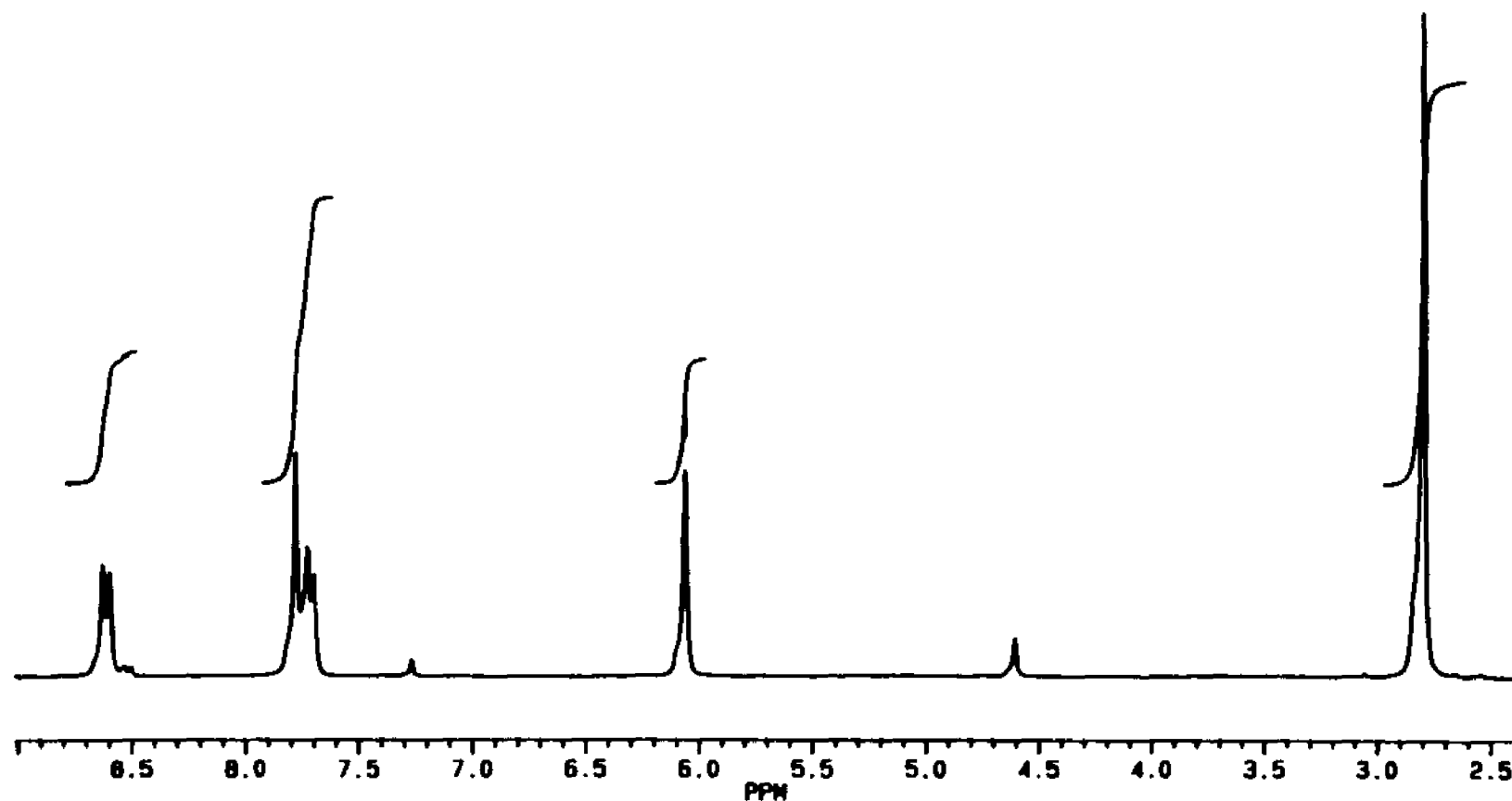
Appendix B: GC/MS spectrum of dibenzo[ghi, mno]cyclopenta[cd]fluoranthene, (16).



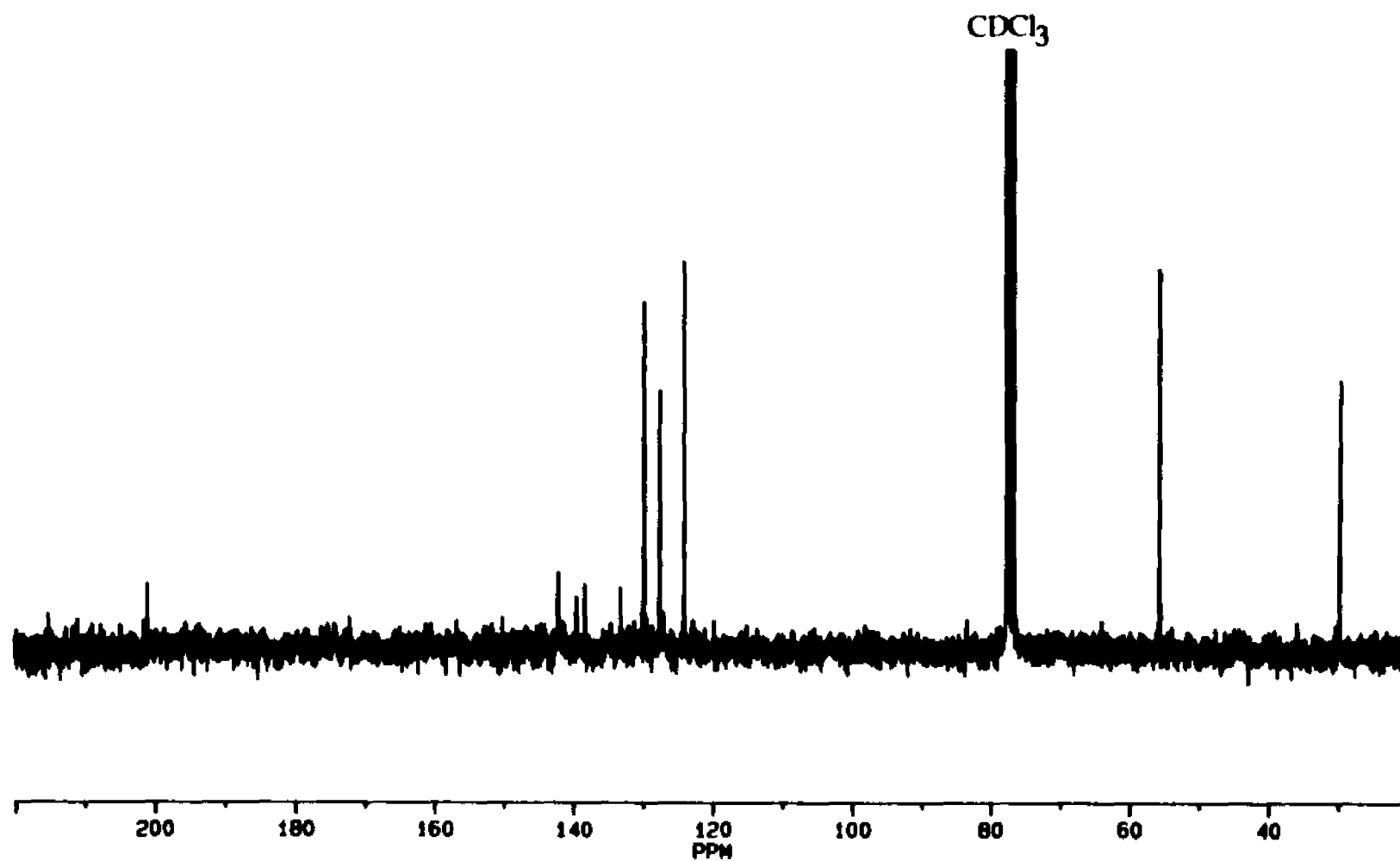
Appendix 9: ^1H NMR spectrum of compound 17.



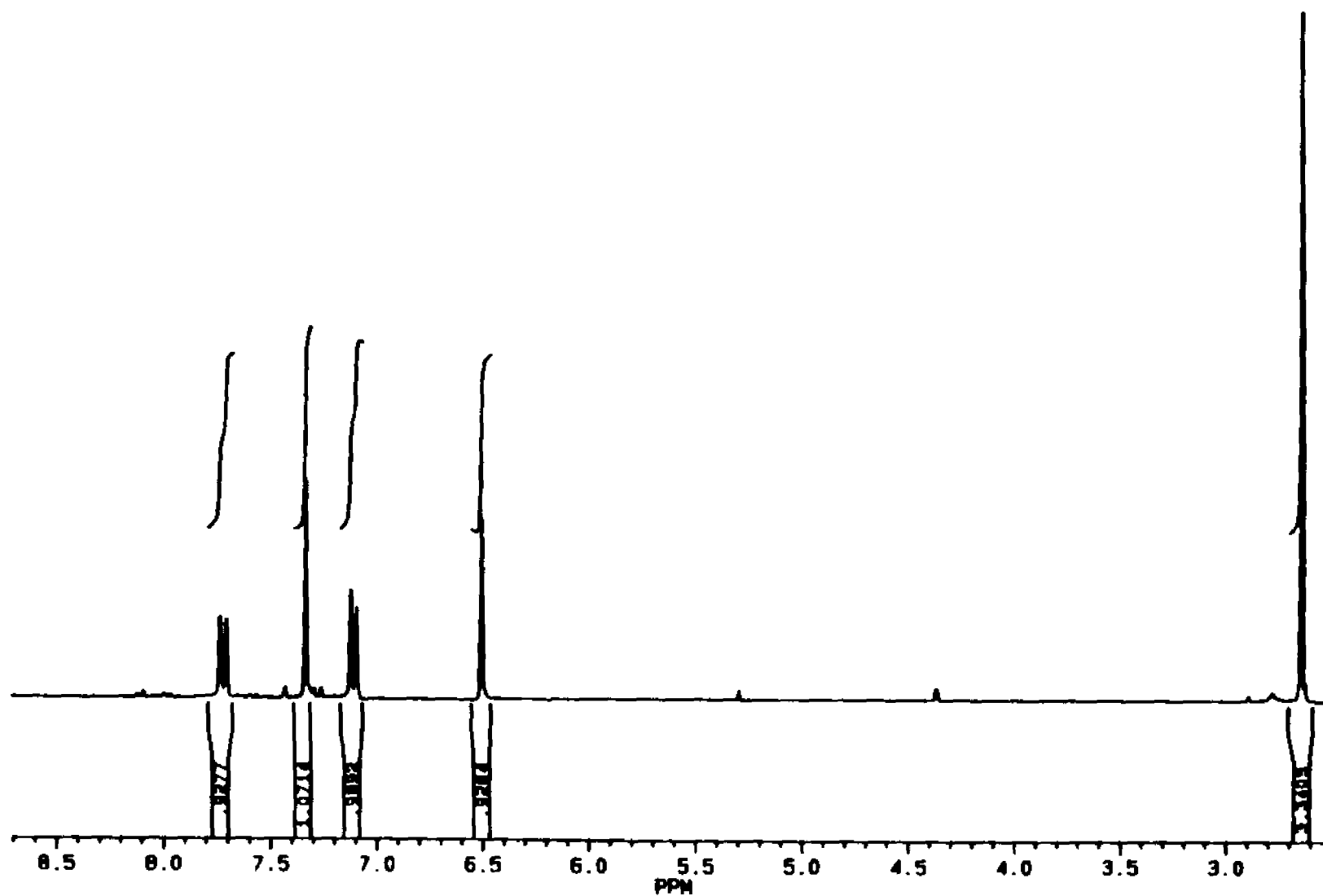
Appendix 10: GC/MS spectrum of compound 17.



Appendix 11: ^1H NMR spectrum of 7,10-diacetyl-3,4-(1,2-dibromoethano)fluoranthene, (18).



Appendix 12: ^{13}C NMR spectrum of 7,10-diacetyl-3,4-(1,2-dibromoethano)fluoranthene, (18).



Appendix 13: ^1H NMR spectrum of 7,10-diacetyl-3,4-ethenofluoranthene, (19).



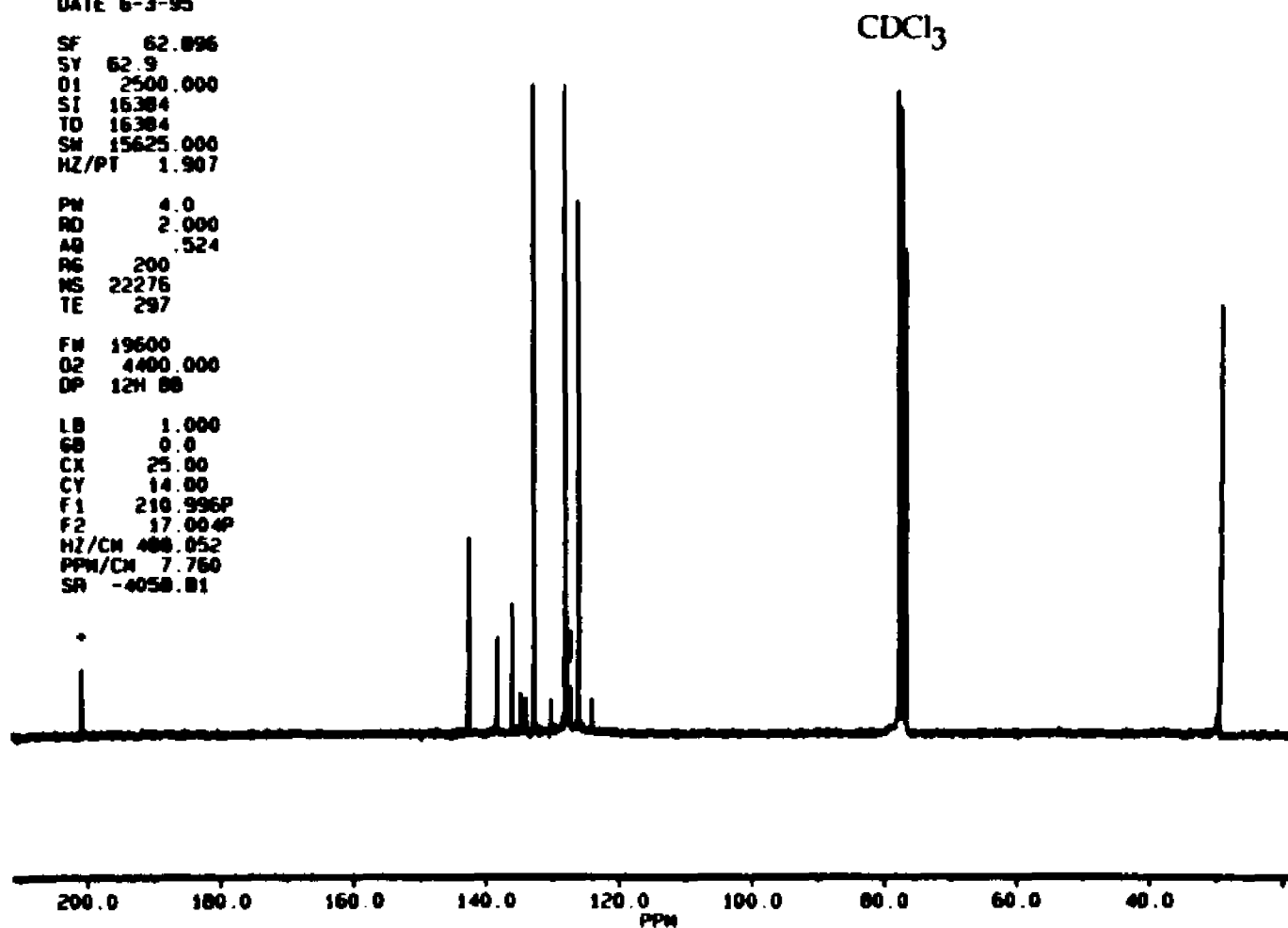
AB000305.001
DATE 6-3-95

SF 62.896
SY 62.9
OI 2500.000
SI 16384
TD 16384
SN 15625.000
HZ/PT 1.907

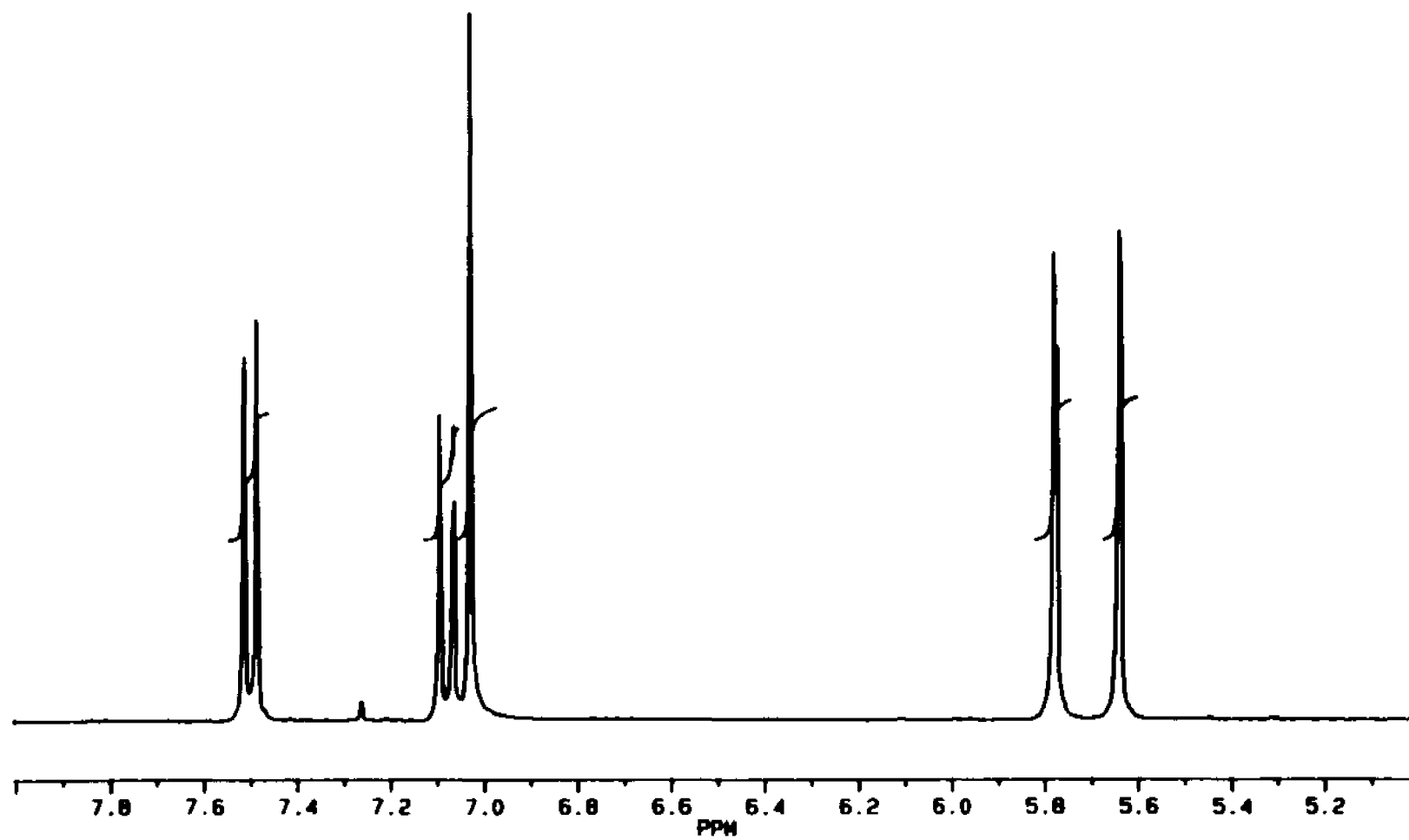
PN 4.0
RD 2.000
AQ .524
RG 200
NS 22276
TE 297

FW 19600
OZ 4400.000
OP 12H 00

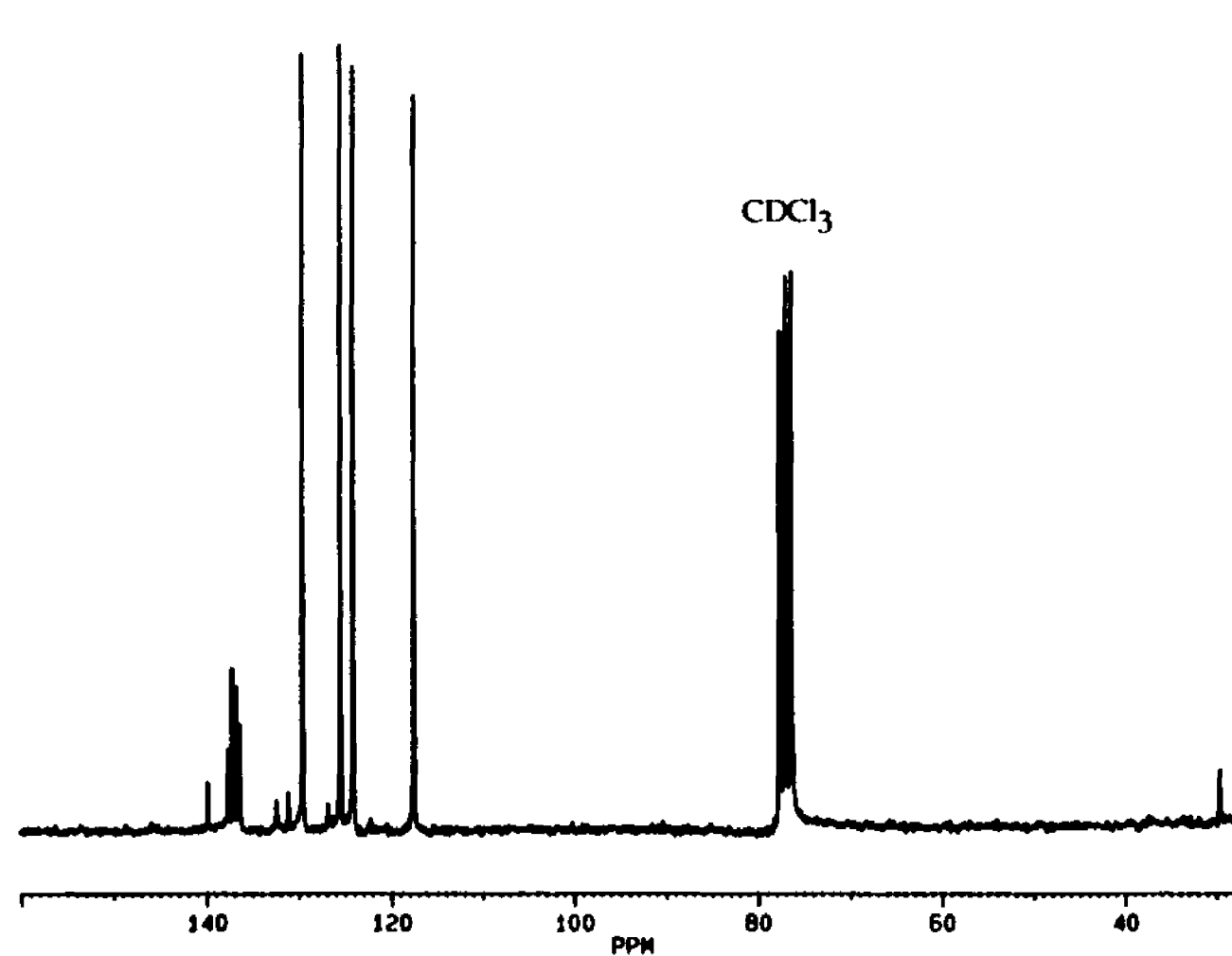
LB 1.000
GB 0.0
CX 25.00
CY 14.00
F1 210.996P
F2 17.004P
HZ/CM 400.052
PPM/CM 7.760
SR -4050.01




Appendix 14: ¹³C NMR spectrum of 7,10-diacetyl-3,4-ethenofluoranthene, (19).

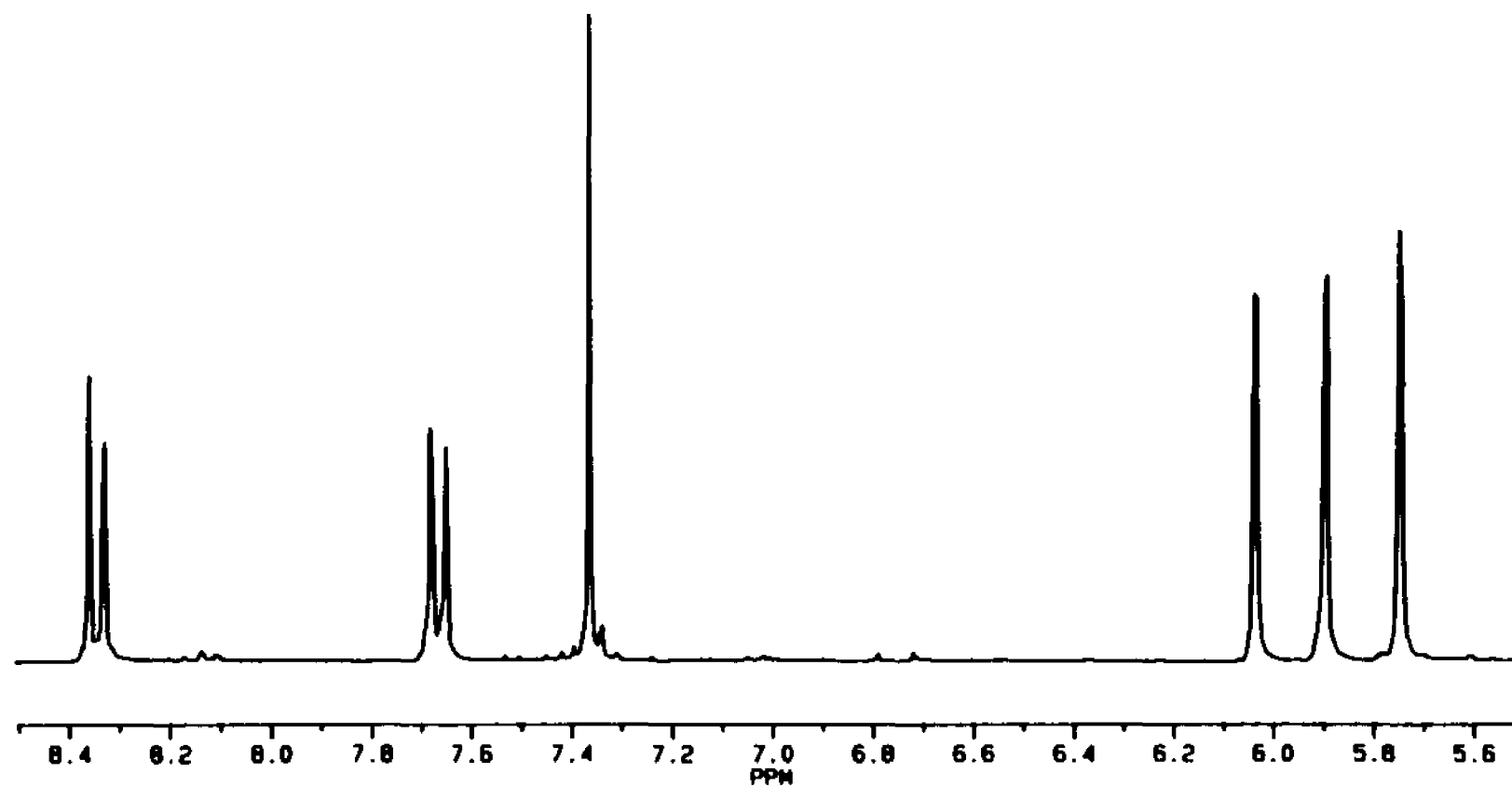


Appendix 15: ^1H NMR spectrum of compound 20.

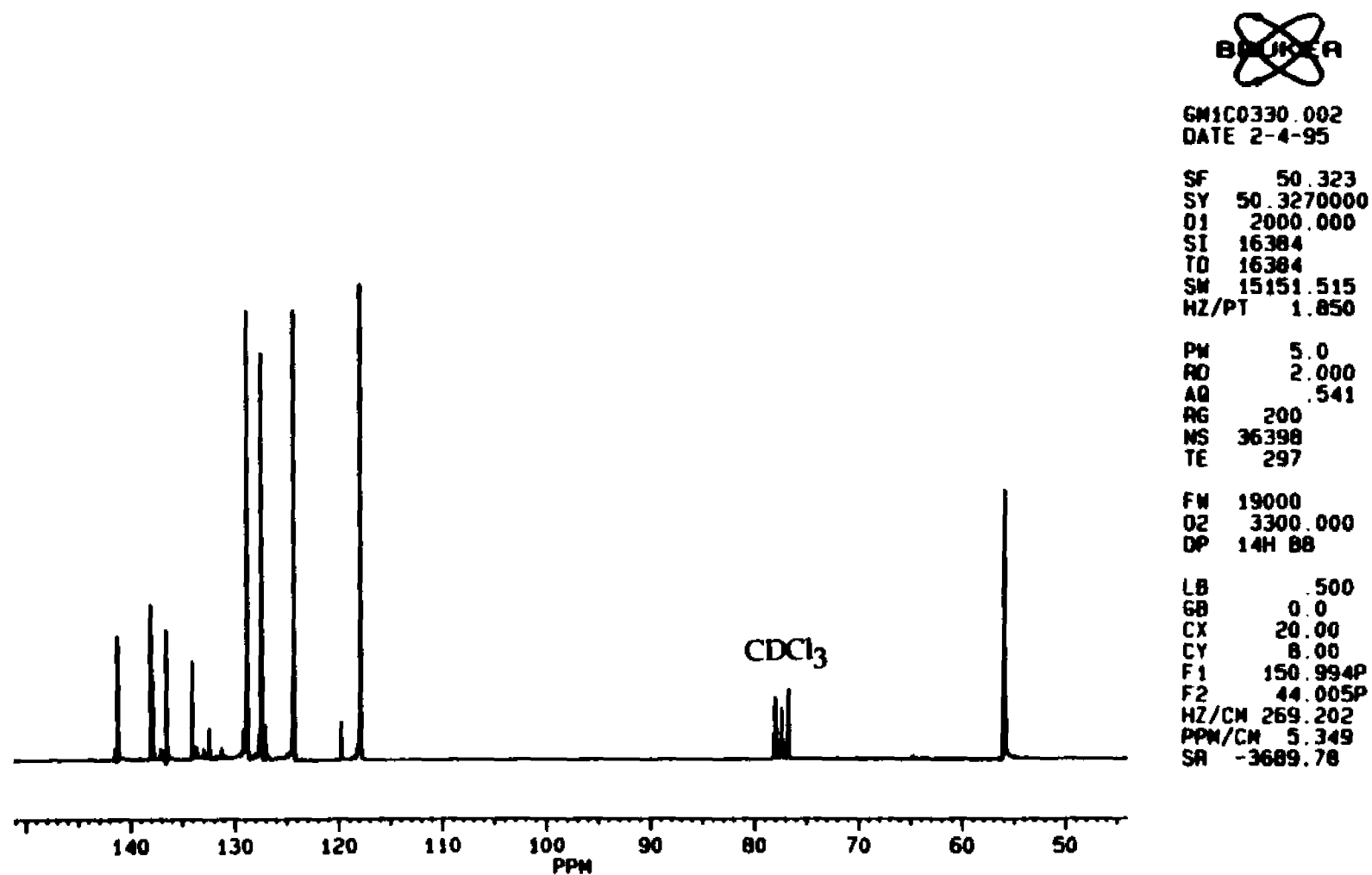



 AB00324.001
 DATE 25-3-95
 SF 50.323
 SY 50.3270000
 O1 2000.000
 S1 16384
 TD 16384
 SN 15151.515
 HZ/PT 1.850
 PW 5.0
 RD 2.000
 AQ .541
 RG 200
 NS 25767
 TE 297
 FN 19000
 O2 3300.000
 OP 14H 88
 LB 2.000
 GB 0.0
 CX 20.00
 CY 12.00
 F1 160.026P
 F2 27.052P
 HZ/CM 334.584
 PPM/CM 6.649
 SR -3683.76

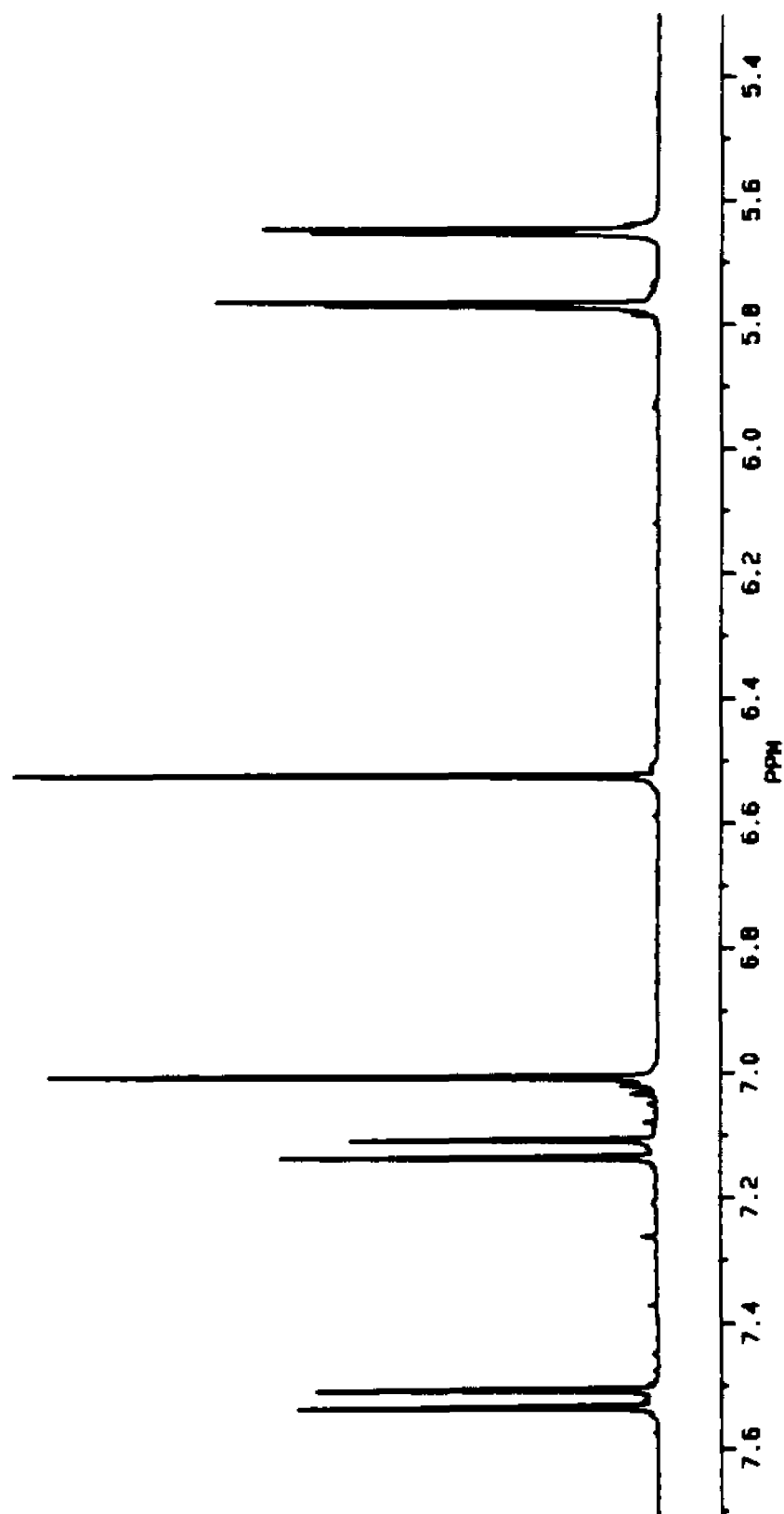
Appendix 16: ^{13}C NMR spectrum of compound 20.



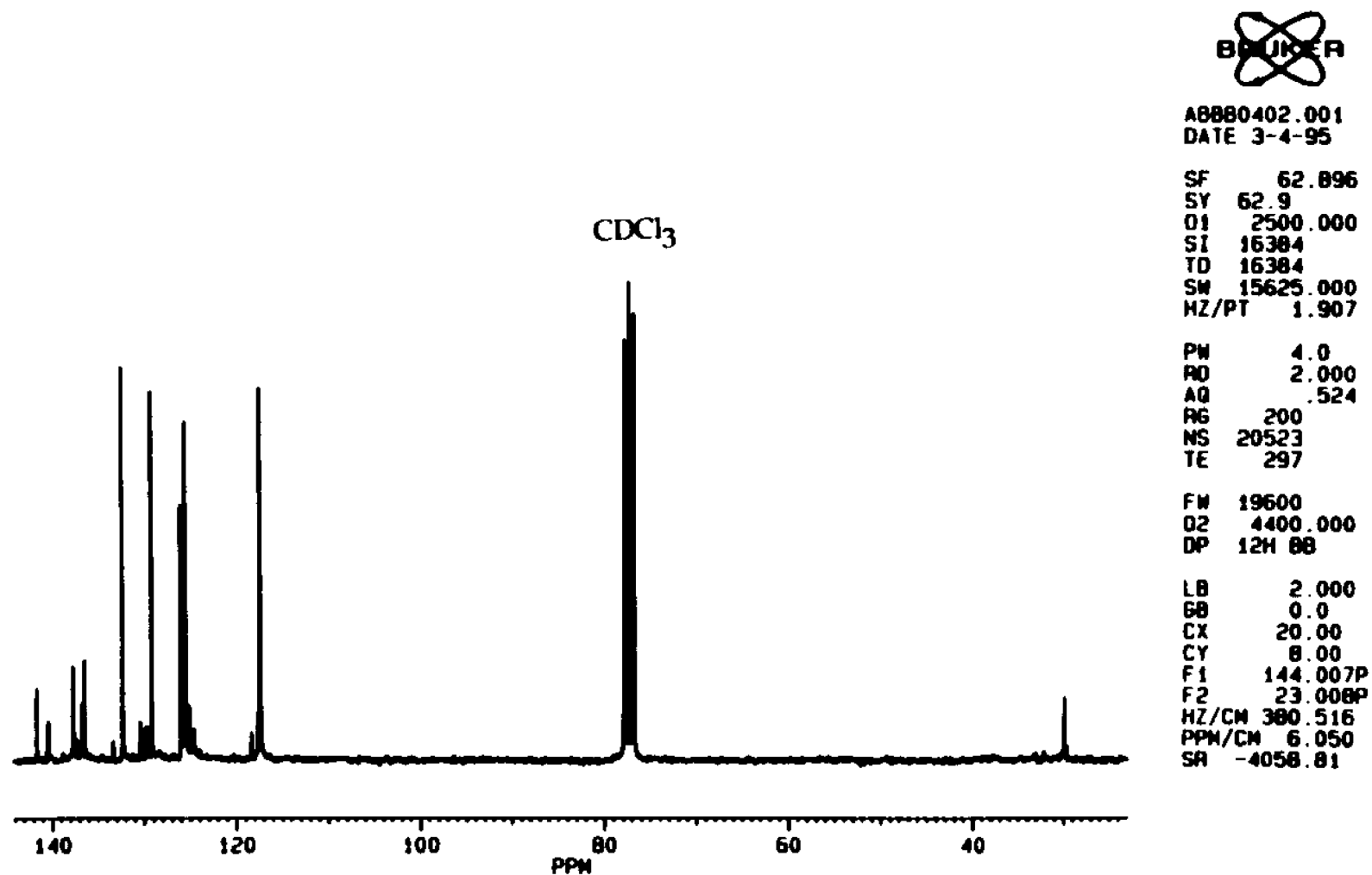
Appendix 17: ^1H NMR spectrum of 7,10-(1-chloroethenyl)-3,4-(dibromoethano)fluoranthene, (21).



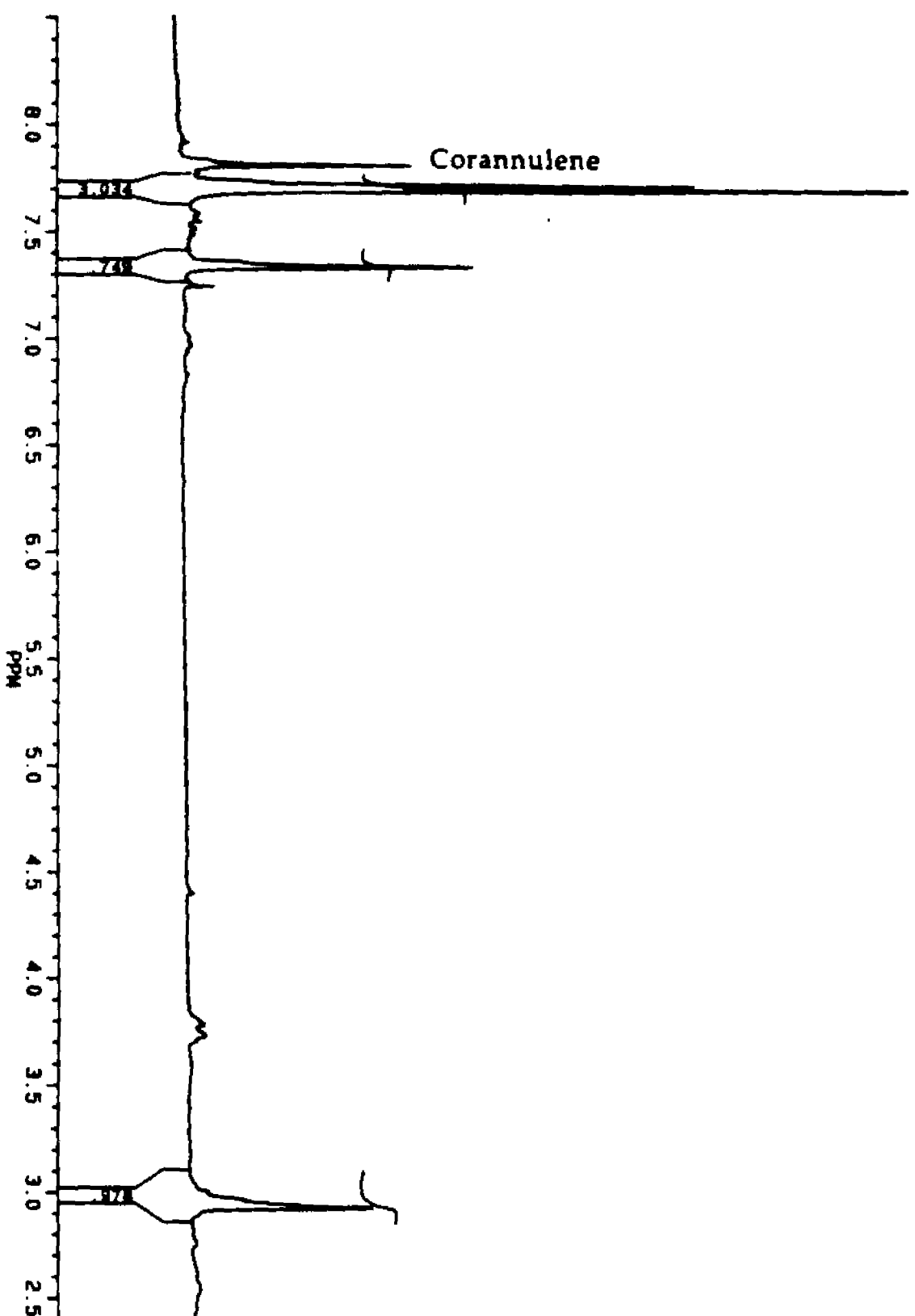
Appendix 18: ^{13}C NMR spectrum of 7,10-(1-chloroethyl)-3,4-(dibromoethano)fluoranthene, (21).



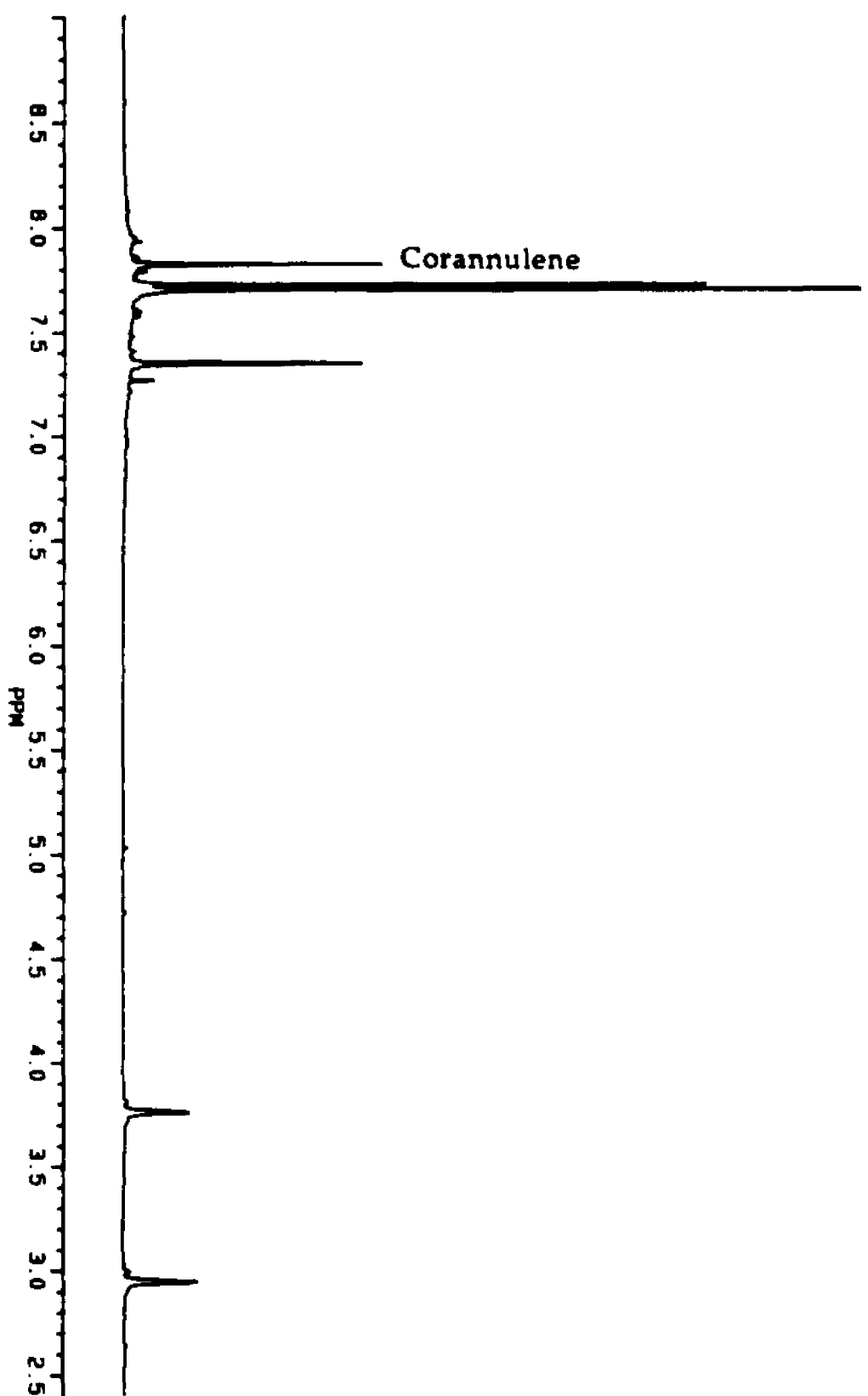
Appendix 19: ^1H NMR spectrum of 7,10-di(1-chloroethenyl)-3,4-ethenofluoranthene, (22).



Appendix 20: ¹³C NMR spectrum of 7,10-di(1-chloroethenyl)-3,4-etheno- fluoranthene, (22).



Appendix 21: ^1H NMR spectrum of 23 before equilibration in CDCl_3 .



Appendix 22: ^1H NMR spectrum of 23 after equilibration in CDCl_3 .



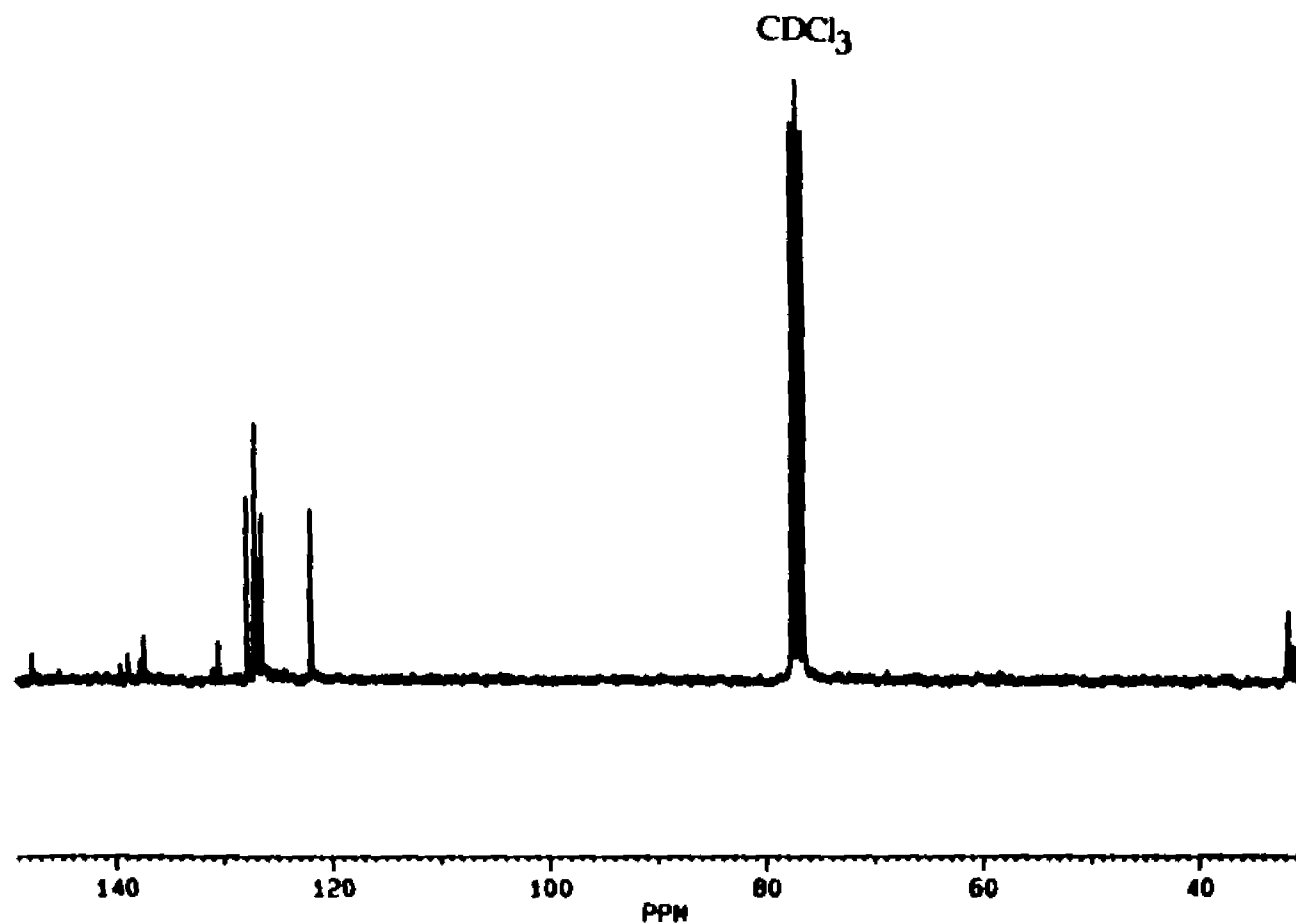
AB00415.001
DATE 15-4-95

SF 62.896
SY 62.9
D1 2500.000
SI 16384
TO 16384
SW 15625.000
HZ/PT 1.907

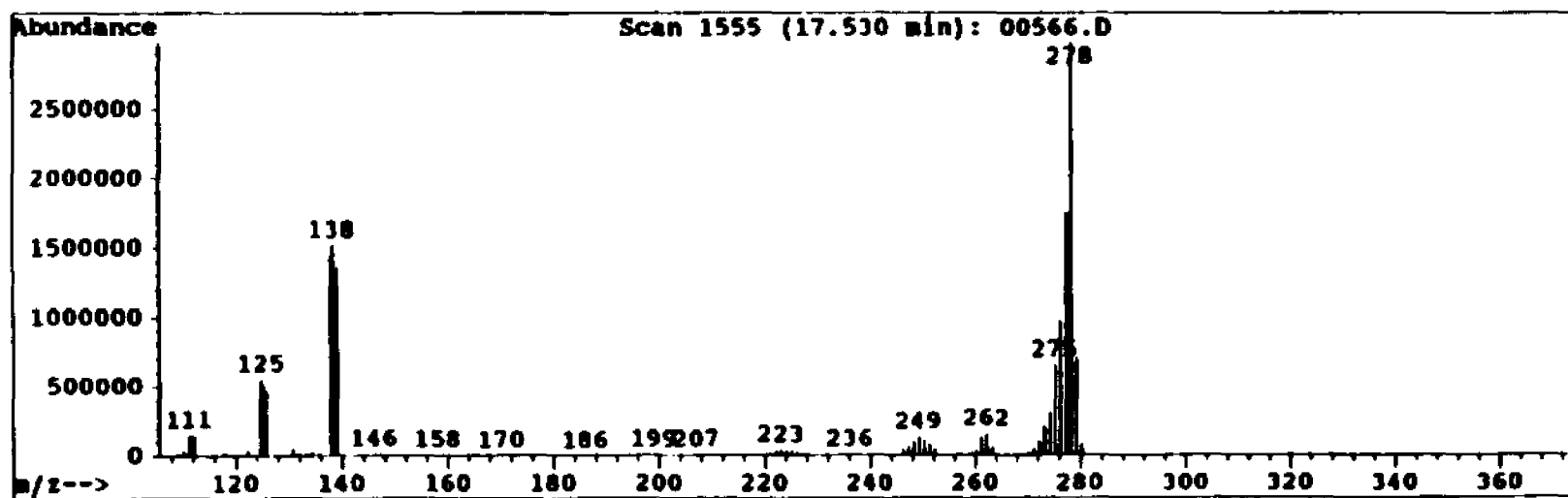
PW 4.0
RD 2.000
AQ .524
RG 200
NS 7221
TE 297

FM 19600
D2 4400.000
DP 12H 88

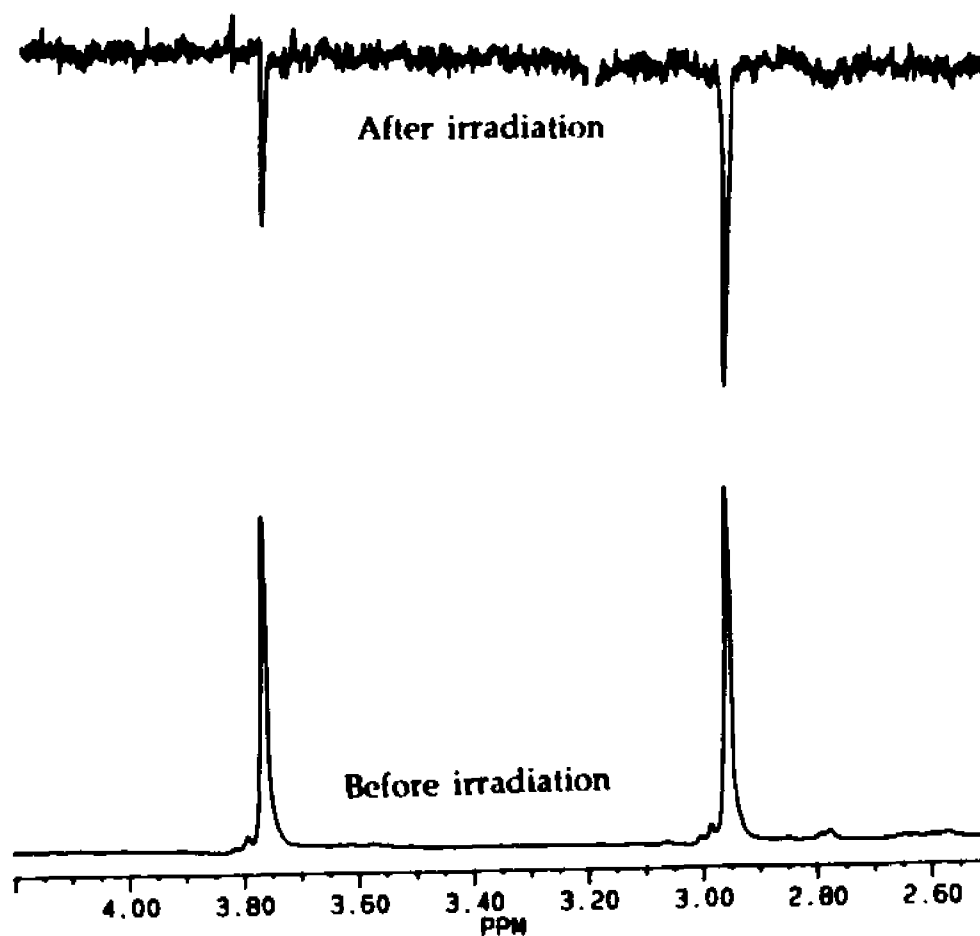
LB 2.000
GB 0.0
CX 20.00
CY 0.00
F1 140.993P
F2 29.814P
HZ/CM 374.794
PPM/CM 5.959
SR -4044.34



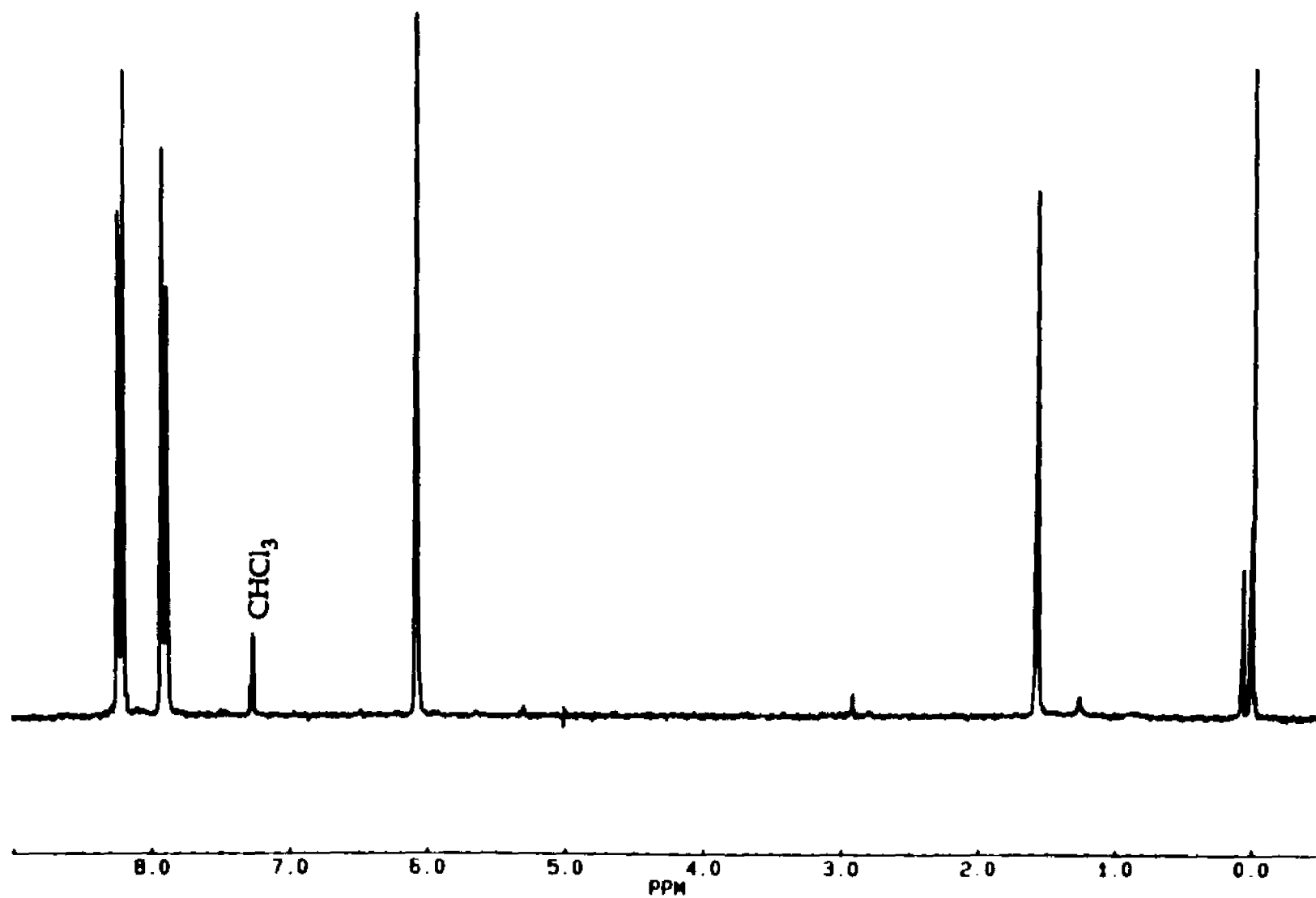
Appendix 23: ¹³C NMR spectrum of 23 after equilibration in CDCl₃.



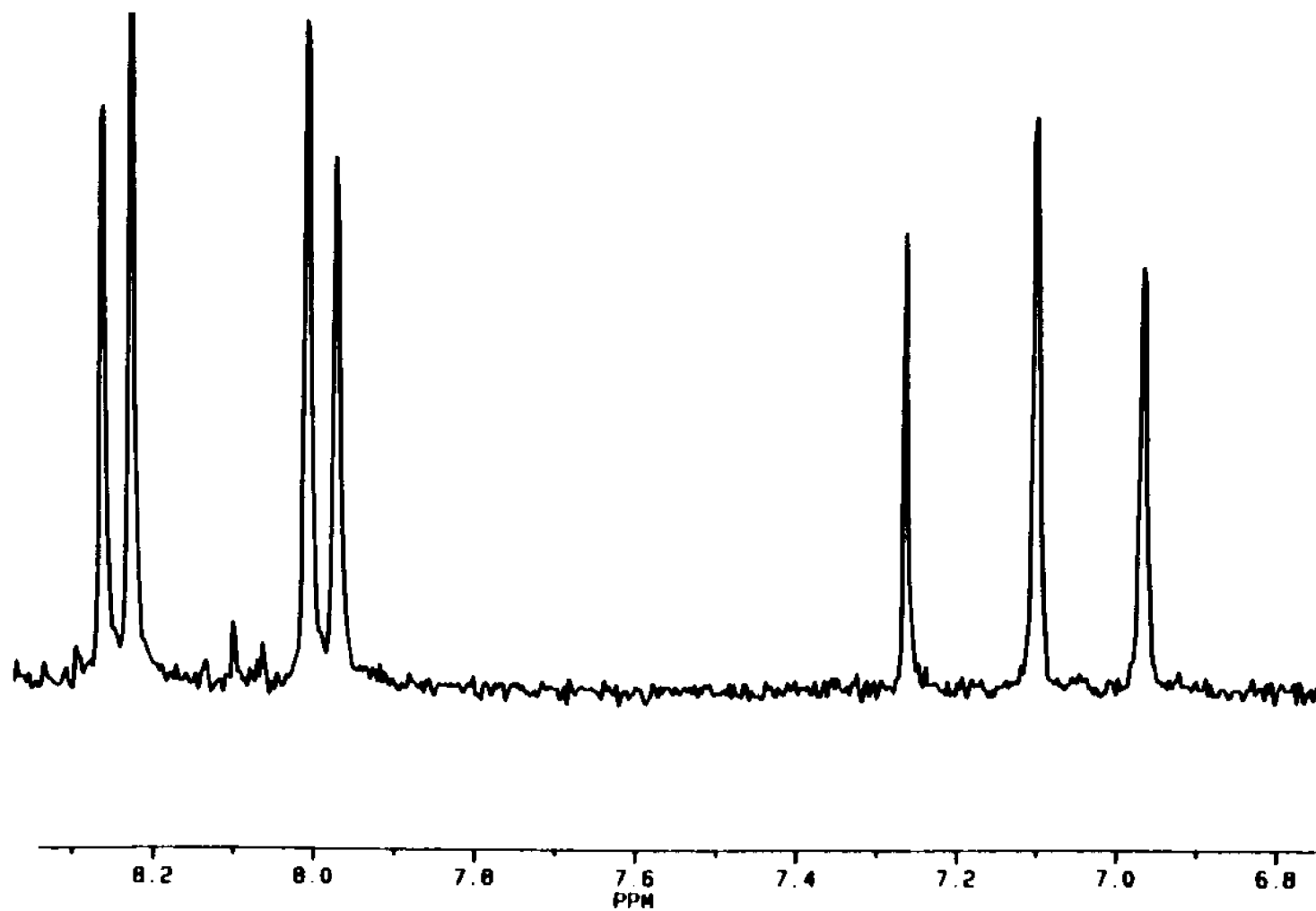
Appendix 24: GC/MS spectrum of 23.



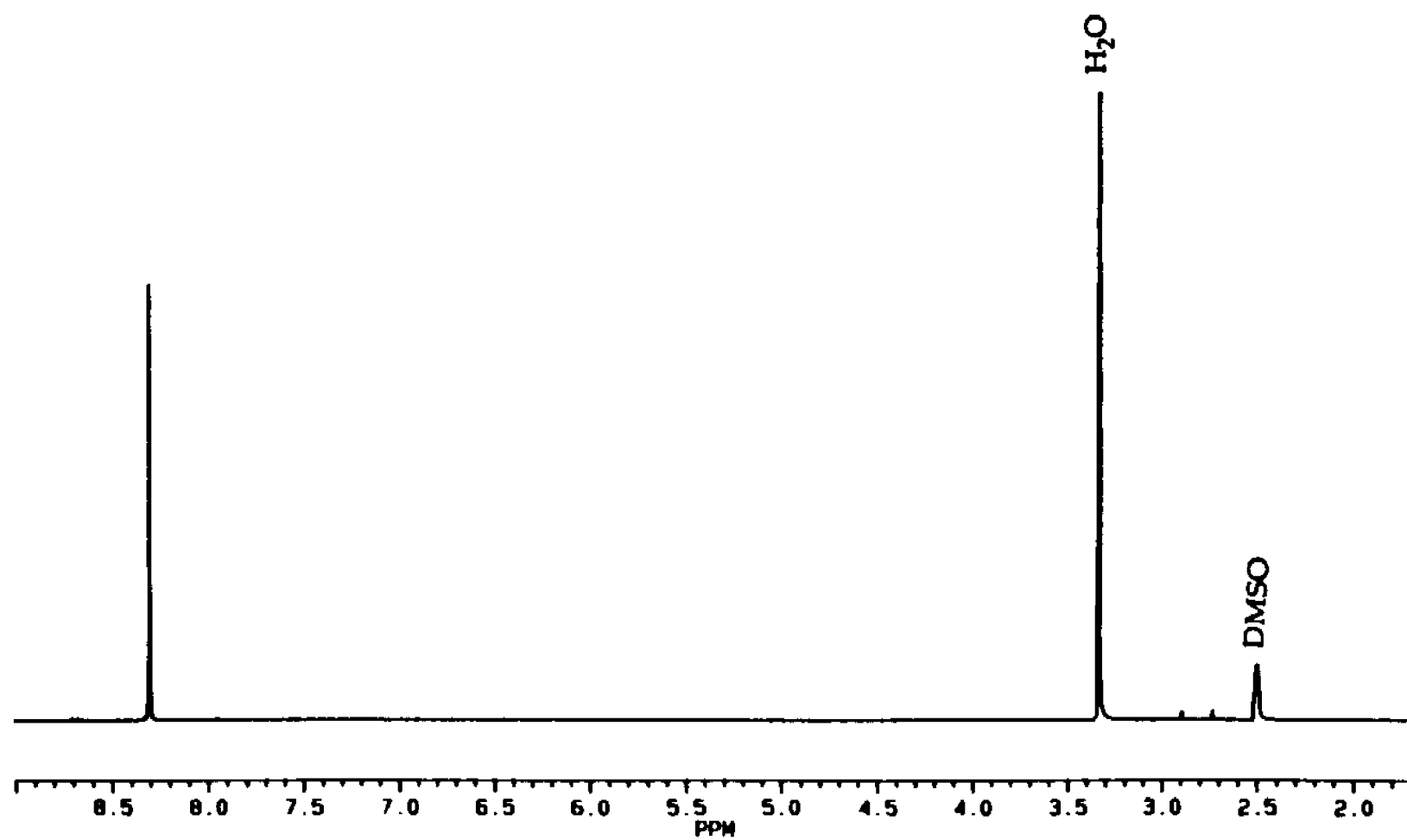
Appendix 25: NOE effect on the benzylic protons of the equilibrated mixture of **23** in CDCl_3 after irradiation of the aromatic proton at 7.32 ppm ($D1 = 5$, $D2 = 5$, $DP = 30L$).



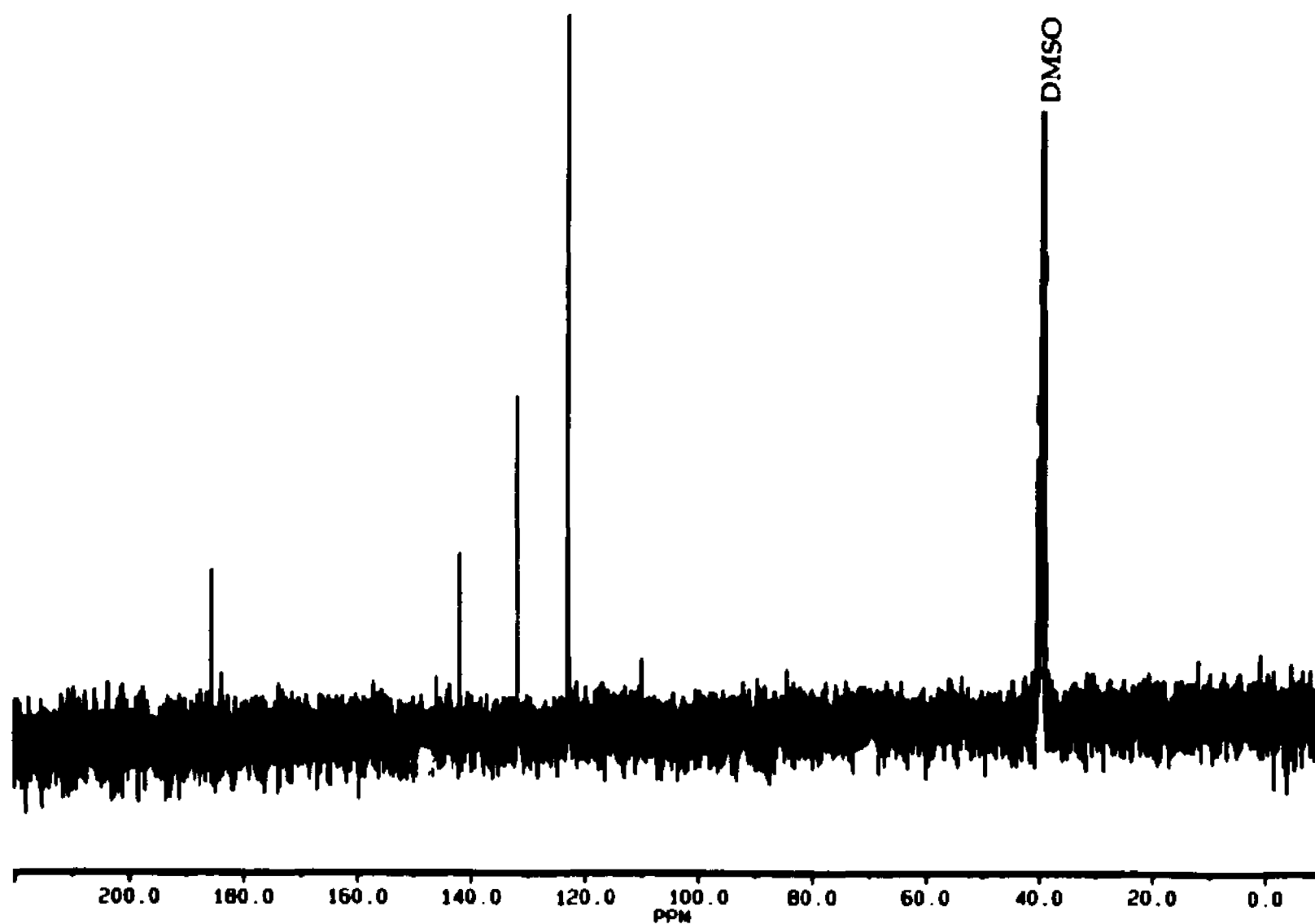
Appendix 26: ^1H NMR spectrum of 5,6-dibromo-5,6-dihydrocyclopent[fg]acenaphthylene-1,2-dione, (33).



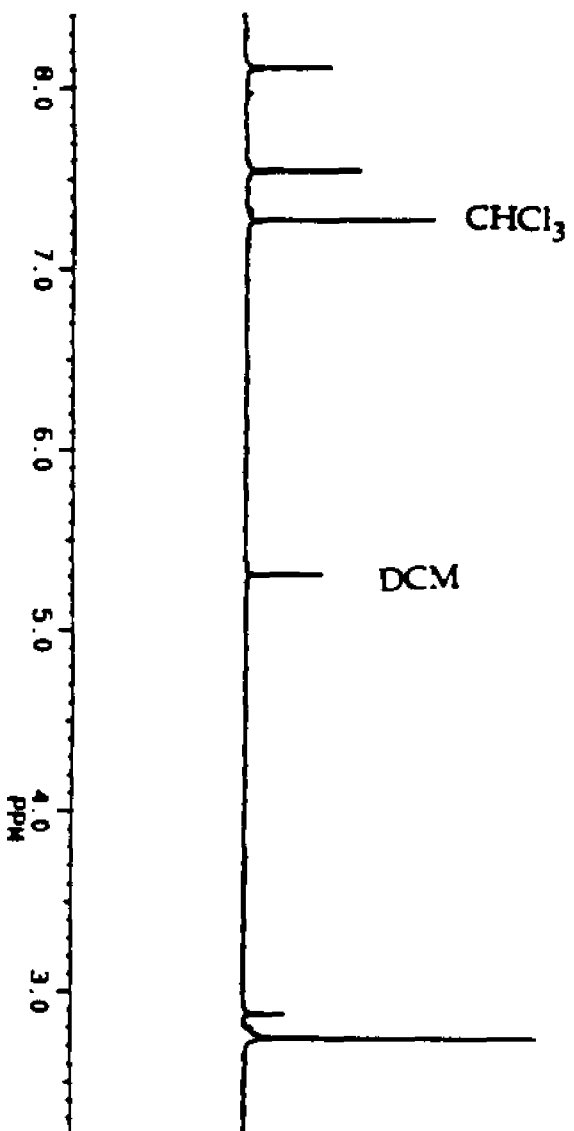
Appendix 27: ^1H NMR spectrum of 5,6-dihydro-5,6-bis(nitrooxy)cyclopent[fg]acenaphthylene-1,2-dione, (34).



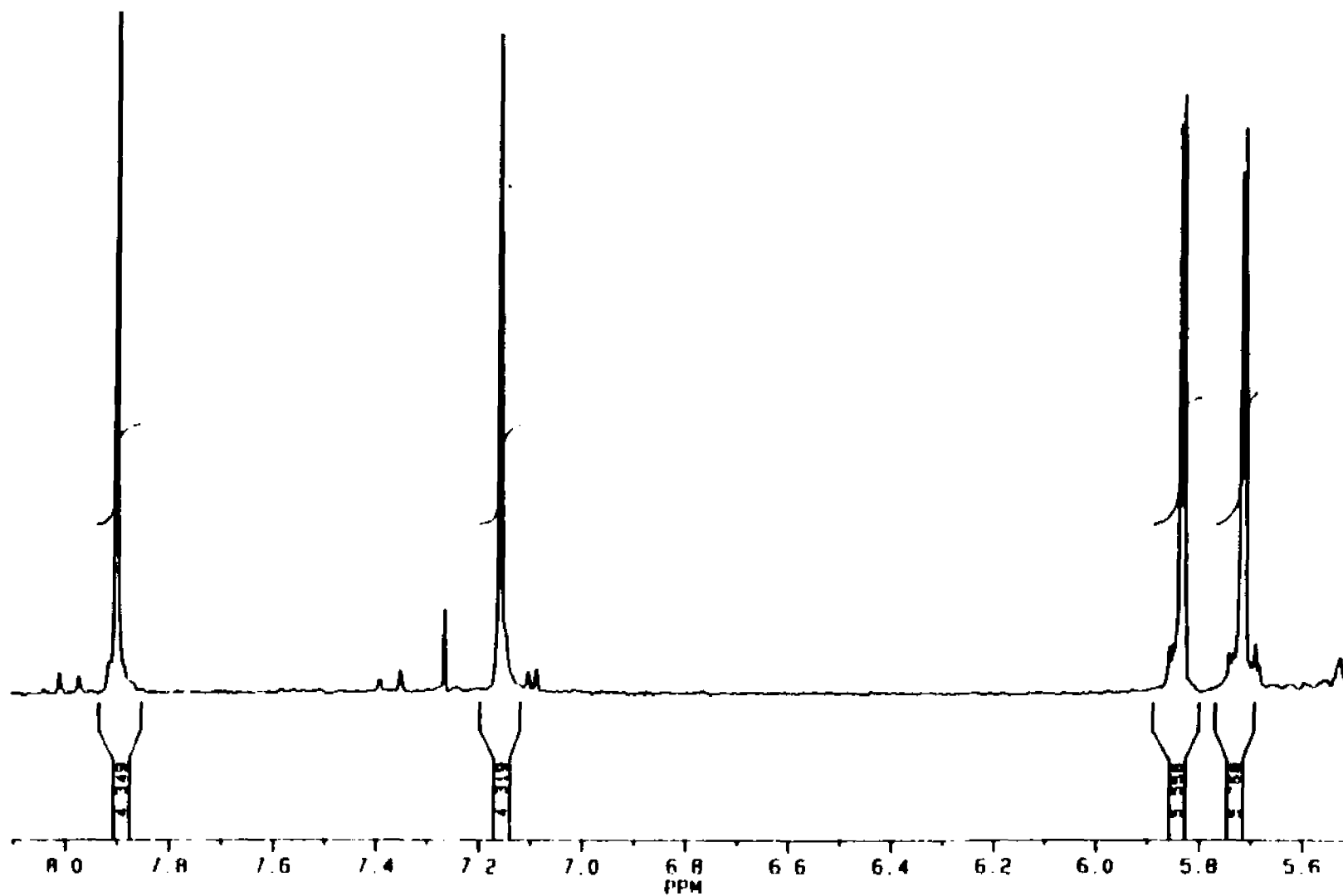
Appendix 28: ^1H NMR spectrum of cyclopent[fg]acenaphthylene-1,2,5,6-tetrone, (31) in DMSO-d_6 .



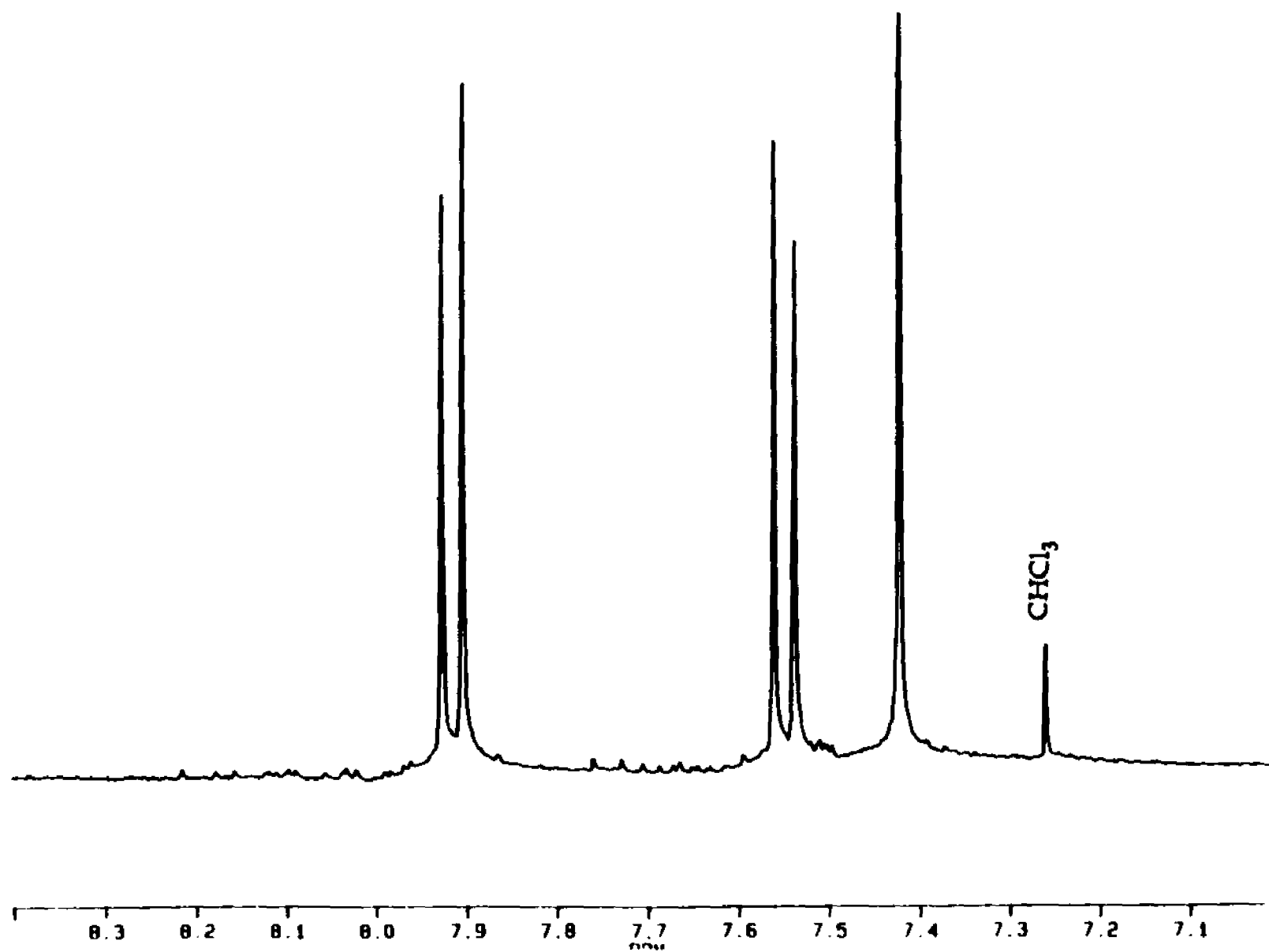
Appendix 29: ^{13}C NMR spectrum of cyclopent[fg]acenaphthylene-1,2,5,6-tetrone, (31) in DMSO-d_6 .



Appendix 30: ^1H NMR spectrum of 1,4,7,10-tetraethanone-indeno[1,2,3-*cd*]fluoranthene, (35).



Appendix 31: ^1H NMR spectrum of 1,4,7,10-tetrakis(1-chloroethenyl)-indeno[1,2,3-cd]fluoranthene, (36).



Appendix 32: ^1H NMR spectrum of diacenaphtho[3,2,1,8-cdefg: 3',2',1',8'-lmnop]chrysene, (24).



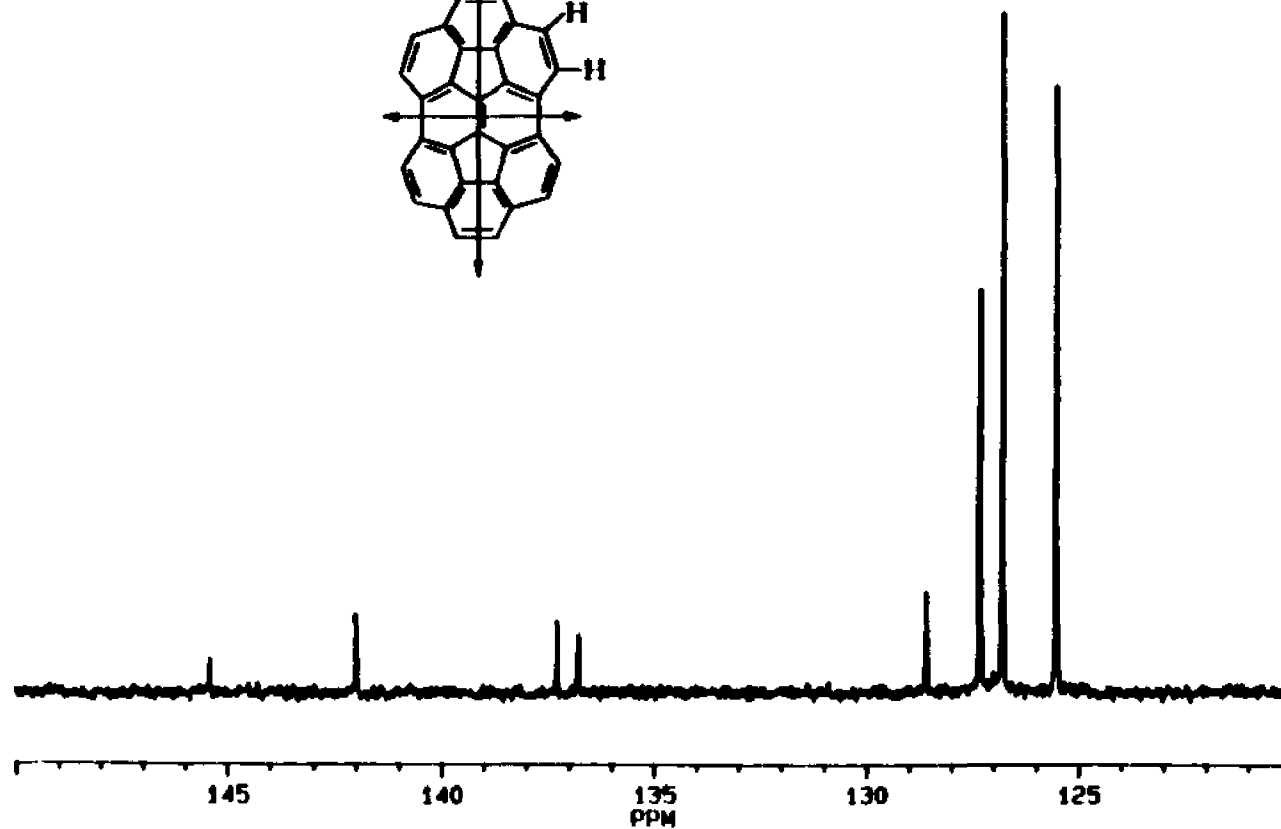
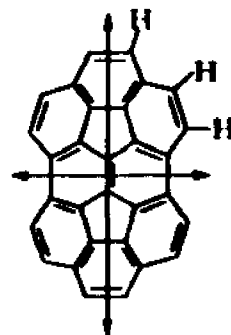
DATE 22-9-92

SF 100.614
SY 169.0
D1 4406.940
SI 32760
TD 32760
SM 25000.000
HZ/PT 1.526

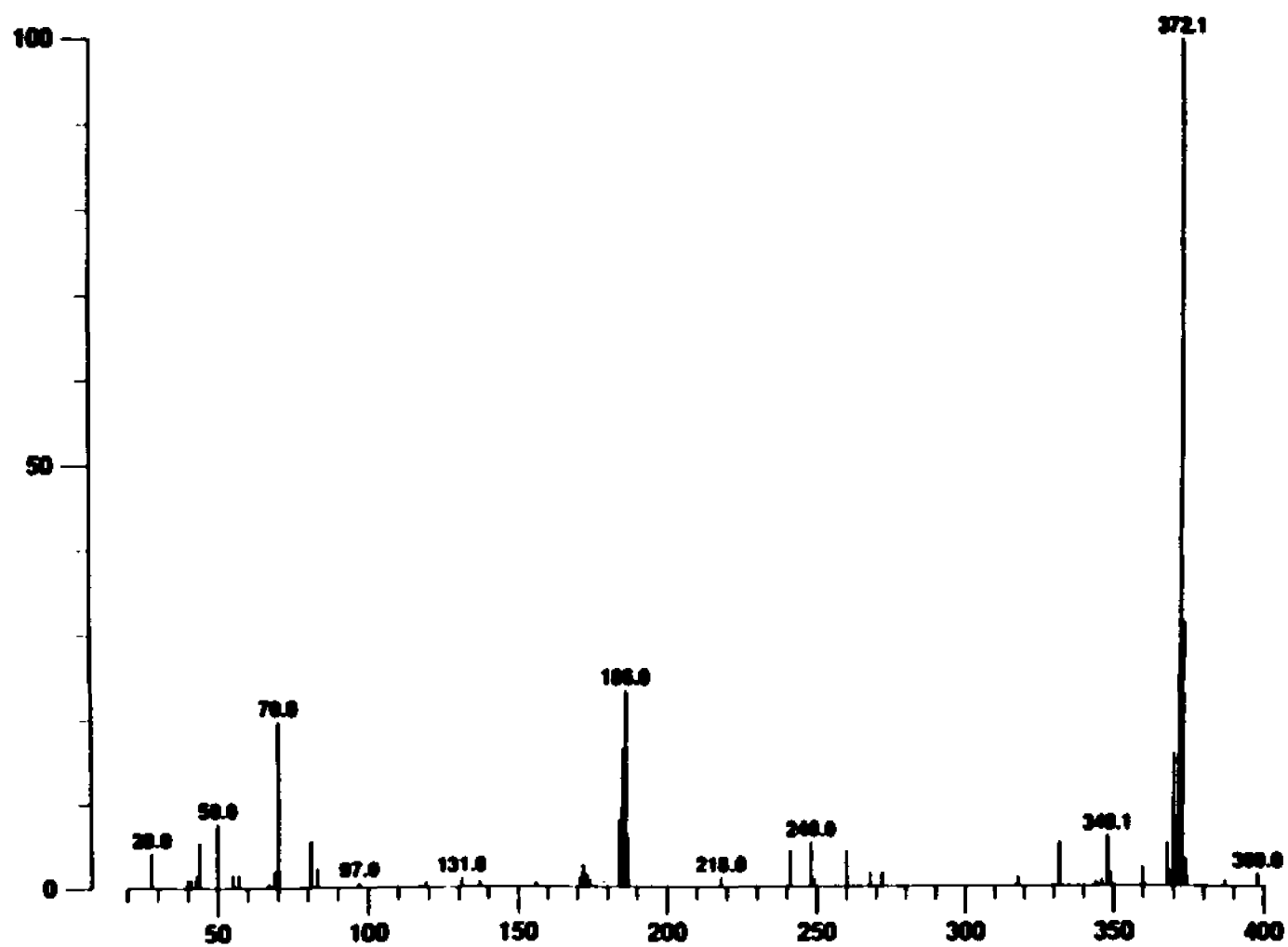
PW 0.5
RO 5.000
AQ .655
RG 32760
NS 9603
TE 298

FW 31300
D2 6400.000
DP 22L CPO

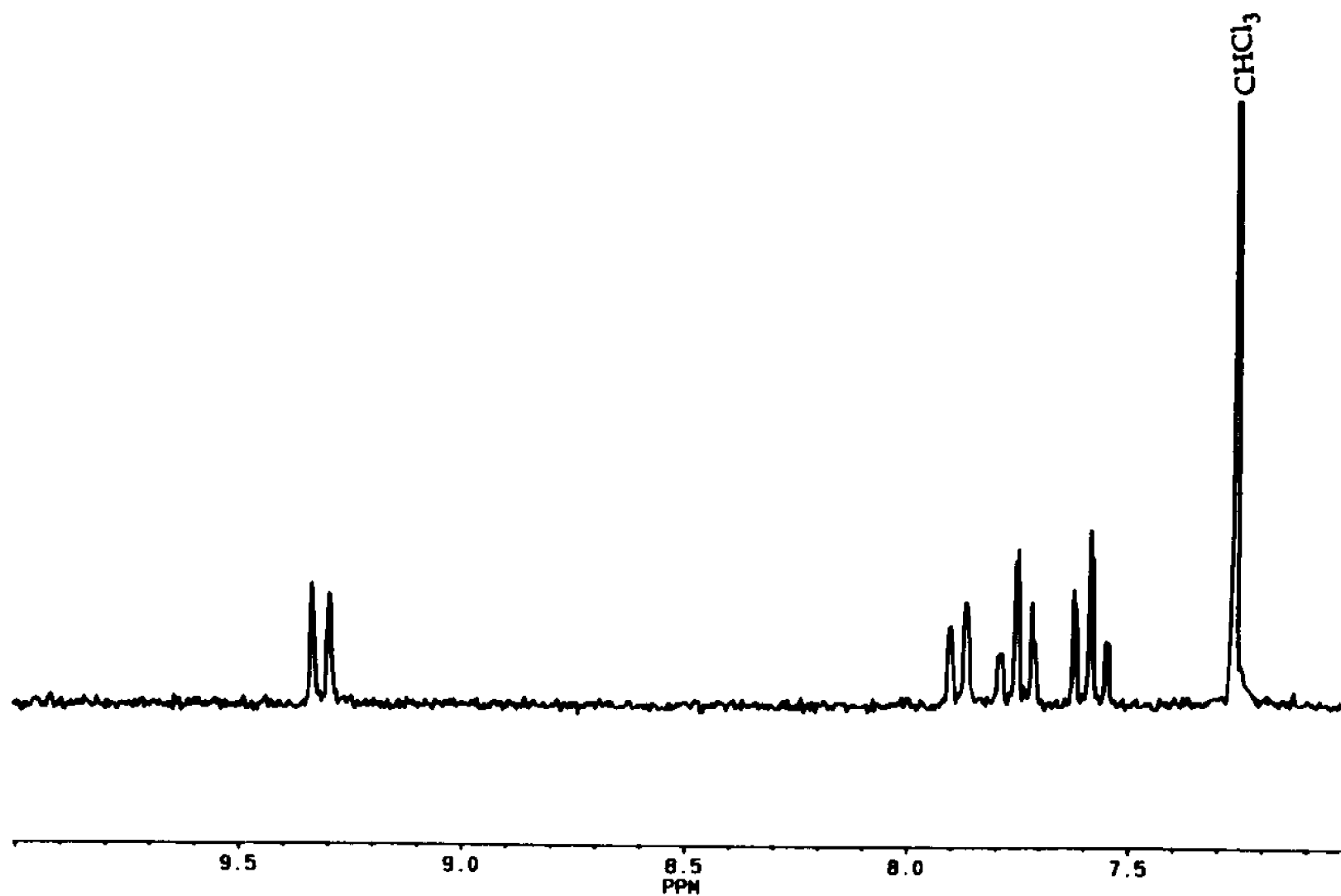
LB 1.000
GB 0.0
CX 20.00
CY 10.00
F1 150.008P
F2 120.010P
HZ/CW 150.909
PPM/CW 1.500
SR -6126.58



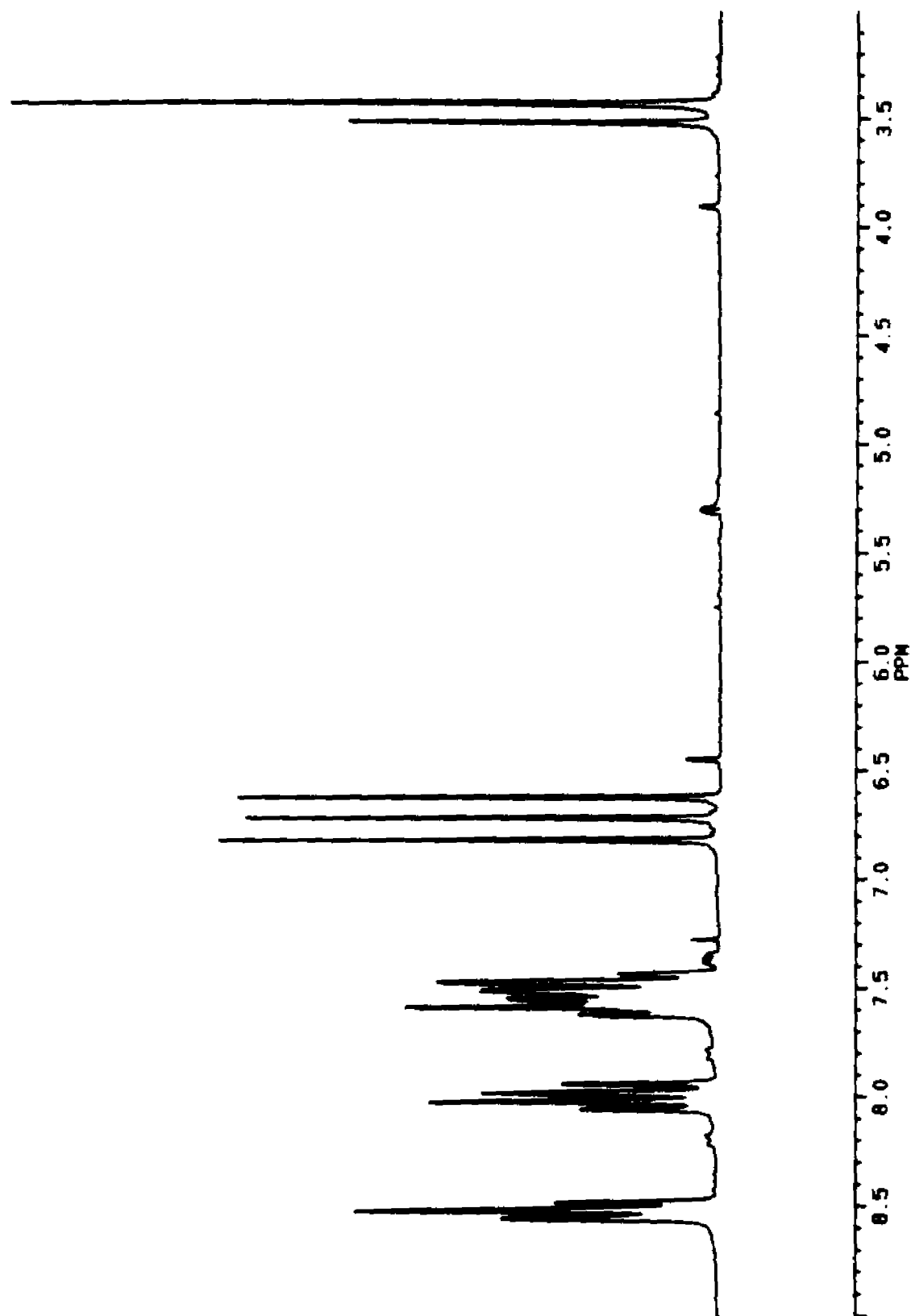
Appendix 33: ^{13}C NMR spectrum of diacenaphtho[3,2,1,8-*cdefg*:3',2',1',8'-*lmnop*]chrysene, (24).



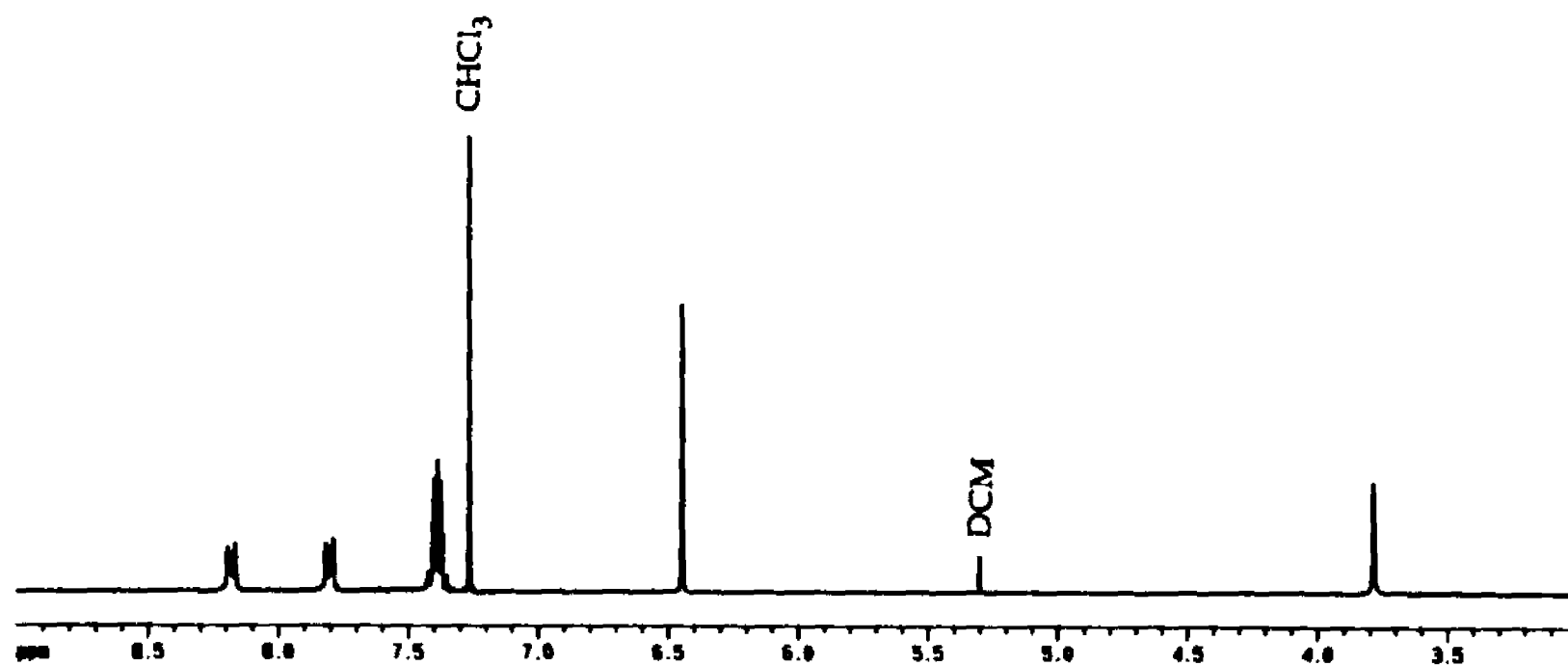
Appendix 34: HR/MS spectrum of diacenaphtho[3,2,1,8-cdefg: 3',2',1',8'-lmnop]chrysene, (24).



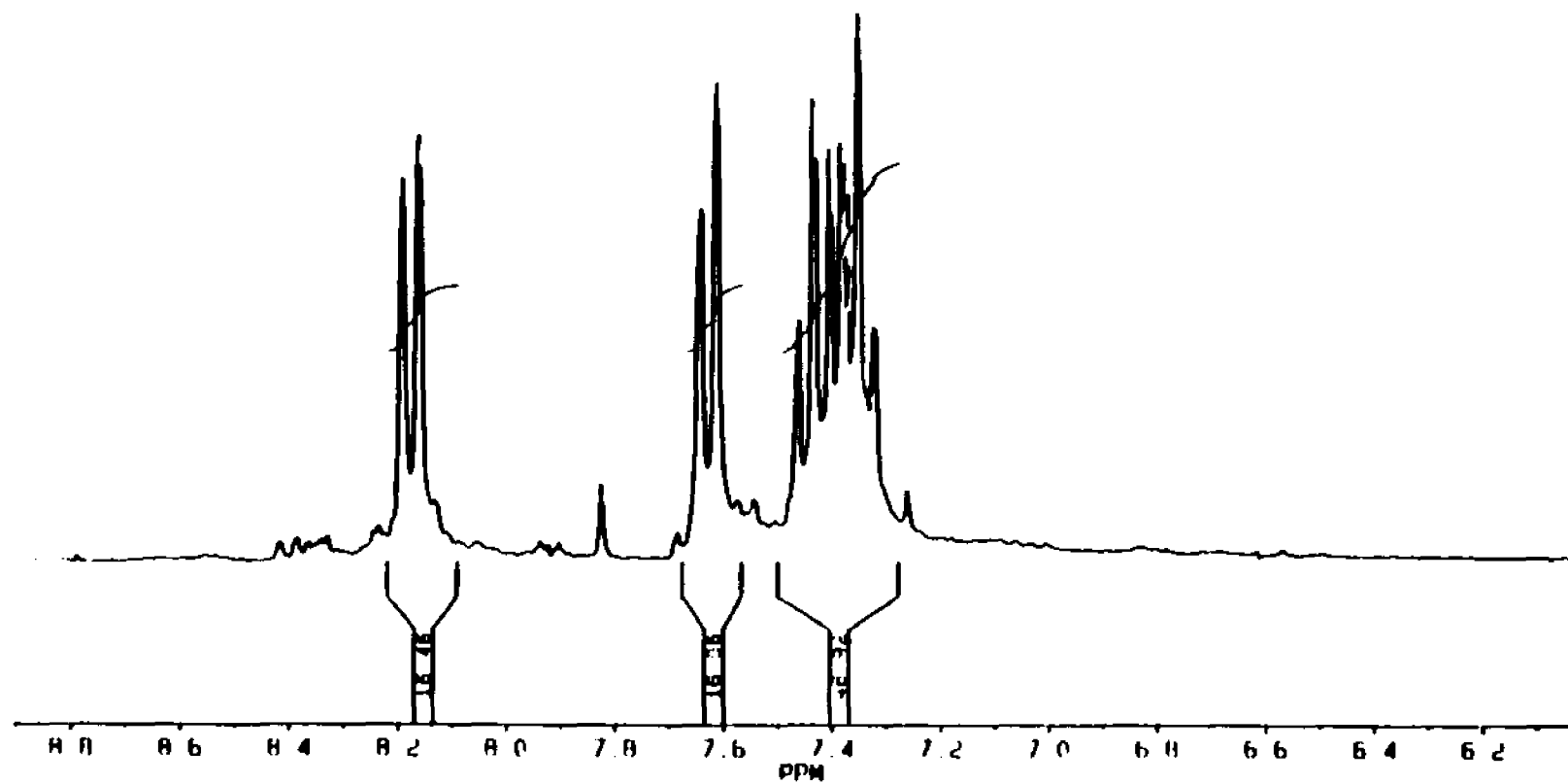
Appendix 35: ^1H NMR spectrum of 5H-diindeno[1,2-a:1',2'-c]fluorene-5,10,15-trione, (27).



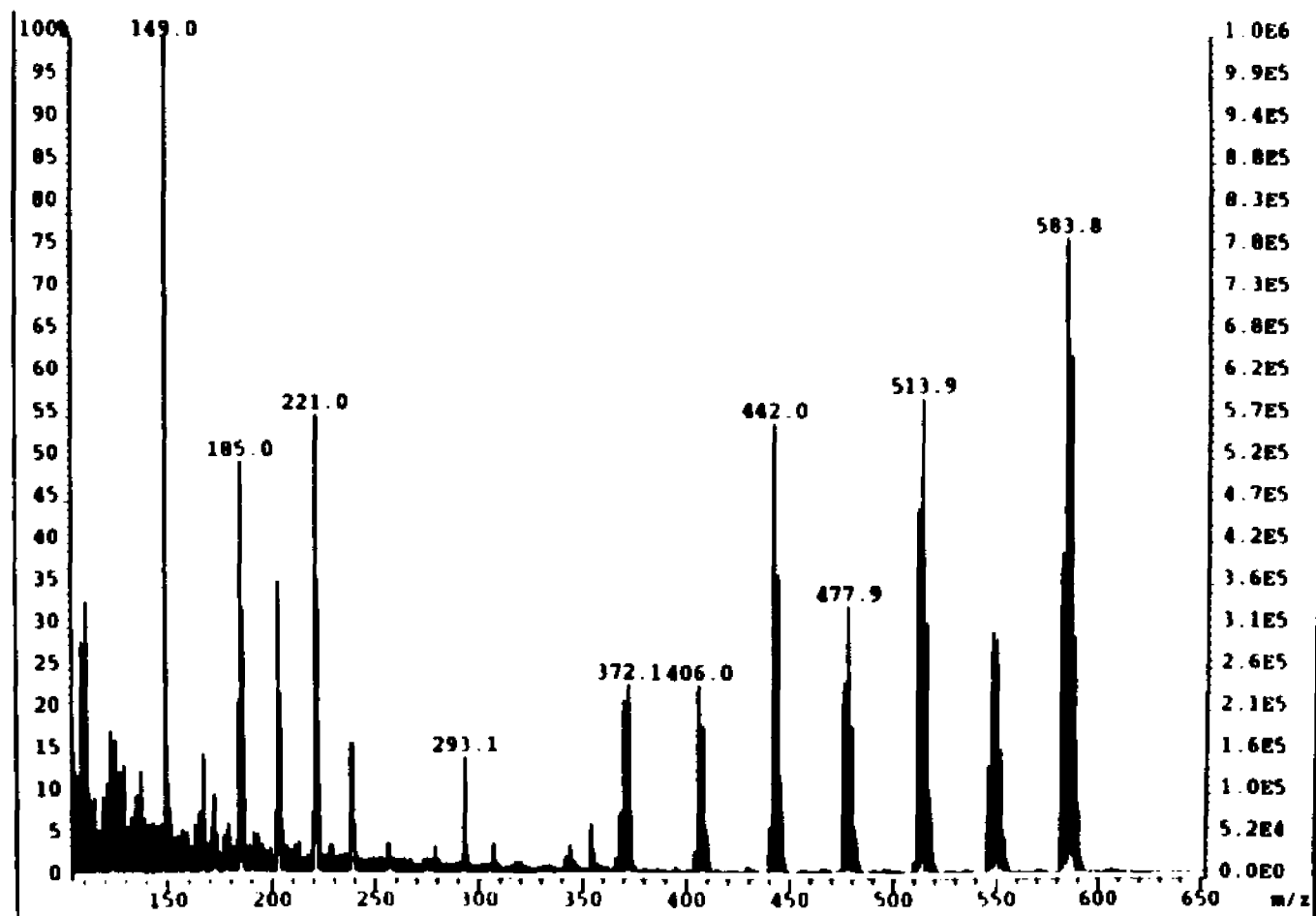
Appendix 36: ^1H NMR spectrum of 5,10,15-trihydroxy-5H-diindenol[1, 2-a:1', 2'-c]fluorene, anti-(40).



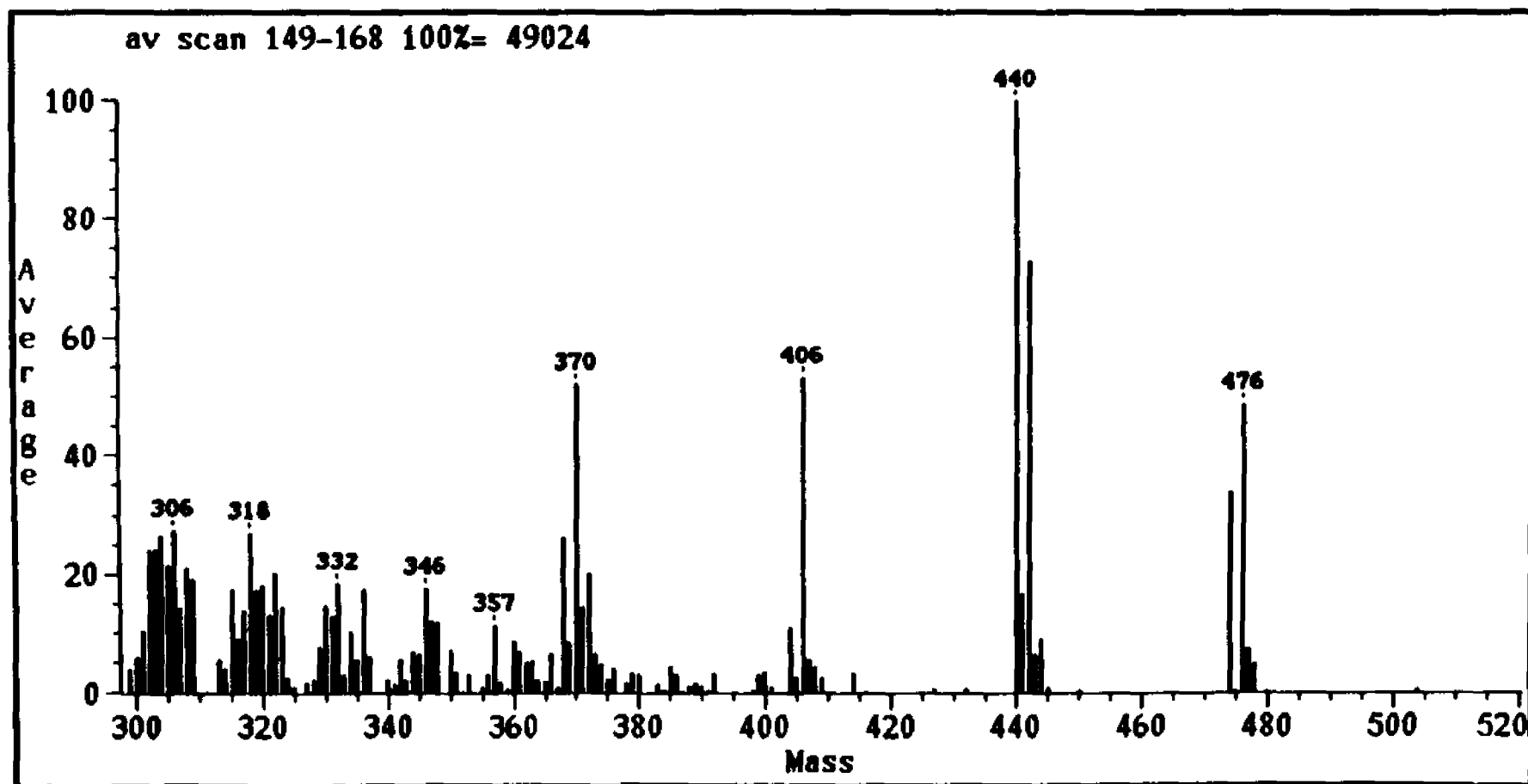
Appendix 37: ^1H NMR spectrum of 5,10,15-trihydroxy-5H-diideno[1, 2-*a*:1', 2'-*c*]fluorene, syn-(40).



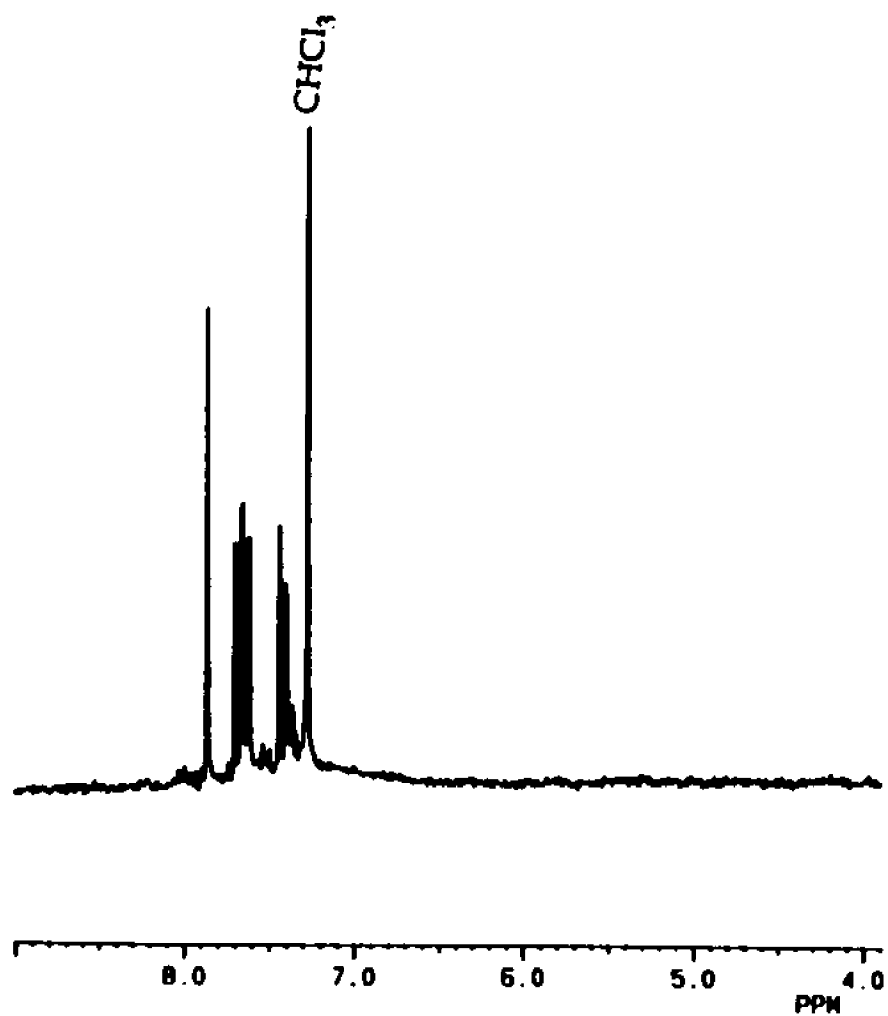
Appendix 38: ^1H NMR spectrum of 5,10,15-tris(dichloromethylene)-5H-diindeno[1,2-a:1',2'-c]fluorene, (41).



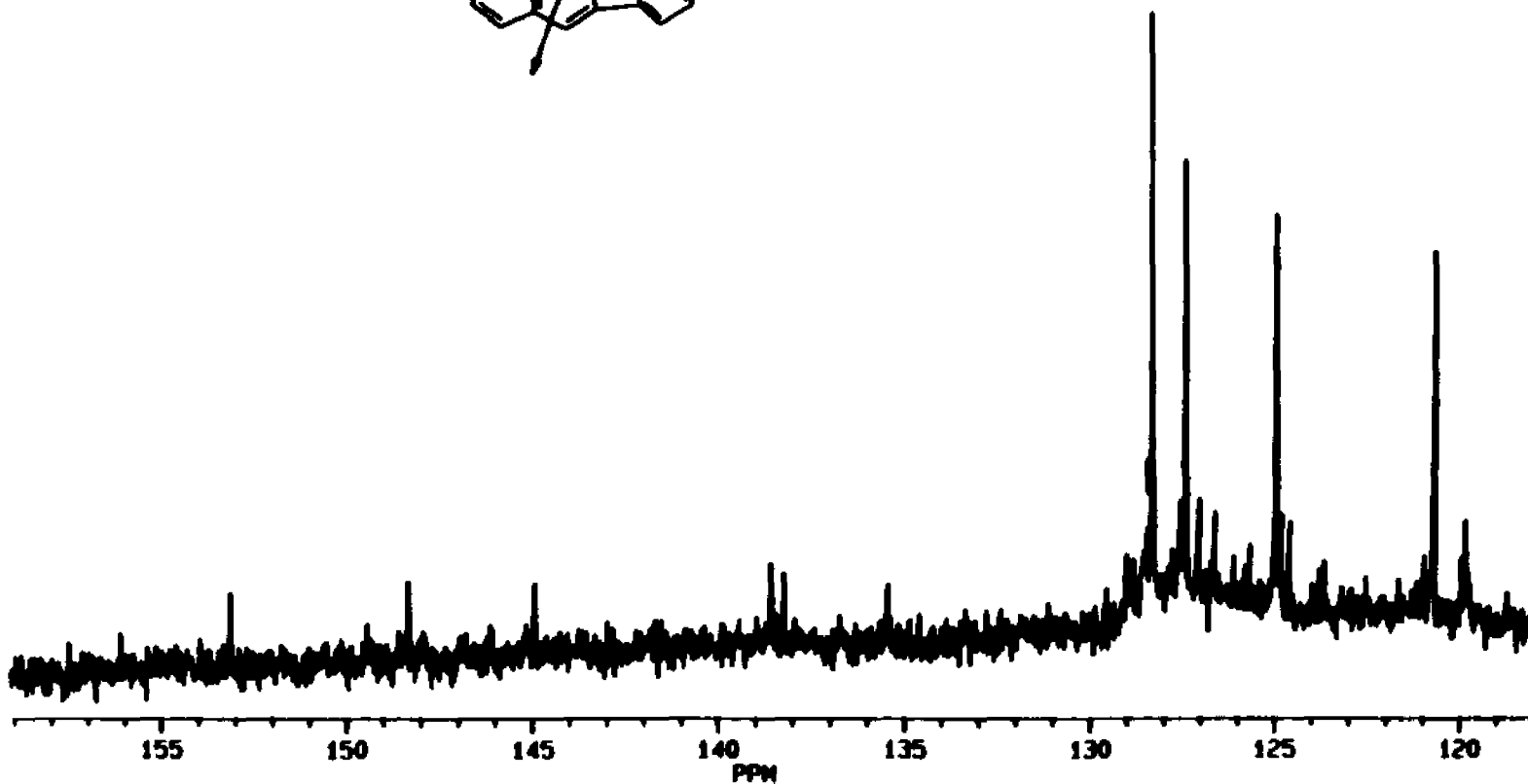
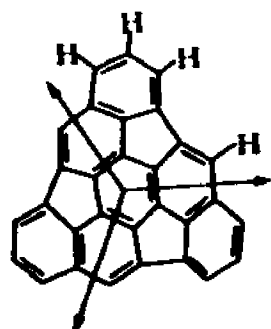
Appendix 39: HR/MS spectrum of 5,10,15-tris(dichloromethylene)-5H-diindeno[1, 2-a:1', 2'-c]fluorene, (41).



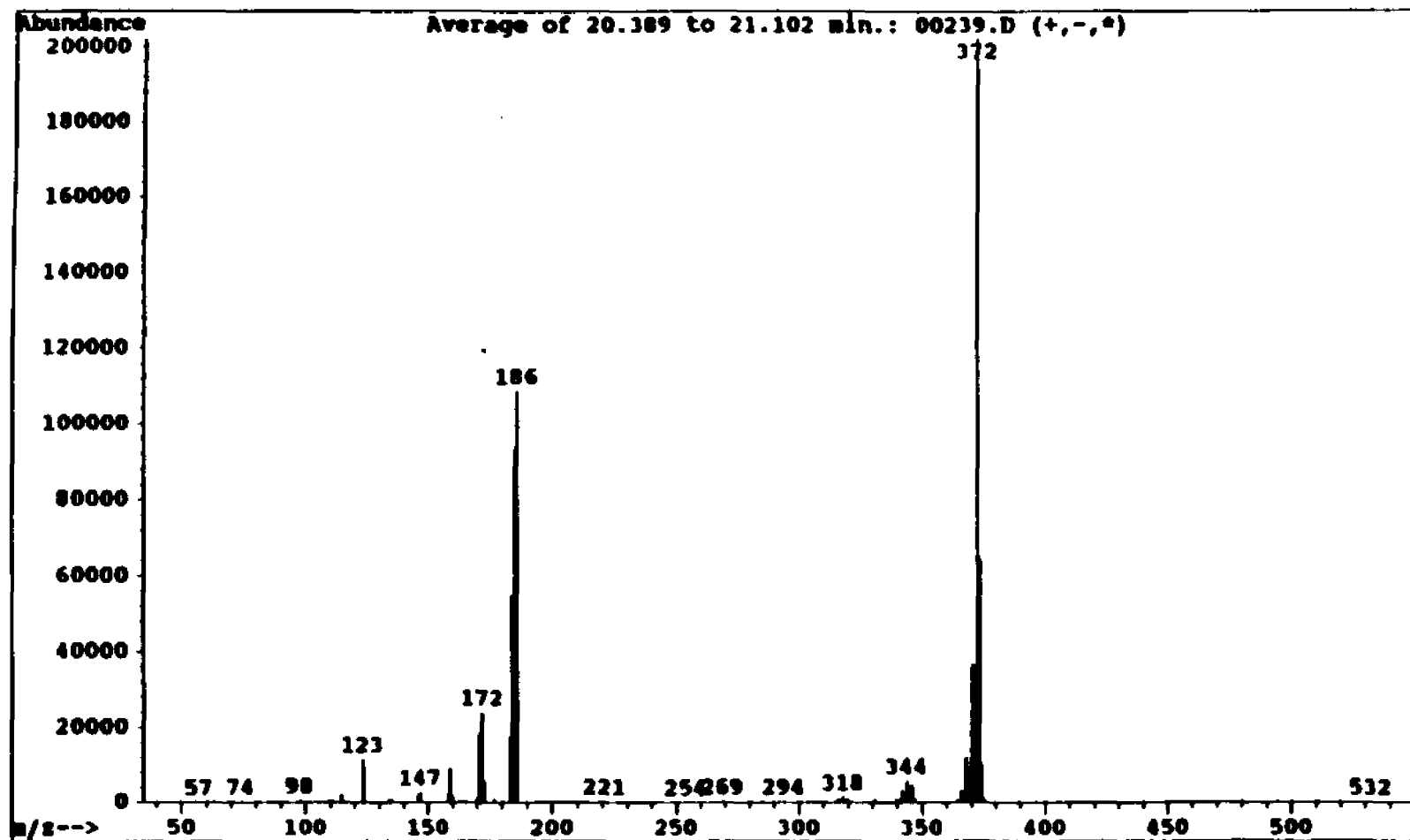
Appendix 40: LC/MS spectrum of the pyrolysis products of 5,10,15-tris-(dichloromethylene)-5H-diindeno[1, 2-a:1', 2'-c]fluorene, (41).



Appendix 41: ^1H NMR spectrum of benz[5,6]-as-indaceno[3,2,1,8,7-*mnopqr*]indeno[4,3,2,1-*cdef*]chrysene, (25).



Appendix 42: ^{13}C NMR spectrum of benz[5,6]-*as*-indaceno[3,2,1,8,7-*mnopqr*]indeno[4,3,2,1-*cdef*]chrysene, (25).



Appendix 43: GC/MS spectrum of benz[5,6]-as-indaceno[3,2,1,8,7-mnopqr]indeno[4,3,2,1-cdef]chrysene, (25).

VITA

Atteye H. Abdourazak was born in Djibouti, Republic of Djibouti. He Graduated from the "Lyceé d' Etat de Djibouti" in 1982 with a National Scholarship to study in France. He received his B.S. degree in 1986, and his M.S. degree in 1987, from the Université de Reims, Champagne-Ardennes (France). After three years spent teaching Physical Sciences in Djibouti, he came to the United States where he started the English Language Orientation Program at Louisiana State University in the Fall of 1990. He began pursuing his doctorate degree in Organic Chemistry in the Fall of 1991 under the direction of Dean Peter W. Rabideau. Currently, he is a candidate for the degree of Doctor of Philosophy in the Department of Chemistry.

DOCTORAL EXAMINATION AND DISSERTATION REPORT

Candidate: Atteye H. Abdourazak

Major Field: Chemistry

Title of Dissertation: Polynuclear Aromatic Hydrocarbons with Curved Surfaces:
Models and Precursors for Fullerenes

Approved:


Major Professor and Chairman


Dean of the Graduate School

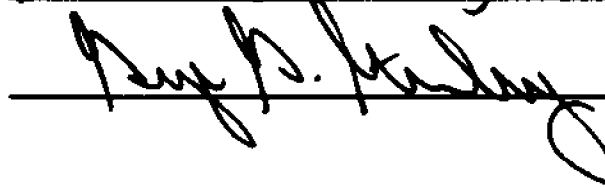
EXAMINING COMMITTEE:











Date of Examination:

July 7, 1995